The Official Journal of the Chinese Stomatological Association (CSA)

Chinese Journal of Dental Research

CJDR

VOLUME 28 NUMBER 2 2025

Join us in celebration and explore our special anniversary offers

These and many other anniversary offers:
www.quint.link/anniversary

QUINTESSENCE PUBLISHING

75 YEARS

Chinese Journal of Dental Research

The Official Journal of the Chinese Stomatological Association (CSA)

Chinese Journal of Dental Research

The Official Journal of the Chinese Stomatological Association (CSA)

Review

Original article

Case report

Chinese Journal of Dental Research

CN 10-1194/R • ISSN 1462-6446 • eISSN 1867-5646 • Quarterly

The Official Journal of the Chinese Stomatological Association
Co-sponsor: Peking University School of Stomatology, Quintessenz Verlag

Publication Department

Production Manager: Megan Platt (London, UK)
Managing Editor: Xiao Xia ZHANG (Beijing, P.R. China)

Address: 4F, Tower C, Jia 18#, Zhongguancun South Avenue, HaiDian District, 100081, Beijing, P.R. China.
Tel: 86 10 82195785, **Fax:** 86 10 62173402
Email: editor@cjdrcsa.com

Manuscript submission: Information can be found on the Guidelines for Authors page in this issue. To submit your outstanding research results more quickly, please visit: http://mc03.manuscriptcentral.com/cjdr

Administrated by: China Association for Science and Technology
Sponsored by: Chinese Stomatological Association and Popular Science Press
Published by: Popular Science Press
Printed by: Beijing ARTRON Colour Printing Co Ltd
Subscription (domestically) by Post Office

Chinese Journal of Dental Research is indexed in MEDLINE.

For more information and to download the free full text of the issue, please visit
www.quint.link/cjdr
http://www.cjdrcsa.com

Acknowledgements

We would like to express our gratitude to the peer reviewers for their great support to the journal in 2024.

Abdulmajeed, Aous (USA)
Afify, Ahmed (Egypt)
Ahmad, Basaruddin (Malaysia)
Akbarizadeh, Fatemeh (Iran)
Aly, Yousra (Egypt)
An, Na (China)
Arpornmaeklong, Premjit (Thailand)
Asaumi, Rieko (Japan)
Aslan, Tugrul (Turkey)
Attard, N (Malta)
Ayan, Gizem (Turkey)
Ayna, Emrah (Turkey)
Aytaç Bal, Fatma (Turkey)
Bacci, Christian (Italy)
Ballal, Nidambur (India)
Ballal, Vasudev (USA)
Bayoumi, Amr (Egypt)
Belli, Sema (Turkey)
Boffano, Paolo (Italy)
Buldur, Burak (Turkey)
Cao, Ye (China)
Caplin, Jennifer (USA)
Chabbra, Dr Ajay (India)
Chen, Chen (China)
Chen, Feng (China)
Chen, Jian Huan (China)
Chen, Jiang (China)
Chen, Jing (China)
Chen, Li Li (China)
Chen, Peng (China)
Chen, Zhi (China)
Dalben, Gisele da Silva (Brazil)
de Oliveira-Neto, O B (Brazil)
de-Jesus-Soares, Adriana (Brazil)
Dede, Dogu Omur (Turkey)
Dedeoğlu, Numan (Turkey)
Delaney, Eliza (France)
Deng, Ke (China)
Ding, Chun Mei (China)
Doğan Çankaya, Tülin (Turkey)
Dong, Yan Mei (China)
Duman, Şuayip Burak (Turkey)
EKINCI, Merve Sena (Turkey)
Fan, Zhi Peng (China)
Flores-Mir, Carlos (Canada)
Fu, Bai Ping (China)
Gao, Xue Mei (China)
Garoushi, Sufyan (Finland)
Gaur, Sumit (India)
Gautam, Chandkiram (India)
GÖK, Tuba (Turkey)
Gruber, Reinhard (Austria)
Gu, Li Sha (China)
Gundala, Rupasree (India)
Guo, Jie (China)
HafeziMotlagh, Kimia (Iran)
Hajeer, Mohammad Y (Syria)
Hamdy, Tamer (Egypt)
Han, Dong (China)
Han, Xiang Long (China)
Hasan, Arshad (Pakistan)
He, Jing Wei (China)
He, Miao (China)
Hourfar, Jan (Germany)
Hua, Cheng Ge (China)
Huang, Xin (China)
Huang, Yi Ping (China)
Huang, Zheng Wei (China)
Hür Şahin, Özge (Turkey)
Hussein, Ahmed (Egypt)
Hussein, Seenaa (Iraq)
Ismail, Hadi (Iraq)
Jakovljevic, Aleksandar (Syria)
Jamilian, Abdolreza (Iran)
JE, LeÃ³n (Brazil)
Jepsen, Soren (Germany)
Jia, Ling Fei (China)
Jiang, Hong Bing (China)
Jiang, Shao Yun (China)
Jotikasthira, Dhirawat (Thailand)
Katbeh, Imad (Russia)
Kinzinger, Gero (Germany)
Korucu, Hulde (Turkey)
Kuwata, Hirotaka (Japan)
Lagravere, Manuel O (Canada)
Li, Gang (China)
Li, Xiaodong (China)
Li, Zehan (China)
Liu, Jian Zhang (China)
Liu, Li Bing (China)
Liu, Ou Sheng (China)
Liu, Xue Nan (China)
Liu, Yan (China)
Long, Anna E (UK)
Long, Hu (China)
Ma, Ning (China)
Magan-Fernandez, Antonio (Spain)
Mancini, Manuele (Italy)
Markande, Dr Archana (India)
Mavragani, Maria (Norway)
Miron, Richard J (Switzerland)
Motgi, Anagha A (India)
Nagarajappa, Ramesh (India)
Ngeow, Wei Cheong (Malysia)
Nuvvula, Sivakumar (India)
Okutan, Alev (Turkey)
Osman, Ranjdar (Iraq)
Özdemir, Burcu (Turkey)
Pan, Ya Ping (China)
Park, Joo-Cheol (Korea)
Ramalingam, Karthikeyan (India)
Ramesan, Manammel Thankappan (India)
Rezaeifar, Kosar (Iran)
Rodrigues, Renata Cristina Silveira (Brazil)
Rong, Wen Sheng (China)
Sadrzadeh-Afshar, Maryam-Sadat (Iran)
Saul, Pavle (Ukraine)
Scribante, Andrea (Italy)
Shetty, Shishir Ram (United Arab Emirates)
Si, Yan (China)
Song, Jiang Yuan (China)
Srilatha, Adepu (India)
Su, Jia Zeng (China)
Sui, Lei (China)
Sun, Yu Chun (China)
Sun, Zhi Jun (China)
Sun, Zhi Peng (China)
Tagg, John R (New Zealand)
Tang, Xiao Lin (China)
Tao, Ren Chuan (China)
Tatakis, Dimitris (USA)
Tian, Fu Cong (China)
Trophimos, Akeem (Switzerland)
Uctasli, Sadullah (Turkey)
Valente, Nicola Alberto (Italy)
Viana Casarin, Renato Correa (Brazil)
Viktar, Muthoni (Algeria)
Wang, Fu (China)
Wang, Jing (China)
Wang, Peng Fei (China)
Wang, Wei Qi (China)
Wang, Wen Mei (China)
Wang, Yi Xiang (China)
Wang, Zuo Min (China)
Wu, Xiao Shan (China)
Xi, Tong (China)
Xia, Bin (China)
Xia, Lun Guo (China)
Xing, Hai Xia (China)
Yang, Bo (China)
Yang, Jing (China)
Yang, Yan Qi (China)
Yu, Jin Hua (China)
Yuan, Xue (China)
Zhang, Cheng Fei (China)
Zhang, Ran (China)
Zhang, Xu (China)
Zhang, Yu Feng (China)
Zhang, Zhi Hui (China)
Zhao, Yu Ming (China)
Zhao, Zhong Fang (China)
Zheng, Shu Guo (China)
Zheng, Yun Fei (China)
Zhong, Lai Ping (China)
Zhou, Bo (China)
Zhou, Xuan (China)
Zhu, Gui Quan (China)
Zhuang, Zi Yao (China)
Zong, Chen (China)
Zou, Jing (China)

Editorial Office
Chinese Journal of Dental Research

Lineage Tracing Identified Cell Populations within Adult Stem Cell Niches for Oral Maxillofacial Hard Tissue Formation

Shuang YANG[1], Chang Hao YU[1,2], Fei Fei LI[1,3], Yu SHI[1], Hui WANG[1], Wei Dong TIAN[1], Quan YUAN[1], Ling YE[1,2], Fan Yuan YU[1,2]

The regeneration of oral maxillofacial hard tissues is currently one of the issues of most concern in public health. This complex process involves a variety of cell types residing in a specialised microenvironment known as the adult stem cell niche in living organisms. Within this niche, adult stem cells are considered to play a central role in the regeneration of hard tissues, which undergo rapid proliferation and differentiation into progenitor cells to replace lost tissue, throughout postnatal life. Their fate is tightly regulated by the niche factors secreted by the non-stem niche cells present within the same microenvironment. Over the past decades, the advent of lineage tracing techniques has revolutionised the in vivo study of cell dynamics. Through tissue- and temporally-specific labelling of Cre-expressing cells, this method enables researchers to depict the defined cell fates and differentiation trajectories. The present review summarises the progress made in lineage tracing studies of hard tissue formation cell populations residing in the oral and maxillofacial regions, with a focus on stem cells, progenitor cells and niche cells. The aim is to provide new clues for future research endeavours.

Keywords: *adult stem cell niche, hard tissue formation, lineage tracing, niche cell, oral maxillofacial region, progenitor cell, stem cell*

Chin J Dent Res 2025;28(2):89–104; doi: 10.3290/j.cjdr.b6260563

The oral maxillofacial region is a prominent anatomical area with the jaw as the principal skeletal support. Its complex structures, including the teeth, jawbones, temporomandibular joints and various soft tissues, confer significant physiological functions. However, the global prevalence of oral diseases, such as dental caries, periodontal disease and tumours, is increasing, primarily resulting in the destruction of hard tissues in this region.[1,2] This leads to alterations in facial appearance and dysfunctions in chewing and speech. Consequently, enhancing the regeneration of oral maxillofacial hard tissues has become a critical focus in clinical interventions.[3,4]

Adult stem cells play a central role in the homeostasis and regeneration of postnatal tissues.[5] They reside within a specific anatomical location called the adult stem cell niche, which supports their normal function and fate determination through various intercellular interactions.[5] Typically, the adult stem cell niche is composed of cellular components (such as stem/progenitor cells and non-stem niche cells) and acellular components (such as extracellular matrix and long-distance signals from blood vessels, neurons and immune cells) (Fig 1).[6] When hard tissue is lost due to trauma, stem cells undergo asymmetrical division and differ-

1 State Key Laboratory of Oral Diseases & National Center for Stomatology & National Clinical Research Center for Oral Diseases, West China Hospital of Stomatology, Sichuan University, Chengdu, Sichuan Province, P.R. China
2 Department of Endodontics, West China Stomatology Hospital, Sichuan University, Chengdu, Sichuan Province, P.R. China
3 Department of Pediatric Dentistry, West China Stomatology Hospital, Sichuan University, Chengdu, Sichuan Province, P.R. China

Corresponding author: Dr Fan Yuan YU, State Key Laboratory of Oral Diseases & National Center for Stomatology & National Clinical Research Center for Oral Diseases, West China Hospital of Stomatology, Sichuan University, Chengdu 610041, Sichuan Province, P.R. China. Tel: 86-28-85503497. Email: fanyuan_yu@outlook.com

This work was supported by National Natural Science Foundation of China 82201045 (FY); and Sichuan Province Science and Technology Program 2024ZYD0172 (FY), 25NSFSC2450 (FL) and 2025NSFJQ0071 (FY).

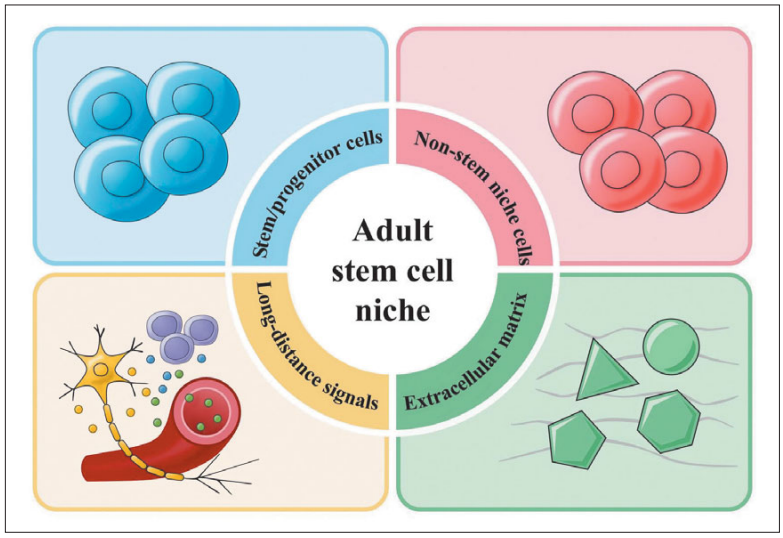

Fig 1 Components of the adult stem cell niche.

entiate into lineage-committed progenitor cells that further differentiate into specific hard tissue–forming cells, contributing to the repair of damaged tissues.[7] Moreover, niche cells play a vital role in regulating stem cell activity through paracrine signalling pathway during this process.[6] However, due to the inability to replicate the intricate microenvironment within a living organism, previous in vitro studies failed to accurately capture the characteristics of the cell population in vivo.[8] As a consequence, some stem cells exhibit enhanced plasticity and proliferation capabilities when isolated from the in vivo environment, even if they are not normally involved in homeostasis maintenance.[9,10]

Advances in transgenic animals have revolutionised the investigation of cell fate in vivo.[11] The lineage tracing technique utilising the Cre/loxP system has been widely employed in the study of oral maxillofacial hard tissues. Targeted gene-driven Cre recombinase enters the nucleus and specifically recognises the loxP sequences.[12] The stop codon flanked by loxP sequences is then removed to allow downstream fluorescent protein gene expression, achieving spatial-specific labelling of cell populations.[12] When the Cre recombinase is further fused with the ligand-binding domain of oestrogen receptor (ER), CreER recombinase can change conformation and enter the nucleus to exert recombinase activity only with the addition of tamoxifen, further realising the temporal-specific regulation of cell labelling.[13] This method enables the permanent labelling and visualisation of Cre- or CreER-expressing cells and their progeny. By virtue of its high efficiency, specificity, continuity and controllability, lineage tracing provides fresh perspectives on realistic cell activities in vivo, thus expanding understanding of cell fate determination during tissue formation and regeneration.

Currently, the lineage tracing technique has identified various cell populations within adult stem cell niches that are involved in the formation of oral maxillofacial hard tissues (Fig 2). In this review, the present authors summarise discoveries obtained through lineage tracing regarding the cellular components of adult stem cell niches, including stem, progenitor and niche cells. The aim of this review is to enhance comprehension of the ongoing research on adult stem cell niches in vivo, and to provide insight into the processes of development, homeostasis and regeneration of hard tissues in the oral maxillofacial region.

Stem cells

Adult stem cells possess the unique ability to undergo continuous self-renewal and differentiate into specific cell types associated with particular tissues.[14] The identification of stem cells through lineage tracing typically requires that all cells within the hierarchy be permanently labelled over an extended tracing period.[14] Current findings have led to the recognition of several well-defined populations of stem cells in the oral maxillofacial regions.

Sox2$^+$ cells

Sox2 is a member of the Sox family of transcription factors with highly conserved HMG-box DNA-binding domains.[15] It is expressed prominently in epithelial tissues across various organs and is established as an iconic marker of epithelial stem cells.[16,17] Recent studies have highlighted the pivotal role of Sox2$^+$ dental epithelial stem cells (DESCs) in tooth development.

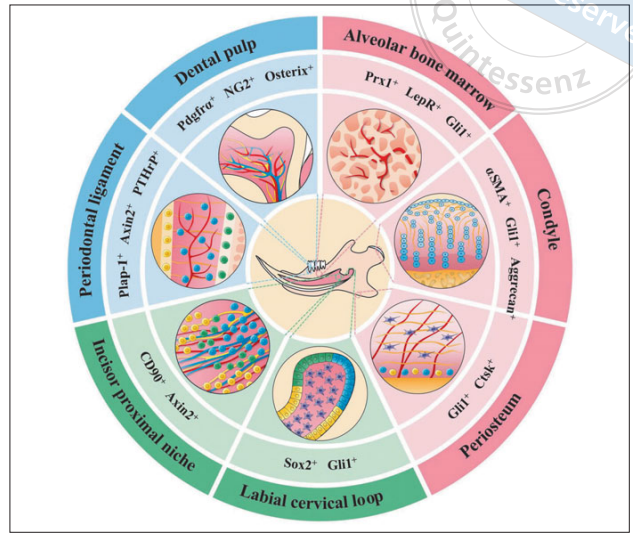

Fig 2 Lineage tracing identified representative cell populations within different adult stem cell niches in the oral maxillofacial region.

Rodent incisors retain the ability of continuous growth after birth due to the presence of the labial cervical loop (laCL), a well-known adult stem cell niche at the proximal end of the incisor.[18,19] Research by Juuri et al[20] indicated a gradual localisation of Sox2 expression from the entire oral epithelium to the laCL, followed by postnatal generation of all epithelial cell lineages, including ameloblasts, outer enamel epithelium, stellate reticulum and stratum intermedium, which were also generated by Sox2$^+$ cells in adult mouse incisors. Conversely, in mouse molars, Sox2$^+$ cells are transiently present during the embryonic period and contribute to all epithelial cell lineages, but disappear after birth synchronously with the loss of cervical loops.[21] Therefore, the different fates of Sox2$^+$ DESCs in the murine incisor and molar provide an acceptable explanation for different postnatal growth potential at the cellular level.

Prx1$^+$ cells

Paired related homeobox 1 (Prx1 or Prrx1) is a transcription factor expressed in the mesenchymal tissues.[22] Prx1$^+$ cells are well recognised as important mesenchymal stem cells (MSCs) in long bones and calvaria.[23,24] Application of lineage tracing in oral maxillofacial hard tissues has yielded valuable insight into the functions of Prx1$^+$ MSCs.

Prx1$^+$ cells may be responsible for tooth morphogenesis

Teeth are different shapes to accommodate a wide variety of functions.[25] In tapered mouse incisors, Prx1$^+$ cells nest in the dental follicle and dental pulp, but not in epithelial lineage cells.[26,27] Intriguingly, Prx1$^+$ cells exhibit varying distributions in different molars: they are widely present within the dental pulp of the first molar (M1), have a reduced distribution in the second molar (M2) and are nearly absent in the third molar (M3) during early tooth development.[26,28] Given the morphological differences among murine molars, it is tempting to speculate about a potential correlation between Prx1$^+$ MSCs and tooth morphogenesis.

Prx1$^+$ cells support the formation of jawbone

Prx1$^+$ cells also engage in jawbone development and the maintenance of homeostasis after birth. Cui et al[27] identified a large number of Prx1$^+$ cells surrounding incisors and at the molar base that subsequently differentiated into osteocytes in neonatal Prx1-Cre mice. However, in adult Prx1-CreER mice, only a few Prx1$^+$ cells were detected in the periodontal ligament (PDL), supporting the turnover of periodontal tissues.[29] Overall, the contribution of Prx1$^+$ cells to alveolar bone formation appears to be more significant in infancy.

Nevertheless, Prx1$^+$ cells remain crucial for alveolar bone remodelling and regeneration in adulthood. The most recent study by Feng et al[30] demonstrated the necessity of Prx1$^+$ cells for implant osseointegration. To investigate the role of Prx1$^+$ cells in jawbone regeneration, Zhao et al[31] established a full-thickness mandibular defect model by osteotomy, and found that Prx1$^+$ cells were activated and clustered on the surface of trabecular bone in the defect area. In contrast, ablation of Prx1$^+$ cells by inducing endogenous cytotoxic diphtheria toxin A resulted in impaired alveolar bone repair in non-critical size periodontal defects, suggesting the significance of Prx1$^+$ MSCs in the process of jawbone damage repair.[29]

LepR$^+$ cells

The leptin receptor (LepR) has been identified as a marker of adult bone marrow mesenchymal cells in long bones.[32,33] LepR$^+$ cells serve as a significant source of osteoprogenitor cells and are capable of secreting various cytokines to maintain a conducive microenvironment for hematopoietic stem cells, thereby supporting the maintenance of adult bone homeostasis and facilitating timely fracture repair.[34,35] In the oral maxillofacial region, the functions of LepR$^+$ cells have also garnered increasing attention.

LepR$^+$ cells play a minor role in cementum formation

Under physiological conditions, LepR$^+$ cells are predominantly located in the apical region of the PDL in 4-week-old juvenile LepR-Cre mice, with a smaller presence in the gingiva, alveolar bone marrow cavity and dental pulp.[9,36] Remarkably, all cementocytes are negative for LepR at the juvenile stage.[36] Extending the tracing period up to 1 year, the progeny of LepR$^+$ PDL cells gradually increase and differentiate into cementocytes at a low frequency.[36] In adult LepR-CreER mice, LepR$^+$ cells also show minimal contribution to cementocytes, even though the ablation of LepR$^+$ cells lead to disturbances in periodontium homeostasis and ultimately result in cementum dysplasia.[9] Based on the existing findings, the contribution of LepR$^+$ cells to cementum formation is minor.

LepR$^+$ cells have a limited effect on the formation of alveolar bone

A quiescent population of LepR$^+$ cells within the bone marrow (BM) can give rise to osteoblastic lineage cells physiologically and contribute to the regeneration of alveolar bone after tooth extraction.[37,38] Ablation of LepR$^+$ BM cells brought about attenuated healing of extraction sockets.[37]

PDL stem cells (PDLSCs) have a high differentiation potential to promote alveolar bone regeneration.[39] The role of LepR$^+$ PDLSCs in the development and homeostasis of alveolar bone has been revealed recently.[9,36] However, research by Oka et al[36] demonstrated a definite but limited effect of LepR$^+$ PDLSCs on new bone formation in tooth extraction sites, with the LepR$^-$ PDL cell subpopulation showing a greater contribution to alveolar bone regeneration. Taken together, the insignificant contribution of LepR$^+$ PDLSCs to both cementum and alveolar bone indicates that they are not the primary source of cells forming oral maxillofacial hard tissues.

CD90$^+$ cells

CD90, also known as Thy1, is a glycophosphatidylinositol-anchored cell membrane protein essential for the pluripotency of MSCs.[40] An et al[41] identified a CD90$^+$ MSC subset responsible for supplying cells for the rapid growth of incisors during early postnatal development and adult clipped incisors regeneration, while only very few were detected during homeostasis. Notably, the reappearing CD90$^+$ cells in clipped incisors were generated by a small and quiescent Celsr1$^+$ cell population located proximal to MSCs, suggesting a potential role of Celsr1$^+$ cells as a stem cell reservoir.[41] Although researchers hypothesised that the blooming of CD90$^+$ cells during incisor regeneration might be related to the loss of occlusal force, the unloaded incisor did not exhibit accelerated growth when clipping the opposing incisor, indicating that Celsr1$^+$ cells were likely triggered by other currently unidentified signals rather than occlusal force change.[41]

Apart from the incisor pulp, a recent study by Zhao et al[42] demonstrated the differentiation of CD90$^+$ cells into cementoblasts in the developing molar PDL and the decreased number in adults. In mild periodontitis, CD90$^+$ cells regain their ability to differentiate into cementoblasts.[42] However, Nagata et al[43] reported no detectable upregulation of CD90 in cementoblasts based on single-cell transcriptomic analysis. This discrepancy may be attributed to variations in experimental methodologies, necessitating further investigation to definitively delineate the lineage hierarchy of cells in periodontal tissues.

Pdgfrα$^+$ cells

Platelet-derived growth factor receptor α (Pdgfrα) is a common marker of stem cells.[44] Adult Pdgfrα-CreER; tdTomato mice could label the majority of dental pulp cells, whereas only a small number of osteocytes in the alveolar bone and very few PDL cells were labelled.[45] Specifically, Yao et al[46] identified a population of CD51$^+$Pdgfrα$^+$ cells that gradually declined with age in the odontoblast layer and pulp core in murine molars. However, the specific role of these cells in tooth homeostasis and age-related changes remains largely unexplored, warranting further research to decipher the mechanisms involved.

Stem/progenitor cells

The characterisation of stem cell markers is notably intricate, making it challenging to differentiate these cells accurately based solely on a single marker.[47] Consequently, the cells labelled by a singular recombinase system are expected to represent a heterogeneous population exhibiting stem-like properties. Furthermore, the absence of data from long-term lineage tracing complicates the direct classification of certain cells as stem cells. Therefore, this review will collectively address these cells in this section for further discussion.

αSMA$^+$ cells

As a characteristic protein of myofibroblasts, alpha-smooth muscle actin (αSMA) is engaged in the movement and contraction of blood vessels.[48,49] Additionally, αSMA is commonly used as a molecular marker for mesenchymal stem/progenitor cells.

αSMA$^+$ cells are responsive to dental tissues injury

Minor subsets of αSMA$^+$ cells have been detected in dental pulp, PDL and the alveolar bone surrounding incisors or molars.[45,50,51] CD31 antibody staining indicated that αSMA$^+$ cells typically reside in perivascular regions.[52] These cells are recognised for their significant involvement in the process of tissue repair. Roguljic et al[50] observed the proliferation and differentiation of αSMA$^+$ PDL cells into various cell types, including cementoblasts, osteoblasts and fibroblasts, in a murine PDL injury model. Additionally, Vidovic et al[51-53] also demonstrated that αSMA$^+$ cells in dental pulp were substantially activated and differentiated into odontoblasts in response to experimental dentine injury and pulp exposure.

αSMA$^+$ cells are fibrocartilage stem cells residing in the condyle cartilage superficial zone

The condylar cartilage is characterised by highly organised cellular zones, which are sequentially arranged from the surface to the interior as the fibrous superficial zone, the proliferative zone, the chondrocyte zone and the mature hypertrophic chondrocyte zone.[54] Research by Embree et al[55] indicated that undifferentiated αSMA$^+$ cells in the superficial zone could spontaneously differentiate into mature chondrocytes, thus maintaining the steady state of condylar cartilage. Therefore, this observation provides powerful evidence for the notion that the superficial zone may serve as a conducive adult stem cell niche for fibrocartilage stem cells (FCSCs).

Gli1$^+$ cells

Hedgehog (Hh) signalling regulates the proliferation and differentiation of stem cells in the nervous, skeletal, digestive and reproductive systems.[56] As an essential transcription factor in Hh signaling, Gli1 serves as a reliable stem/progenitor cell marker.[57] Recently, a series of studies have demonstrated the significance of Gli1$^+$ stem/progenitor cells in the formation, homeostasis and regeneration of oral maxillofacial hard tissues.

Gli1$^+$ cells are heterogeneous populations involved in tooth formation

Tooth formation is a complex process involving reciprocal interactions between the epithelium and mesenchyme.[58] As mentioned above, the laCL is recognised as a niche for DESCs in the mouse incisor.[18,19] Seidel et al[59] identified the label-retaining Gli1$^+$ DESCs in the laCL that gave rise to ameloblasts. The neurovascular bundle (NVB) situated in the mesenchyme adjacent to laCL also harbours Gli1$^+$ MSCs, which continuously generate transit-amplifying progenitors that actively undergo mitosis and differentiate into odontoblasts or dental pulp cells to maintain dental homeostasis.[60] In summary, Gli1$^+$ cells play a crucial role in both epithelial and mesenchymal cell lineages during incisor formation.

Moreover, Gli1$^+$ cells are also involved in the development of molar roots. Wen et al[61] reported the distribution of Gli1$^+$ cells in the molar apical mesenchyme and dental epithelium in postnatal 7.5-day-old mice. Upon completion of root development at 3 weeks old, the main structures, including odontoblasts, dental pulp, PDL and the remaining dental epithelium, were found to be tdTomato$^+$ cells derived from Gli1$^+$ cells.[61] Additionally, a study by Xie et al[62] also asserted the involvement of Gli1$^+$ cells in the formation of both cellular and acellular cementum. Ablation of Gli1$^+$ cells resulted in a noticeable cementum hypoplasia phenotype.[62] Overall, these results provide compelling evidence to support the heterogeneity of Gli1$^+$ stem/progenitor cells in the formation of dental hard tissues.

Gli1$^+$ cells function in alveolar bone regeneration

In the jawbone, Gli1$^+$ BM cells mainly reside along blood vessels within the furcation area of the molar roots.[63] Additionally, a minor population of Gli1$^+$ cells scatter in the periosteum of the mandible.[64] These two distinct

populations of Gli1$^+$ cells participate in the maintenance of local bone homeostasis. Despite lacking various differentiation markers physiologically, Gli1$^+$ BM cells possess the potential to be stimulated into proliferation and differentiation into osteocytes following tooth extraction, contributing to extraction socket healing and implant osseointegration.[63] As a complement, the ablation of Gli1$^+$ BM cells leads to a significant reduction in bone volume around the implant, emphasising the importance of Gli1$^+$ cells in alveolar bone regeneration.[63]

The engagement of Gli1$^+$ PDL cells should not be ignored. Shalehin et al[10] transplanted the maxillary first molars from Gli1-CreERT2 mice into the abdominal subcutaneous connective tissues of wild-type mice, and the results showed that Gli1$^+$ PDL cells were capable of osteogenic differentiation. They also demonstrated that Gli1$^+$ cells in the tooth socket were positive for Periostin 1 day after tooth extraction, indicating the contribution of Gli1$^+$ cells originating from PDL to alveolar bone regeneration.[65]

A notable characteristic of PDLSCs is their responsiveness to mechanical forces.[66] Orthodontic tooth movement (OTM) serves as a well-defined model for investigating the regulatory factors in mechanical-force mediated bone remodelling.[67] Liu et al[68] first revealed a substantial increase in the number of Gli1$^+$ PDL cells on the tension side following 7 days of OTM, contrasting with restricted decreased Gli1$^+$ cells on the pressure side. Subsequent evidence from Seki et al[69] also suggested that Gli1$^+$ PDL cells on the tension side exhibited immediate proliferation in response to tensile stress and further differentiated into mature osteoblasts. Intriguingly, a similar level of increased Gli1$^+$ PDL cells on the pressure side was observed 10 days after OTM, with these cells differentiating into fibroblasts to contribute to PDL reconstruction.[69] Conversely, when unloading the occlusal forces by extracting the opposing teeth, Men et al[45] observed a significant decrease in Gli1$^+$ PDL cells, accompanied by notably reduced alveolar bone height and relative bone density. Collectively, these studies provide sufficient evidence for the diverse responses of Gli1$^+$ stem/progenitor cells to distinct mechanical forces.

Gli1$^+$ cells orchestrate the osteogenesis and chondrogenesis of the condyle

Postnatal Gli1$^+$ cells in the condyle are spatially distributed in two different domains, namely the superficial zone of the cartilage and the subchondral bone immediately beneath the cartilage (chondro-osseous junction).[70,71] The superficial zone provides a niche for FCSCs.[72] Gli1$^+$ FCSCs here could proliferate and migrate into two to four cell layers deeper.[71] However, they do not typically migrate into the mature hypertrophic chondrocyte zones even after 1-year tracing.[71] In contrast, Gli1$^+$ cells at the chondro-osseous junction lack expression of Sox9 and Aggrecan, indicating that they do not belong to the cartilage lineage.[71] Instead, they extend towards the trabecular bone and subsequently exhibit colocalisation with Osterix$^+$ osteoblasts, which verify their osteogenic differentiation ability in the subchondral bone.[70,71] In summary, two unique populations of Gli1$^+$ cells contribute to the growth and development of the condyle, each with distinct characteristics and functions.

Building upon this groundwork, researchers have delved into the contribution of these two Gli1$^+$ cell populations to tissue repair and the adaptive remodelling process. Firstly, Chen et al[70] conducted experiments on a murine condylar fracture model and found that Gli1-lineage cells originating from the chondro-osseous junction could differentiate into osteoblasts and chondrocytes at the fracture site. In a separate study involving a murine model of temporomandibular joint osteoarthritis (TMJOA) induced by partial discectomy, Lei et al[71] demonstrated that the abnormal mechanical loading triggered osteoclast-mediated subchondral bone resorption. This subsequently led to aberrant subchondral bone formation due to the overexpansion of Gli1$^+$ cell progeny, highlighting the significant function of Gli1$^+$ cells at the chondro-osseous junction in response to mechanical stress.[71] Meanwhile, investigations focusing on Gli1$^+$ FCSCs in a murine TMJOA model induced by anterior disc displacement surgery also revealed the activation of the chondrogenic capacity of Gli1$^+$ FCSCs.[73] Collectively, these findings underscore the indispensable role played by Gli1$^+$ stem/progenitor cells in preserving the structural and functional integrity of the condyle.

Plap-1$^+$ cells

PDL associated protein-1 (Plap-1) is an extracellular matrix protein that is highly expressed in the PDL and participates in balancing bone metabolism.[74,75] Iwayama et al[76] documented Plap-1 as a molecular marker that selectively labelled the lineage of periodontal fibroblasts. Through lineage tracing, Plap-1$^+$ cells were detected within the fibroblastic zone in a 3-month tracing period when the PDL turnover was completed, which indicated their identity as stem/progenitor cells involved in PDL homeostasis.[76] Moreover, they were also observed in the cementoblastic and osteoblastic zone during homeostasis maintenance and periodon-

titis repair, suggesting that this is a heterogeneous cell population.[76] As a result, a "PDL single-cell atlas" was conducted and eventually identified a distinct population of Ly6a$^+$ Plap-1 clusters situated in the apical region of the PDL that might represent PDLSCs to serve as a potential source for other PDL cells.[76]

NG2$^+$ cells

Neuron-glial antigen 2 (NG2) is a proteoglycan that is predominantly expressed in mammalian glial cells and pericytes.[77] In recent years, the heterogeneity of NG2$^+$ cells has garnered increasing interest. Lineage tracing investigations have provided compelling evidence that NG2$^+$ pericytes serve as the cellular origin for a minor population of MSCs within the odontogenic mesenchyme.[78] Throughout the development and maintenance of mouse incisors, NG2$^+$ cells primarily contribute to the vascular system, with only a sparse distribution in the pulp and odontoblast layers.[60,78,79] These observations are similarly applicable to mouse molars.[45,60] In response to incisor tooth injury, NG2$^+$ cells exhibit a rapid reaction by proliferating and differentiating into odontoblast-like cells, thereby producing reparative dentine-like tissue.[60,78,80] Nevertheless, the degree to which blood vessels and nerves contribute to the population of stem/progenitor cells remains largely unexplored.

Progenitor cells

Progenitor cells, which exhibit a more defined differentiation trajectory while retaining a degree of stemness, can be labelled with multiple lineages during short-term lineage tracing experiments as well.[14] Nevertheless, the absence of unlimited self-renewal capacity in these labelled progenitor cells results in their eventual disappearance following prolonged tracing periods, thereby differentiating them from stem cells.[14]

Axin2$^+$ cells

The canonical Wnt/β-catenin signalling is indispensable for the development of hard tissues, and Axin2 is the direct transcriptional target gene within this pathway.[81-83] Thus far, Axin2$^+$ cells have been acknowledged as important progenitor cells in the formation and regeneration of oral maxillofacial hard tissues.

Axin2$^+$ cells are widely involved in tooth formation and restoration

Axin2-LacZ reporter mice have become a valuable tool for in vivo studies of Axin2 expression patterns.[84,85] In incisors, X-gal staining showed the extensive expression of Axin2 in the dental mesenchyme, particularly in the proximal regions of incisors.[86,87] After a 1-week lineage tracing in 3 week-old mice, almost all odontoblasts were labelled as tdTomato$^+$ cells, indicating that Axin2$^+$ cells were important cell sources for odontoblasts during postnatal tooth development.[86] However, the fluorescent signals vanished upon prolonging the tracing duration to 1 month.[87] Thus, Axin2$^+$ cells in the mouse incisor mesenchyme represent a rapidly proliferating, non-self-renewing population of progenitors.

In mouse molars, Axin2 also labels odontoblasts and dental pulp cells during homeostasis.[88,89] In addition, Axin2$^+$ cells present in the PDL are essential for cementum formation because the ablation of Axin2$^+$ PDL cells leads to severe cementum hypoplasia.[42,90-92] A study by Xie et al[90] further demonstrated that Axin2$^+$ PDL cells were a shared progenitor source of both cellular and acellular cementum, which promotes a better understanding of the cell origin and formation processes of dental hard tissues.

The pathological change in dentine due to damage is the formation of tertiary dentine at the injury site, which can be further divided into reactionary dentine and reparative dentine according to the degree of damage.[93] Specifically, Axin2$^+$ odontoblasts are triggered to secrete more matrix for reactionary dentine formation following superficial dentine trauma.[88] Under severe pulp exposure, however, a substantial number of odontoblasts undergo cell death.[93] Axin2$^+$ pulp cells proliferate and differentiate into new odontoblast-like cells to form reparative dentine as a protective response to injury.[94] These observations highlight the pronounced contribution of Axin2$^+$ progenitor cells in both tooth development and reparative processes following tooth injury.

Axin2$^+$ cells are supporting actors in alveolar bone regeneration

In addition to pulp Axin2$^+$ cells, PDL-derived Axin2$^+$ cells contribute to alveolar bone regeneration in multiple models. Following tooth extraction, Yuan et al[95] found that Axin2$^+$ PDL cells proliferated, migrated to the tooth socket and subsequently differentiated into osteoblasts to generate new bone. Additionally, Wang et al[96] delineated the property of Axin2$^+$ PDL cells to

be activated in response to mechanical force in mice that underwent OTM. Despite the osteogenic potential demonstrated by Axin2$^+$ PDL cells in multiple models, Xie et al[92] pointed out that their contribution to alveolar bone regeneration was very limited, suggesting Axin2$^+$ cells might not function as the dominant driving force in this process.

Aggrecan$^+$ cells

Aggrecan (Acan) is an important proteoglycan in cartilage extracellular matrix, known for its interaction with hyaluronic acid, which endows cartilage with its elasticity and load-bearing properties.[97,98] Recent lineage tracing studies utilising Acan-CreER mice have revealed the developmental trajectory of chondrocyte progenitor cells within the condyle.

Aggrecan$^+$ cells contribute to chondrocytes in all layers of the condyle

The distribution of Acan$^+$ cells in condylar cartilage is non-uniform during homeostasis, characterised by a higher density observed in the anterior and middle regions compared to the posterior region.[99-101] Additionally, the interspaced patches of Acan$^+$ cells and Acan$^-$ cells respectively extend deeply into the cartilage and reach the hypertrophic chondrocyte layer.[101] These observations indicate the ability of Acan$^+$ cells to generate chondrocytes across different layers and suggest a regional variation in cellular composition in condylar cartilage. In line with this phenomenon, the reduction in chondrocyte count is more pronounced in the anterior and middle regions of Acan$^+$ cells ablation mice.[100,101] More importantly, despite the surviving cells subsequently initiating proliferation to restore the cell count, these newly-formed cells exhibit a clustered distribution on the surface without extending into the cell-depleted areas in the hypertrophic chondrocyte layers.[101] Further study of the mechanisms involved may enrich knowledge of the pathogenesis of osteoarthropathy.

Aggrecan$^+$ cells transdifferentiated into osteocytes

It was traditionally believed that chondrocytes underwent apoptosis prior to endochondral ossification.[102] However, by tracing Acan$^+$ cell lineage, Jing et al[103] demonstrated that chondrocytes could directly transdifferentiate into bone lineage cells in vivo, bypassing apoptosis, which greatly promoted understanding of cartilage cell transdifferentiation. Furthermore, in a study conducted on mice with unstable mandible ramus fracture, Wong et al[104] also observed the transdifferentiation of Acan$^+$ chondrocyte cells into osteoblasts contributing to the formation of fracture callus, which underscored the significance of Acan$^+$ progenitor cells in the regeneration process of condylar fractures.

Osterix$^+$ cells

Osterix (Osx), also known as specificity protein 7 (Sp7), is an osteoblast-specific transcription factor that determines the directional differentiation of osteoblasts.[105] Recent research has expanded understanding of Osx$^+$ cells beyond their involvement in osteoblast differentiation to their contribution to root morphogenesis.

Tracing Osx-Cre mice from birth until postnatal day 30, cells originating from the odontogenic mesenchyme within the dental follicle and dental papilla of incisors/molars were predominantly labelled, whereas odontogenic epithelium-derived cells, such as ameloblasts and epithelial root sheaths, remained unmarked.[106-108] Additionally, Rakian et al[109] observed the temporal emergence of the Osx$^+$ cells from M1 to M3, suggesting a strong link between Osx activity and tooth development stage.

Root morphogenesis commences with the formation of a bilayered epithelial structure known as the Hertwig epithelial root sheath (HERS).[110] Notably, some Osx$^+$ cells were observed in close proximity to the HERS of neonatal mice.[111,112] A long-term tracing experiment revealed that these Osx$^+$ cells eventually differentiated into odontoblasts and cementoblasts, contributing to root maintenance even after the completion of root development.[112]

PTHrP$^+$ cells

Parathyroid hormone-related protein (PTHrP) is a locally acting autocrine/paracrine ligand that is widely expressed in a variety of tissues, including teeth and bones.[113,114] It plays a unique biological role by binding to parathyroid hormone type 1 receptor (PTH1R).[115] Recent in-depth studies have progressively elucidated an inseparable relationship between PTHrP$^+$ cells and Osx$^+$ cells.

PTHrP$^+$ cells represent a more localised subpopulation of dental mesenchymal cells compared to Osx$^+$ cells. To be specific, PTHrP$^+$ cells are exclusively found in the dental follicle but absent from the dental papilla and pulp.[43,111,116] At postnatal day 7, when molar root formation begins, PTHrP$^+$ cells show active

proliferation in the immediate vicinity of the HERS in the dental follicle and then differentiate into PDL cells, cementoblasts and alveolar cryptal bone osteoblasts.[111,116] Even after tooth eruption, PTHrP$^+$ cells persist on the root surface, predominantly on the acellular cementum.[111,116]

Ctsk$^+$ cells

Cathepsin K (Ctsk), a member of the papain family of cysteine proteases, was initially discovered as a collagenase expressed by activated osteoclasts to degrade collagen and other matrix proteins during bone resorption.[117,118] Remarkably, Ctsk$^+$ cells exemplify the heterogeneity of osteogenesis progenitor cells.

Under physiological conditions, Ctsk-Cre extensively labelled periosteum cells in the mandible, with a fraction of Ctsk$^+$ cells present in the bone marrow and a small number in the dental pulp and odontoblasts.[119,120] Notably, Ctsk$^+$ cells in the periosteum were positive for stem cell markers and osteogenic markers.[120] The diphtheria toxin receptor-mediated ablation of Ctsk$^+$ cells resulted in decreased Ctsk$^+$ cells and delayed bone defect healing.[120] Thus, Ctsk$^+$ cells are considered to be an important population responsible for intramembranous osteogenesis in the jawbone.

The identification of Ctsk$^+$ cell subtype significantly advocates the heterogeneity within Ctsk$^+$ cells. For example, Ding et al[120] identified a specific subset of Ly6a$^+$Ctsk$^+$ cells restricted to the jawbone periosteum. These Ly6a$^+$Ctsk$^+$ periosteal cells could aggregate in the callus and differentiated into osteogenic lineages in response to jaw defects.[120] Given the reported involvement of Ly6a$^+$ cells in angiogenesis, whether Ly6a$^+$Ctsk$^+$ cells make more multifaceted contributions to the repair of hard tissue injury requires further research. Additionally, Weng et al[121] documented a subpopulation of Krt14$^+$Ctsk$^+$ osteoprogenitor cells with dual epithelial and mesenchymal properties around the mucosa–bone interface. These Krt14$^+$Ctsk$^+$ cells contributed to alveolar bone homeostasis and especially osteogenesis induced by maxillary sinus floor lifting, which highlighted the potential contribution of epithelium-derived cells to the process of bone formation.[121] Intriguingly, during the formation and maturation of new bone tissue, these Krt14$^+$Ctsk$^+$ cells underwent a transformation into Krt14$^-$Ctsk$^+$ cells, accompanied by enhanced osteogenic capacity.[121] To investigate the physiological significance of this shift in cellular identity and function, further studies are warranted regarding the unidentified regulatory mechanisms involved in this process.

Niche cells

In contrast to stem cells and progenitor cells, certain cell types within the stem cell niche lack the characteristic properties of stemness.[6] Although these cells do not engage in tissue homeostasis and repair through direct differentiation into terminally differentiated cells, they play a crucial role in supporting the survival and functionality of stem and progenitor cells via paracrine signalling and other mechanisms.[6] Consequently, these cells warrant particular consideration in the study of stem cell biology.

Runx2$^+$ cells

Runt-related transcription factor 2 (Runx2) is a bone-specific transcription factor that is essential for the differentiation commitment of MSCs to osteoblasts.[122] Surprisingly, Chen et al[123] found a subpopulation of Runx2-expressing mesenchymal cells in the proximal region of mouse incisors, located adjacent to MSCs and transit-amplifying progenitors. Under physiological conditions, these Runx2$^+$ cells maintain a quiescent state.[123] Additionally, no significant changes were observed in their distribution or quantity during the injury repair process for clipped incisors.[123] Furthermore, EdU staining also revealed their low proliferative activity.[123] Thus, Runx2$^+$ cells were identified as non-stem niche cells. Mechanistic studies further revealed that these Runx2$^+$ cells can secret insulin-like growth factor binding-protein-3 (Igfbp3) to activate insulin-like growth factor-2 (IGF-2) signalling, regulating the proliferation and differentiation of transit-amplifying cells, to maintain niche homeostasis and promote incisor growth.[123]

SM22α$^+$ cells

Smooth muscle protein 22-α (SM22α) is a 22 kDa globular protein primarily present in vascular smooth muscle, visceral smooth muscle and myofibroblasts.[124,125] Previous studies have demonstrated the important role played by SM22α$^+$ cells in vascular homeostasis and remodelling.[126] However, understanding of the behaviour of SM22α$^+$ cells in oral maxillofacial hard tissues is still in its inception. A recent study by Zhou et al[127] demonstrated the proliferation of a physiologically quiescent SM22α$^+$ cell population at the tooth extraction socket, engaging in intramembranous bone regeneration. However, these SM22α$^+$ cells did not express classical MSC markers or differentiate into osteocytes for new bone formation.[127] Instead, they were identified as niche cells indirectly supporting bone regeneration by

secreting H_2S in a Pdgfrβ-dependent manner.[127] Overall, these findings serve as a reminder to emphasise the indispensable contribution of niche cells to the regeneration of oral maxillofacial hard tissues.

Discussion

In this review, the present authors have discussed lineage tracing-identified cell populations in the oral maxillofacial region. In addition to these extensively studied cells, recent years have also witnessed other scattered reports on potential stem and progenitor cell populations associated with oral and maxillofacial hard tissue formation, such as rapidly dividing $Lgr5^+$ cells in laCL,[128] $Bmi1^+$ epithelial stem cells in incisors[129] and glia-derived PLP^+ mesenchymal stem cells.[130] These findings further contribute to the growing body of research in stem cell biology. The present authors' objective is to delineate a framework for the adult stem cell niche in the context of hard tissue homeostasis and regeneration. These findings are underpinned by advancements in lineage tracing methodologies, which continuously update comprehension of adult stem cells and guide us in the pursuit of future investigative endeavours.

The progress of lineage tracing methodology brings about new insights

Lineage tracing has become the cornerstone technique for studying cellular dynamics in vivo. In its infancy, the non-inducible Cre system was pervasive due to its straightforward operability and high efficiency in genetic recombination.[12] However, the constitutively expressing recombinases are associated with several challenges, such as unspecific postnatal labelling, spatiotemporal administration difficulty and risk of germline leakage.[131,132] To address these issues, there has been a shift towards the adoption of the inducible CreER system, which is exemplified by the tamoxifen administered genetic recombination.[13] Consequently, the extent of labelled cells through these two methodologies exhibits dominant discrepancies. As described by Ono et al,[111] 2 days after tamoxifen injection on postnatal day 3, Osx-CreER tagged Osx^+ cells were primarily distributed in the odontoblast layer of the mandibular M1, with sparse presence in the dental follicle and papilla. Conversely, Osx-Cre labelled most mesenchymal cells in the dental follicle and dental papilla by postnatal day 5.[111] This extent discrepancy amplifies as the mice grow older. Thus, the validity of findings from some non-inducible Cre designated studies in the adult stem cell niche may be questionable (Table 1).

Despite these improvements, the side effects of tamoxifen with regard to interference with bone metabolism remain concerning. As an oestrogen analogue, tamoxifen inevitably stimulates the growth of both cortical and trabecular bone in a dose-dependent manner.[133] The potential adverse impact of β-catenin depletion in $Prx1^+$ cells on osteogenesis was even reversed by higher doses of tamoxifen.[134] The impact of tamoxifen induction is also associated with changes in osteoclast activity.[134] Thus, a systematic tamoxifen injection guideline serves as a necessary basis for obtaining reliable results. Nevertheless, the lack of standardised protocols for tamoxifen administration results in varying administration regimens across different studies, further complicating the interpretation of experimental outcomes (Table 2).

On the other hand, the choice of reporter gene also matters. Initially, the LacZ gene was substantially used in murine embryonic development research, whereas its limitations, such as its technical sensitivity, non-quantitative nature and incompatibility with immunohistochemistry, restricted its broader application.[135,136] The groundbreaking discovery of fluorescent proteins opens up new possibilities for cell labelling, with tdTomato being the most extensively employed reporter protein in diverse studies.[137] However, as research evolves, the limitations of monocolour reporter systems have become apparent. Specifically, these systems are unable to distinguish the differentiation trajectories of individual progeny cells. Thus, the innovation of multicolour reporter gene systems is necessary to accurately depict the lineage origins of each progeny cell.[138] Up to now, a dual recombinases-mediated double labelling lineage tracing approach has allowed researchers to track the transition of $Krt14^+Ctsk^+$ cells into $Krt14^-Ctsk^+$ cells that exhibit a stronger capacity for osteogenic differentiation in the oral and maxillofacial region.[121] Similarly, in the study of long bones, the utilisation of Rainbow mice has facilitated the identification of distinct skeletal stem cell populations that play a critical role in postnatal bone homeostasis and regeneration.[139,140] Given their vast potential, multicolour reporter gene systems are anticipated to serve as a countermeasure to elucidate the hierarchical relationships between different cell populations.

More questions to be addressed

The utilisation of transgenic tools has facilitated the identification of cell populations residing in the adult stem cell niche in the oral maxillofacial region. Nevertheless, some subjects still require additional investigation. First,

Table 1 Genetic recombination system used in oral maxillofacial lineage tracing.

System	Driver	Application fields	References
Non-inducible	Prx1-Cre	Development, homeostasis, regeneration	26-28,31,142
	LepR-Cre	Development, homeostasis, regeneration	36,37,45
	CD90-Cre	Development, homeostasis, regeneration	41,42
	NG2-Cre	Development, homeostasis, regeneration	60,78,79
	Osx-Cre	Development	106,107,109,111,142
	Ctsk-Cre	Development, homeostasis, regeneration, inflammation	119,120
	SM22α-Cre	Regeneration	127
Inducible	Sox2-CreERT2	Development, homeostasis	20
	Prx1-CreER	Development, regeneration	29
	LepR-CreER	Development, homeostasis, mechanical remodelling	9
	Pdgfrα-CreER	Homeostasis, aging	45,46
	Gli1-CreERT2	Development, homeostasis, regeneration, OTM, implant osseointegration, TMJOA, periodontitis	10,59-65,68-73,143,144
	αSMA-CreERT2	Development, homeostasis, dentine injury	45,50-53,55
	Plap-1-CreER	Homeostasis, periodontitis	76
	NG2-CreERT	Homeostasis, regeneration	45,80
	Axin2-CreERT2	Development, homeostasis, regeneration, OTM	86-92,94-96
	Acan-CreERT2	Development, homeostasis, regeneration	99-101,103,104,145-147
	Osx-CreERT2	Development	108,111,112
	PTHrP-CreER	Development	43,116
	Ctsk-CreER	Maxillary sinus floor lifting	121

CreERT and CreERT2 are modified variants of CreER.
OTM, orthodontic tooth movement; TMJOA, temporomandibular joint osteoarthritis.

the heterogeneity of the same marker identified cell population in different niches remains unresolved. In the case of $Gli1^+$ cells, they play diverse roles in the oral maxillofacial region: as DESCs in laCL,[59] as MSCs in the incisor proximal niche,[60] and as FCSCs in the superficial zone of condylar cartilage.[71] While their differentiation trajectories are radically distinct, the elucidation of how divergent cell fate is determined remains insufficient.

Another expansive area of research involves exploring the relationship and interplay between different cell populations within a shared location. As described above, various cell populations identified by distinct markers are frequently detected within the same niche, and they exhibit similar functions in maintaining homeostasis and facilitating regeneration. For instance, Osx^+ cells and $PTHrP^+$ cells within the dental follicle and dental papilla both play crucial roles in postnatal root morphogenesis in a comparable fashion,[111,112] and both αSMA^+ cells and $Axin2^+$ cells in dental pulp are actively engaged in the formation of the tertiary dentine following dentine injury.[51,94] The question of whether they represent distinct cell populations exhibiting synergistic effects, subgroups of the same functional cell population characterised by different markers or derived cells situated at different levels of the differentiation hierarchy requires additional empirical research for clarification.

Investigating and effectively harnessing the regulatory mechanisms that govern cell activity is essential for translating basic research into practical applications, particularly when considering various identities and functions of different cell types. The challenge arises from the intricate regulatory network of overlapping signalling pathways. While a singular signal can widely influence the biological functions of multiple cell populations, the activity of a specific cell population is concurrently modulated by signals originating from diverse sources.[29,62,90] Furthermore, there has been growing recognition of the role played by neurovascular regulation within the adult stem cell niche. Notable examples include the Hh signal activated by NVB sensory nerves and the PDGF signal provided by arterial cells.[60,141] Consequently, it is imperative that further investigation be carried out into the mechanisms that govern cell behaviour within the niche, as such insights could enhance current clinical attempts substantially.

Conclusion

In summary, current lineage tracing on cell fate determination in the oral maxillofacial region has yielded significant advancements, greatly enhancing comprehension of the adult stem cell niche. However, the potential

Table 2 Tamoxifen administration regimen in the inducible genetic recombination system.

Driver	Application fields	Time of induction	Number of injections	Dosage of tamoxifen	References
Prx1-creER	Development	Postnatal day 3	10 consecutive days	40 mg/kg b.w	29
	Regeneration	7–9 weeks old	10 consecutive days	40 mg/kg b.w	29
LerR-CreER	Development	Postnatal day 5	2 consecutive days	1 mg	9
		Postnatal day 21			
	Mechanical remodelling	6 weeks old	5 consecutive days	1 mg	9
	Homeostasis	3 months old	5 consecutive days	1 mg	9
Pdgfrα-CreER	Homeostasis	5–8 weeks old[45]	1 time[46]	70 mg/kg b.w[46]	45,46
		3 months old[46]	2 consecutive days[45]	1.5 mg/10 g b.w[45]	
	Aging	14 months old[46]	1 time[46]	70 mg/kg b.w[46]	46
Gli1-CreERT2	Development	Postnatal day 0.5[70]	1 time[61,62,70,143] 2 consecutive days[64,72]	75 mg/kg b.w[62,72] 1.5 mg/10 g b.w[61,70,143] 1.5 mM/g b.w[64]	61,62,64,70,72,143
		Postnatal day 3.5[61]			
		Postnatal day 12[72]			
		postnatal day 13[64]			
		Postnatal day 16[143]			
		Postnatal day 21[62]			
	Homeostasis	4–6 weeks old[60]	1 time[59]	10 mg[59,60] 1.5 mg/10 g b.w[45]	45, 59, 60
		5–8 weeks old[45]	2 consecutive days[45]		
		8–10 weeks old[59]	3 consecutive days[60]		
	Tooth extraction	4 weeks old[65]	2 consecutive days[10,65]	10 mg[10,65]	10,65
		8 weeks old[10]			
	OTM	8 weeks old[69]	2 consecutive days[69]	10 mg[69]	68,69
		10–12 weeks old[68]	3 consecutive days[68]	100 μg/g b.w[68]	
	Implant osseointegration	6 weeks old	2 consecutive days	1.5 mg/10 g b.w	63
	TMJOA	4 weeks old[73]	2 consecutive days[73]	75 mg/kg b.w[73]	71,73
		6 weeks old[71]	3 consecutive days[71]	1.5 mg/10 g b.w[71]	
	Periodontitis	6–8 weeks old	2 consecutive days	4 mg	144
αSMA-CreERT2	Development	Postnatal day 16[55]	1 time[55]	75 μg/g b.w[50]	50,55
		3–4 weeks old[50]	2 consecutive days[50]	62.5 mg/g b.w[55]	
	Homeostasis	5–8 weeks	2 consecutive days	1.5 mg/10 g b.w	45
	Dentine injury	Postnatal day 4[51]	2 consecutive days[51]	75 μg/g b.w[51-53]	51-53
		4 weeks old[52,53]	2 at 24-h intervals[52,53]		
NG2-CreER	Homeostasis	5–8 weeks old	2 consecutive days	1.5 mg/10 g b.w	45
	Regeneration	6 weeks old	5 consecutive days	75 mg/kg b.w	80
Axin2-CreERT2	Development	Postnatal day 12[143]	1 time[89,90,92,143] 3 consecutive days[42,86,88,91]	75 mg/kg b.w[86,89,90,92]	42,86,88-92,143
		Postnatal day 14[42]		2 mg/30 g b.w[42]	
		Postnatal day 21[86,89,92]		0.15 mg/g b.w[143]	
		Postnatal day 28[90]		4 mg/25 g b.w[88,91]	
		1 month old[91]			
		Postnatal day 90[88]			
	Homeostasis	Adult[42]	3 consecutive days[42]	2 mg/30 g b.w[42]	42
	Dentine injury	6 weeks[94]	3 consecutive days[88,94]	0.1 mg/g b.w[94]	88,94
		Adult[88]		4 mg/25 g b.w[88]	
	Tooth extraction	Adult	3 consecutive days	4 mg/25 g b.w	95
	OTM	Postnatal day 28	1 time	75 mg/kg b.w	96
Acan-CreERT2	Development	Postnatal day 3[145,147]	1 time[103,145-147] 3 consecutive days[101]	1.5 mg/10 g b.w[101,103]	101,103,145-147
		Postnatal day 7[101]		1 mg/13 g b.w[146]	
		Postnatal day 14[103,146]		75 mg/kg b.w[147]	
	Homeostasis	5 weeks old[99]	3 consecutive days[100]	1 mg/10 g b.w[99]	99,100
		9 weeks old[100]	5 consecutive days[99]	150 mg/kg b.w[100]	
	Regeneration	10–16 weeks old	5 consecutive days	75 mg/kg b.w	104

CreERT2 is a modified variant of CreER with three points mutations.
b.w, body weight; OTM, orthodontic tooth movement; TMJOA, temporomandibular joint osteoarthritis.

systematic errors in the current experiments need to be ruled out by rigorous experimental design. Further questions about the hierarchical relationship and the interaction between different cell populations have not been answered precisely due to the limitations of the tools. It is anticipated that improvements in technology and methodology will further reveal the enigmatic nature of cell populations in the formation of oral maxillofacial hard tissues, thus making a significant contribution to the rapid development of regenerative medicine.

Conflicts of interest

The authors declare no conflicts of interest related to this study.

Author contribution

Dr Shuang YANG contributed literature collection and manuscript draft; Drs Chang Hao YU, Fei Fei LI, Yu SHI, Hui WANG, Wei Dong TIAN, Quan YUAN and Ling YE contributed to the manuscript revision; Dr Fan Yuan YU contributed to the conception, supervision and revision.

(Received Sep 15, 2024; accepted Mar 10, 2025)

References

1. Benzian H, Watt R, Makino Y, Stauf N, Varenne B. WHO calls to end the global crisis of oral health. Lancet 2022;400: 1909–1910.
2. Liu J, Zhang SS, Zheng SG, Xu T, Si Y. Oral health status and oral health care model in China. Chin J Dent Res 2016;19: 207–215.
3. Jazayeri HE, Tahriri M, Razavi M, et al. A current overview of materials and strategies for potential use in maxillofacial tissue regeneration. Mater Sci Eng C Mater Biol Appl 2017;70: 913–929.
4. Liu J, Ruan J, Weir MD, et al. Periodontal bone-ligament-cementum regeneration via scaffolds and stem cells. Cells 2019; 8:537.
5. Mannino G, Russo C, Maugeri G, et al. Adult stem cell niches for tissue homeostasis. J Cell Physiol 2022;237:239–257.
6. Rezza A, Sennett R, Rendl M. Adult stem cell niches: Cellular and molecular components. Curr Top Dev Biol 2014;107: 333–372.
7. Scadden DT. Nice neighborhood: Emerging concepts of the stem cell niche. Cell 2014;157:41–50.
8. Matarese G, La Cava A, Horvath TL. In vivo veritas, in vitro artificia. Trends Mol Med 2012;18:439–442.
9. Zhang D, Lin W, Jiang S, et al. Lepr-expressing PDLSCs contribute to periodontal homeostasis and respond to mechanical force by Piezo1. Adv Sci (Weinh) 2023;10:e2303291.
10. Shalehin N, Seki Y, Takebe H, et al. Gli1^{+}-PDL cells contribute to alveolar bone homeostasis and regeneration. J Dent Res 2022; 101:1537–1543.
11. Yao M, Ren T, Pan Y, et al. A new generation of lineage tracing dynamically records cell fate choices. Int J Mol Sci 2022; 23:5021.
12. Couasnay G, Madel MB, Lim J, Lee B, Elefteriou F. Sites of Cre-recombinase activity in mouse lines targeting skeletal cells. J Bone Miner Res 2021;36:1661–1679.
13. Kretzschmar K, Watt FM. Lineage tracing. Cell 2012;148: 33–45.
14. Grompe M. Tissue stem cells: New tools and functional diversity. Cell Stem Cell 2012;10:685–689.
15. Lefebvre V, Dumitriu B, Penzo-Méndez A, Han Y, Pallavi B. Control of cell fate and differentiation by Sry-related high-mobility-group box (Sox) transcription factors. Int J Biochem Cell Biol 2007;39:2195–2214.
16. Arnold K, Sarkar A, Yram MA, et al. Sox2(+) adult stem and progenitor cells are important for tissue regeneration and survival of mice. Cell Stem Cell 2011;9:317–329.
17. Ohmoto M, Nakamura S, Wang H, Jiang P, Hirota J, Matsumoto I. Maintenance and turnover of Sox2+ adult stem cells in the gustatory epithelium. PLoS One 2022;17:e0267683.
18. Harada H, Kettunen P, Jung HS, Mustonen T, Wang YA, Thesleff I. Localization of putative stem cells in dental epithelium and their association with Notch and FGF signaling. J Cell Biol 1999;147:105–120.
19. Lin Y, Cheng YS, Qin C, Lin C, D'Souza R, Wang F. FGFR2 in the dental epithelium is essential for development and maintenance of the maxillary cervical loop, a stem cell niche in mouse incisors. Dev Dyn 2009;238:324–330.
20. Juuri E, Saito K, Ahtiainen L, et al. Sox2+ stem cells contribute to all epithelial lineages of the tooth via Sfrp5+ progenitors. Dev Cell 2012;23:317–328.
21. Li J, Feng J, Liu Y, et al. BMP-SHH signaling network controls epithelial stem cell fate via regulation of its niche in the developing tooth. Dev Cell 2015;33:125–135.
22. Huang Z, Su X, Julaiti M, Chen X, Luan Q. The role of PRX1-expressing cells in periodontal regeneration and wound healing. Front Physiol 2023;14:978640.
23. Fan Y, Hanai JI, Le PT, et al. Parathyroid hormone directs bone marrow mesenchymal cell fate. Cell Metab 2017;25: 661–672.
24. Wilk K, Yeh SA, Mortensen LJ, et al. Postnatal calvarial skeletal stem cells expressing PRX1 reside exclusively in the calvarial sutures and are required for bone regeneration. Stem Cell Reports 2017;8:933–946.
25. Jernvall J, Thesleff I. Tooth shape formation and tooth renewal: Evolving with the same signals. Development 2012;139: 3487–3497.
26. Gong X, Zhang H, Xu X, et al. Tracing PRX1+ cells during molar formation and periodontal ligament reconstruction. Int J Oral Sci 2022;14:5.
27. Cui C, Bi R, Liu W, et al. Role of PTH1R signaling in Prx1+ mesenchymal progenitors during eruption. J Dent Res 2020;99:1296–1305.
28. Wang H, Lv C, Gu Y, et al. Overexpressed Sirt1 in MSCs promotes dentin formation in Bmi1-deficient mice. J Dent Res 2018;97:1365–1373.
29. Bassir SH, Garakani S, Wilk K, et al. Prx1 expressing cells are required for periodontal regeneration of the mouse incisor. Front Physiol 2019;10:591.
30. Feng X, Wang H, Weng Y, Chen Y, Huang J, Wang Z. Paired-related homeobox 1-positive cells are needed for osseointegration. Int J Oral Maxillofac Implants 2024;39:893–903.
31. Zhao W, Cao Y, Chen Y, et al. NLRP3 regulates mandibular healing through interaction with UCHL5 in MSCs. Int J Biol Sci 2023;19:936–949.

32. Zhou BO, Yue R, Murphy MM, Peyer JG, Morrison SJ. Leptin-receptor-expressing mesenchymal stromal cells represent the main source of bone formed by adult bone marrow. Cell Stem Cell 2014;15:154–168.
33. Shu HS, Liu YL, Tang XT, et al. Tracing the skeletal progenitor transition during postnatal bone formation. Cell Stem Cell 2021;28:2122–2136.e3.
34. Jeffery EC, Mann TLA, Pool JA, Zhao Z, Morrison SJ. Bone marrow and periosteal skeletal stem/progenitor cells make distinct contributions to bone maintenance and repair. Cell Stem Cell 2022;29:1547–1561.e6.
35. Kara N, Xue Y, Zhao Z, et al. Endothelial and Leptin Receptor+ cells promote the maintenance of stem cells and hematopoiesis in early postnatal murine bone marrow. Dev Cell 2023;58:348–360.e6.
36. Oka H, Ito S, Kawakami M, et al. Subset of the periodontal ligament expressed leptin receptor contributes to part of hard tissue-forming cells. Sci Rep 2023;13:3442.
37. Zhang D, Zhang S, Wang J, et al. LepR-expressing stem cells are essential for alveolar bone regeneration. J Dent Res 2020;99:1279–1286.
38. Chen Y, Weng Y, Huang J, et al. Leptin receptor (+) stromal cells respond to periodontitis and attenuate alveolar bone repair via CCRL2-mediated Wnt inhibition. J Bone Miner Res 2024;39:611–626.
39. Seo BM, Miura M, Gronthos S, et al. Investigation of multipotent postnatal stem cells from human periodontal ligament. Lancet 2004;364:149–155.
40. Saalbach A, Anderegg U. Thy-1: More than a marker for mesenchymal stromal cells. FASEB J 2019;33:6689–6696.
41. An Z, Sabalic M, Bloomquist RF, Fowler TE, Streelman T, Sharpe PT. A quiescent cell population replenishes mesenchymal stem cells to drive accelerated growth in mouse incisors. Nat Commun 2018;9:378.
42. Zhao J, Faure L, Adameyko I, Sharpe PT. Stem cell contributions to cementoblast differentiation in healthy periodontal ligament and periodontitis. Stem Cells 2021;39:92–102.
43. Nagata M, Chu AKY, Ono N, Welch JD, Ono W. Single-cell transcriptomic analysis reveals developmental relationships and specific markers of mouse periodontium cellular subsets. Front Dent Med 2021;2:679937.
44. Kunisaki Y. Pericytes in bone marrow. Adv Exp Med Biol 2019;1122:101–114.
45. Men Y, Wang Y, Yi Y, et al. Gli1+ periodontium stem cells are regulated by osteocytes and occlusal force. Dev Cell 2020;54:639–654.e6.
46. Yao L, Li F, Yu C, et al. Chronological and replicative aging of CD51+/PDGFR-α+ pulp stromal cells. J Dent Res 2023;102:929–937.
47. Viswanathan S, Shi Y, Galipeau J, et al. Mesenchymal stem versus stromal cells: International Society for Cell & Gene Therapy (ISCT®) Mesenchymal Stromal Cell committee position statement on nomenclature. Cytotherapy 2019;21:1019–1024.
48. Shinde AV, Humeres C, Frangogiannis NG. The role of α-smooth muscle actin in fibroblast-mediated matrix contraction and remodeling. Biochim Biophys Acta Mol Basis Dis 2017;1863:298–309.
49. Sá da Bandeira D, Casamitjana J, Crisan M. Pericytes, integral components of adult hematopoietic stem cell niches. Pharmacol Ther 2017;171:104–113.
50. Roguljic H, Matthews BG, Yang W, Cvija H, Mina M, Kalajzic I. In vivo identification of periodontal progenitor cells. J Dent Res 2013;92:709–715.
51. Vidovic I, Banerjee A, Fatahi R, et al. αSMA-expressing perivascular cells represent dental pulp progenitors in vivo. J Dent Res 2017;96:323–330.
52. Vidovic-Zdrilic I, Vijaykumar A, Mina M. Activation of αSMA expressing perivascular cells during reactionary dentinogenesis. Int Endod J 2019;52:68–76.
53. Vidovic-Zdrilic I, Vining KH, Vijaykumar A, Kalajzic I, Mooney DJ, Mina M. FGF2 enhances odontoblast differentiation by αSMA+ progenitors in vivo. J Dent Res 2018;97:1170–1177.
54. Kuroda S, Tanimoto K, Izawa T, Fujihara S, Koolstra JH, Tanaka E. Biomechanical and biochemical characteristics of the mandibular condylar cartilage. Osteoarthritis Cartilage 2009;17:1408–1415.
55. Embree MC, Chen M, Pylawka S, et al. Exploiting endogenous fibrocartilage stem cells to regenerate cartilage and repair joint injury. Nat Commun 2016;7:13073.
56. Petrova R, Joyner AL. Roles for Hedgehog signaling in adult organ homeostasis and repair. Development 2014;141:3445–3457.
57. Hosoya A, Shalehin N, Takebe H, Shimo T, Irie K. Sonic hedgehog signaling and tooth development. Int J Mol Sci 2020;21:1587.
58. Yu T, Klein OD. Molecular and cellular mechanisms of tooth development, homeostasis and repair. Development 2020;147:dev184754.
59. Seidel K, Ahn CP, Lyons D, et al. Hedgehog signaling regulates the generation of ameloblast progenitors in the continuously growing mouse incisor. Development 2010;137:3753–3761.
60. Zhao H, Feng J, Seidel K, et al. Secretion of shh by a neurovascular bundle niche supports mesenchymal stem cell homeostasis in the adult mouse incisor. Cell Stem Cell 2014;14:160–173 [erratum 2018;23:147].
61. Wen Q, Jing J, Han X, et al. Runx2 regulates mouse tooth root development via activation of WNT inhibitor NOTUM. J Bone Miner Res 2020;35:2252–2264.
62. Xie X, Xu C, Zhao H, Wang J, Feng JQ. A biphasic feature of Gli1+-mesenchymal progenitors during cementogenesis that is positively controlled by Wnt/β-catenin signaling. J Dent Res 2021;100:1289–1298.
63. Yi Y, Stenberg W, Luo W, Feng JQ, Zhao H. Alveolar bone marrow Gli1+ stem cells support implant osseointegration. J Dent Res 2022;101:73–82.
64. Zhang N, Barrell WB, Liu KJ. Identification of distinct subpopulations of Gli1-lineage cells in the mouse mandible. J Anat 2023;243:90–99.
65. Fujii S, Takebe H, Mizoguchi T, Nakamura H, Shimo T, Hosoya A. Bone formation ability of Gli1+ cells in the periodontal ligament after tooth extraction. Bone 2023;173:116786.
66. Jin SS, He DQ, Wang Y, et al. Mechanical force modulates periodontal ligament stem cell characteristics during bone remodelling via TRPV4. Cell Prolif 2020;53:e12912.
67. Huang H, Yang R, Zhou YH. Mechanobiology of periodontal ligament stem cells in orthodontic tooth movement. Stem Cells Int 2018;2018:6531216.
68. Liu AQ, Zhang LS, Chen J, et al. Mechanosensing by Gli1+ cells contributes to the orthodontic force-induced bone remodelling. Cell Prolif 2020;53:e12810.
69. Seki Y, Takebe H, Mizoguchi T, et al. Differentiation ability of Gli1+ cells during orthodontic tooth movement. Bone 2023;166:116609.
70. Chen S, Lan L, Lei J, He Y, Zhang Y. Gli1+ Osteogenic progenitors contribute to condylar development and fracture repair. Front Cell Dev Biol 2022;10:819689.

71. Lei J, Chen S, Jing J, et al. Inhibiting Hh signaling in Gli1+ osteogenic progenitors alleviates TMJOA. J Dent Res 2022;101: 664–674.
72. Bi R, Luo X, Li Q, et al. Igf1 regulates fibrocartilage stem cells, cartilage growth, and homeostasis in the temporomandibular joint of mice. J Bone Miner Res 2023;38:556–567.
73. Bi R, Li Q, Li H, et al. Divergent chondro/osteogenic transduction laws of fibrocartilage stem cell drive temporomandibular joint osteoarthritis in growing mice. Int J Oral Sci 2023;15:36.
74. Kinoshita M, Yamada S, Sasaki J, et al. Mice lacking PLAP-1/Asporin show alteration of periodontal ligament structures and acceleration of bone loss in periodontitis. Int J Mol Sci 2023;24:15989.
75. Liu S, Yan X, Guo J, et al. Periodontal ligament-associated protein-1 knockout mice regulate the differentiation of osteoclasts and osteoblasts through TGF-β1/Smad signaling pathway. J Cell Physiol 2024;239:e31062.
76. Iwayama T, Iwashita M, Miyashita K, et al. Plap-1 lineage tracing and single-cell transcriptomics reveal cellular dynamics in the periodontal ligament. Development 2022; 149:dev201203.
77. Ampofo E, Schmitt BM, Menger MD, Laschke MW. The regulatory mechanisms of NG2/CSPG4 expression. Cell Mol Biol Lett 2017;22:4.
78. Feng J, Mantesso A, De Bari C, Nishiyama A, Sharpe PT. Dual origin of mesenchymal stem cells contributing to organ growth and repair. Proc Natl Acad Sci U S A 2011;108: 6503–6508.
79. Pang YW, Feng J, Daltoe F, et al. Perivascular stem cells at the tip of mouse incisors regulate tissue regeneration. J Bone Miner Res 2016;31:514–523.
80. Fu Y, Ju Y, Zhao S. Ca(v)1.2 regulated odontogenic differentiation of NG2+ pericytes during pulp injury. Odontology 2023; 111:57–67.
81. Järvinen E, Shimomura-Kuroki J, Balic A, Jussila M, Thesleff I. Mesenchymal Wnt/β-catenin signaling limits tooth number. Development 2018;145:dev158048.
82. Lim WH, Liu B, Mah SJ, Yin X, Helms JA. Alveolar bone turnover and periodontal ligament width are controlled by Wnt. J Periodontol 2015;86:319–326.
83. Moshkovsky AR, Kirschner MW. The nonredundant nature of the Axin2 regulatory network in the canonical Wnt signaling pathway. Proc Natl Acad Sci U S A 2022;119:e2108408119.
84. Minear S, Leucht P, Jiang J, et al. Wnt proteins promote bone regeneration. Sci Transl Med 2010;2:29ra30.
85. Menon S, Salhotra A, Shailendra S, et al. Skeletal stem and progenitor cells maintain cranial suture patency and prevent craniosynostosis. Nat Commun 2021;12:4640.
86. Shi P, Xie X, Xu C, Wu Y, Wang J. Activation of Wnt signaling in Axin2(+) cells leads to osteodentin formation and cementum overgrowth. Oral Dis 2023;29:3551–3558.
87. An Z, Akily B, Sabalic M, Zong G, Chai Y, Sharpe PT. Regulation of mesenchymal stem to transit-amplifying cell transition in the continuously growing mouse incisor. Cell Rep 2018;23:3102–3111.
88. Zhao Y, Yuan X, Liu B, Tulu US, Helms JA. Wnt-responsive odontoblasts secrete new dentin after superficial tooth injury. J Dent Res 2018;97:1047–1054.
89. Xu C, Xie X, Shi P, Wu Y, Wang J. Axin2-CreERT2 mediated knockout of bone morphogenetic protein receptor type 1A caused abnormal secondary dentine and altered cell fate of Axin2-expressing odontogenic cells. Int Endod J 2023;56: 1000–1010.
90. Xie X, Wang J, Wang K, et al. Axin2+-mesenchymal PDL cells, instead of K14(+) epithelial cells, play a key role in rapid cementum growth. J Dent Res 2019;98:1262–1270.
91. Turkkahraman H, Yuan X, Salmon B, Chen CH, Brunski JB, Helms JA. Root resorption and ensuing cementum repair by Wnt/β-catenin dependent mechanism. Am J Orthod Dentofacial Orthop 2020;158:16–27.
92. Xie X, Xu C, Zhao L, Wu Y, Feng JQ, Wang J. Axin2-expressing cells in the periodontal ligament are regulated by bone morphogenetic protein signalling and play a pivotal role in periodontium development. J Clin Periodontol 2022;49:945–956.
93. Galler KM, Weber M, Korkmaz Y, Widbiller M, Feuerer M. Inflammatory response mechanisms of the dentine-pulp complex and the periapical tissues. Int J Mol Sci 2021;22:1480.
94. Babb R, Chandrasekaran D, Carvalho Moreno Neves V, Sharpe PT. Axin2-expressing cells differentiate into reparative odontoblasts via autocrine Wnt/β-catenin signaling in response to tooth damage. Sci Rep 2017;7:3102.
95. Yuan X, Pei X, Zhao Y, Tulu US, Liu B, Helms JA. A Wnt-responsive PDL population effectuates extraction socket healing. J Dent Res 2018;97:803–809.
96. Wang K, Xu C, Xie X, et al. Axin2+ PDL cells directly contribute to new alveolar bone formation in response to orthodontic tension force. J Dent Res 2022;101:695–703.
97. Alcaide-Ruggiero L, Cugat R, Domínguez JM. Proteoglycans in articular cartilage and their contribution to chondral injury and repair mechanisms. Int J Mol Sci 2023;24:10824.
98. Krawetz RJ, Wu YE, Bertram KL, et al. Synovial mesenchymal progenitor derived aggrecan regulates cartilage homeostasis and endogenous repair capacity. Cell Death Dis 2022;13:470.
99. Liao L, Zhang S, Zhou GQ, et al. Deletion of Runx2 in condylar chondrocytes disrupts TMJ tissue homeostasis. J Cell Physiol 2019;234:3436–3444.
100. He Y, Zhang M, Huang AY, Cui Y, Bai D, Warman ML. Confocal imaging of mouse mandibular condyle cartilage. Sci Rep 2017;7:43848.
101. He Y, Zhang M, Song J, Warman ML. Cell depleted areas do not repopulate after diphtheria toxin-induced killing of mandibular cartilage chondrocytes. Osteoarthritis Cartilage 2021;29:1474–1484.
102. Gibson G. Active role of chondrocyte apoptosis in endochondral ossification. Microsc Res Tech 1998;43:191–204.
103. Jing Y, Zhou X, Han X, et al. Chondrocytes directly transform into bone cells in mandibular condyle growth. J Dent Res 2015;94:1668–1675.
104. Wong SA, Hu DP, Slocum J, et al. Chondrocyte-to-osteoblast transformation in mandibular fracture repair. J Orthop Res 2021;39:1622–1632.
105. Liu Q, Li M, Wang S, Xiao Z, Xiong Y, Wang G. Recent advances of Osterix transcription factor in osteoblast differentiation and bone formation. Front Cell Dev Biol 2020;8:601224.
106. Wang Y, Cox MK, Coricor G, MacDougall M, Serra R. Inactivation of Tgfbr2 in Osterix-Cre expressing dental mesenchyme disrupts molar root formation. Dev Biol 2013;382:27–37.
107. Guo J, Yu S, Zhang H, et al. Klf4 haploinsufficiency in Sp7+ lineage leads to underdeveloped mandibles and insufficient elongation of mandibular incisor. Biochim Biophys Acta Mol Basis Dis 2023;1869:166636.
108. Liang J, Wang J, Ye C, et al. Ptip is essential for tooth development via regulating Wnt pathway. Oral Dis 2024;30:1451–1461.
109. Rakian A, Yang WC, Gluhak-Heinrich J, et al. Bone morphogenetic protein-2 gene controls tooth root development in coordination with formation of the periodontium. Int J Oral Sci 2013;5:75–84.
110. Wang J, Feng JQ. Signaling pathways critical for tooth root formation. J Dent Res 2017;96:1221–1228.

111. Ono W, Sakagami N, Nishimori S, Ono N, Kronenberg HM. Parathyroid hormone receptor signalling in osterix-expressing mesenchymal progenitors is essential for tooth root formation. Nat Commun 2016;7:11277.
112. Takahashi A, Ono N, Ono W. The fate of Osterix-expressing mesenchymal cells in dental root formation and maintenance. Orthod Craniofac Res 2017;20(suppl 1):39–43.
113. Zhang J, Liao L, Li Y, et al. Parathyroid hormone-related peptide (1-34) promotes tooth eruption and inhibits osteogenesis of dental follicle cells during tooth development. J Cell Physiol 2019;234:11900–11911.
114. Tsutsumi-Arai C, Arai Y, Tran A, et al. A PTHrP gradient drives mandibular condylar chondrogenesis via Runx2. J Dent Res 2024;103:91–100.
115. Martin TJ, Sims NA, Seeman E. Physiological and pharmacological roles of PTH and PTHrP in bone using their shared receptor, PTH1R. Endocr Rev 2021;42:383–406.
116. Takahashi A, Nagata M, Gupta A, et al. Autocrine regulation of mesenchymal progenitor cell fates orchestrates tooth eruption. Proc Natl Acad Sci USA 2019;116:575–580.
117. Drake FH, Dodds RA, James IE, et al. Cathepsin K, but not cathepsins B, L, or S, is abundantly expressed in human osteoclasts. J Biol Chem 1996;271:12511–12516.
118. Costa AG, Cusano NE, Silva BC, Cremers S, Bilezikian JP. Cathepsin K: Its skeletal actions and role as a therapeutic target in osteoporosis. Nat Rev Rheumatol 2011;7:447–456.
119. Yu F, Huo F, Li F, Zuo Y, Wang C, Ye L. Aberrant NF-κB activation in odontoblasts orchestrates inflammatory matrix degradation and mineral resorption. Int J Oral Sci 2022;14:6.
120. Ding Y, Mo C, Geng J, Li J, Sun Y. Identification of periosteal osteogenic progenitors in jawbone. J Dent Res 2022;101:1101–1109.
121. Weng Y, Wang H, Wu D, et al. A novel lineage of osteoprogenitor cells with dual epithelial and mesenchymal properties govern maxillofacial bone homeostasis and regeneration after MSFL. Cell Res 2022;32:814–830.
122. Komori T. Regulation of proliferation, differentiation and functions of osteoblasts by Runx2. Int J Mol Sci 2019;20:1694.
123. Chen S, Jing J, Yuan Y, et al. Runx2+ niche cells maintain incisor mesenchymal tissue homeostasis through IGF signaling. Cell Rep 2020;32:108007.
124. Hoggatt AM, Simon GM, Herring BP. Cell-specific regulatory modules control expression of genes in vascular and visceral smooth muscle tissues. Circ Res 2002;91:1151–1159.
125. Yue Z, Jiang Z, Ruan B, et al. Disruption of myofibroblastic Notch signaling attenuates liver fibrosis by modulating fibrosis progression and regression. Int J Biol Sci 2021;17:2135–2146.
126. Zhang X, Yan X, Cao J, et al. SM22α+ vascular mural cells are essential for vessel stability in tumors and undergo phenotype transition regulated by Notch signaling. J Exp Clin Cancer Res 2020;39:124.
127. Zhou X, Liu J, Zheng Y, et al. SM22α-lineage niche cells regulate intramembranous bone regeneration via PDGFRβ-triggered hydrogen sulfide production. Cell Rep 2022;39:110750.
128. Chang JY, Wang C, Jin C, et al. Self-renewal and multilineage differentiation of mouse dental epithelial stem cells. Stem Cell Res 2013;11:990–1002.
129. Biehs B, Hu JK, Strauli NB, et al. BMI1 represses Ink4a/Arf and Hox genes to regulate stem cells in the rodent incisor. Nat Cell Biol 2013;15:846–852.
130. Kaukua N, Shahidi MK, Konstantinidou C, et al. Glial origin of mesenchymal stem cells in a tooth model system. Nature 2014;513:551–554.
131. Nagao M, Cheong CW, Olsen BR. Col2-Cre and tamoxifen-inducible Col2-CreER target different cell populations in the knee joint. Osteoarthritis Cartilage 2016;24:188–191.
132. Luo L, Ambrozkiewicz MC, Benseler F, et al. Optimizing nervous system-specific gene targeting with Cre driver lines: Prevalence of germline recombination and influencing factors. Neuron 2020;106:37–65.e35.
133. Zhong ZA, Sun W, Chen H, et al. Optimizing tamoxifen-inducible Cre/loxp system to reduce tamoxifen effect on bone turnover in long bones of young mice. Bone 2015;81:614–619.
134. Xie Z, McGrath C, Sankaran J, et al. Low-dose tamoxifen induces significant bone formation in mice. JBMR Plus 2021;5:e10450.
135. Soriano P. Generalized lacZ expression with the ROSA26 Cre reporter strain. Nat Genet 1999;21:70–71.
136. Shimada A, Komatsu K, Nakashima K, Pöschl E, Nifuji A. Improved methods for detection of β-galactosidase (lacZ) activity in hard tissue. Histochem Cell Biol 2012;137:841–847.
137. Li S, Chen LX, Peng XH, et al. Overview of the reporter genes and reporter mouse models. Animal Model Exp Med 2018;1:29–35.
138. Dumas L, Clavreul S, Michon F, Loulier K. Multicolor strategies for investigating clonal expansion and tissue plasticity. Cell Mol Life Sci 2022;79:141.
139. Chan CK, Seo EY, Chen JY, et al. Identification and specification of the mouse skeletal stem cell. Cell 2015;160:285–298.
140. Ambrosi TH, Sinha R, Steininger HM, et al. Distinct skeletal stem cell types orchestrate long bone skeletogenesis. Elife 2021;10:e66063.
141. Guo T, Pei F, Zhang M, et al. Vascular architecture regulates mesenchymal stromal cell heterogeneity via P53-PDGF signaling in the mouse incisor. Cell Stem Cell 2024;31:904–920.e6.
142. Xu X, Gong X, Zhang L, Zhang H, Sun Y. PRX1-positive mesenchymal stem cells drive molar morphogenesis. Int J Oral Sci 2024;16:15.
143. Lav R, Krivanek J, Anthwal N, Tucker AS. Wnt signaling from Gli1-expressing apical stem/progenitor cells is essential for the coordination of tooth root development. Stem Cell Reports 2023;18:1015–1029.
144. Deng Y, Li Q, Svoboda KKH, Opperman LA, Ruest LB, Liu X. Gli1+ periodontal mesenchymal stem cells in periodontitis. J Dent Res 2024;103:279–288.
145. Jing Y, Jing J, Wang K, et al. Vital roles of β-catenin in transdifferentiation of chondrocytes to bone cells. Int J Biol Sci 2018;14:1–9.
146. Kurio N, Saunders C, Bechtold TE, et al. Roles of Ihh signaling in chondroprogenitor function in postnatal condylar cartilage. Matrix Biol 2018;67:15–31.
147. Li H, Jing Y, Zhang R, et al. Hypophosphatemic rickets accelerate chondrogenesis and cell trans-differentiation from TMJ chondrocytes into bone cells via a sharp increase in β-catenin. Bone 2020;131:115151.

Periodontitis Exacerbates Cognitive Impairment via Endothelial Inflammation: Insights from Single-Nucleus Transcriptomics

Zong Shan SHEN[1,#], Ji Chen YANG[1,#], Chuan Jiang ZHAO[1], Bin CHENG[1]

Objective: *To explore the underlying mechanisms of the association between periodontitis and cognitive impairment.*

Methods: *Single-nucleus transcriptomics of mice were used to investigate the impact of periodontitis on brain and hippocampal cells to gain insights into disease progression. After data processing, functional enrichment, pathway analysis and cell-cell communication analysis were used to identify the distinct pathways and genes upregulated in Alzheimer's disease (AD) linked to periodontitis. After cell culture, real-time quantitative polymerase chain reaction (RT-qPCR) and enzyme-linked immunosorbent assay (ELISA) were used to confirm the results.*

Results: *The present authors identified endothelial inflammation as a key factor in periodontitis-related AD. The findings revealed that the upregulation of Mgll expression in endothelial cells was linked to increased antigen presentation and exacerbated neuroinflammation, potentially worsening AD. Moreover, the present authors elucidated MGLL-2AG-CB2 signalling, through which MGLL activation suppresses CB2 expression and leads to heightened inflammation, while MGLL inhibition restores CB2 levels and mitigates inflammation.*

Conclusion: *The present study revealed the role of MGLL in linking periodontitis to hippocampal endothelial inflammation and antigen presentation in cognitive impairment. This research will enhance the understanding of how periodontitis impacts cognition and explore potential therapeutic strategies to alleviate periodontitis-associated cognitive impairment.*

Keywords: *cognitive impairment, endothelial inflammation, MGLL, periodontitis, single-nucleus transcriptomics*

Chin J Dent Res 2025;28(2):105–114; doi: 10.3290/j.cjdr.b6260577

Periodontitis is an inflammatory disease caused by plaque microbiota and results in the degradation of tooth-supporting tissues, which in turn leads to tooth mobility and loss. It has also been reported to be closely associated with cognitive disorders such as Alzheimer's disease (AD) through pathogenic microorganisms and inflammation in both mice and humans.[1,2] Cognitive disorders mainly occur in individuals who are aged over 60 years, with an incidence rate of up to 10%.[3] As the population ages worldwide, the prevalence of these diseases is expected to increase. Currently, effective treatment strategies for both periodontitis and cognitive disorders are lacking. Thus, investigating the mechanisms through which periodontitis influences the development of cognitive disorders and identifying preventive measures could mitigate the risk they pose.

Recent studies have revealed a strong correlation between periodontitis and AD. Individuals with higher levels of periodontitis exhibit faster hippocampal atrophy and cognitive deterioration.[4] Periodontitis can facilitate the infiltration of pathogenic bacteria, virulence factors and inflammatory mediators into the

1 Hospital of Stomatology, Guangdong Provincial Key Laboratory of Stomatology, Guanghua School of Stomatology, Sun Yat-sen University, Guangzhou, P.R. China

# These two authors contributed equally to this work.

Corresponding author: Dr Bin CHENG, Hospital of Stomatology, Guangdong Provincial Key Laboratory of Stomatology, Guanghua School of Stomatology, Sun Yat-Sen University, No. 56, Lingyuan West Road, Guangzhou 510055, P.R. China. Tel: 86-20-83863002. Email: chengbin@mail.sysu.edu.cn

This work was supported by the National Natural Science Foundation of China (grant no. 82201011) and Young Elite Scientist Sponsorship Program by CAST (grant no. 2024QNRC001).

brain via the blood-brain barrier (BBB).[5-7] These substances then change the brain microenvironment, triggering neuroinflammation and neurodegeneration, ultimately leading to cognitive decline. The present authors' previous research showed that periodontitis impairs macrophage function and promotes reactions of hippocampal cells to virulence factors and bacteria, inducing astrocyte abnormalities and neuroinflammation.[8] Nevertheless, the precise mechanisms by which factors damage the BBB and change the microenvironment in the hippocampus require further research.

The brain microvasculature has been proven to be a key player in the development of AD. Previous studies have shown vascular disruption in early AD development.[9,10] Endothelial cells (ECs) are crucial for cleaning beta-amyloid (Aβ) and other harmful substances from the central nervous system, whereas inflammation in them reduces Aβ clearance.[11] Furthermore, ECs can secrete cytokines and directly activate dysfunction of surrounding neurons, astrocytes and microglia, leading to neuroinflammation and cognitive impairment.[12-14] However, the precise mechanisms underlying damage to the brain endothelium from initial contact with periodontitis pathogens and toxins remain unclear.

Single-nucleus transcriptomics enables the examination of cellular changes, shedding light on the mechanisms by which periodontitis impacts cognitive function. In the present study, the authors generated single-nucleus maps of the brain and hippocampus, delineating key cell populations in these regions, and revealed that periodontitis upregulates genes in hippocampal ECs linked to AD and suppresses neurogenesis. Specifically, periodontitis induces the upregulation of monoacylglycerol lipase (MGLL) expression in ECs, leading to neuroinflammation. The authors demonstrated that increasing antigen presentation through MGLL-related pathways in ECs while inhibiting MGLL expression improved periodontitis-induced endothelial dysfunction. This research not only elucidates the pathogenesis of cognitive dysfunction associated with periodontitis but also lays the groundwork for targeted therapeutic interventions for cognitive impairment.

Materials and methods

Data acquisition

The methods used were described in a previous study by the present authors.[8] In brief, male C57BL/6 mice for sequencing were purchased from the National Resource Center of Model Mice (Nanjing, China) and housed in a specific pathogen-free facility at the Laboratory Animal Center of Sun Yat-sen University. The 12-month-old mice were separated into two groups (n = 6 in each group): the healthy group (Heal), which acted as a control, and the periodontitis group (PD). Ligature-induced periodontitis models were generated in PD group mice. After 6 weeks, they were euthanised by CO_2 inhalation for brain and hippocampus collection. All experiments were approved by the Animal Care and Use Committee of Sun Yat-sen University (SYSU-IACUC-2018-109 000135).

Single-nucleus RNA sequencing (snRNA-seq) was performed by the DNBelab C Series High-Throughput Single-Cell System from MGI (Shenzhen, China) and pre-processed by STAR (v2.5.3). The data were uploaded to the National Genomics Data Center (NGDC).

Data processing

The present authors used the Seurat (v5.1.0) package of R (v4.4.0) for subsequent processing.[15] We selected cells that contained between 500 and 4,000 genes and had less than 10% mitochondrial DNA and normalised the data with the *SCTransform* function (Fig S1, provided on request). After data integration and principal component analysis (PCA), we removed batch effects from the data with the *RunHarmony* function of the Harmony (v1.2.0) package[16] and used uniform manifold approximation and projection (UMAP) for dimensionality reduction in the PCA embeddings. Then, we annotated cell clusters based on marker genes identified by the *FindAllMarkers* function (Fig S2, provided on request) and mentioned in previous studies.[8,17-20]

Functional enrichment, pathway analysis and scoring

Differentially expressed genes (DEGs) were identified by the *FindMarkers* Seurat function with a Wilcoxon test ($P < 0.05$). DEGs in the brain and hippocampal ECs between the PD group and Heal group were selected with a minimum expression ratio of 0.2 and an average log fold change (avg logFC) of positive number. DEGs of hippocampal ECs with high *Mgll* expression (expression > 0) were selected with a minimum average log fold change (avg logFC) of 3 or a maximum average log fold change (avg logFC) of −3. Functional enrichment and pathway analyses were performed using Metascape (https://www.metascape.org) based on the selected DEGs to identify enriched functional terms.[21] Then, we integrated the results and visualised them in R with the Treemapify (v2.5.6) package. We chose visualised terms with the 10 highest counts. In addition, we calculated

module scores of significant functional terms with the *AddModuleScore* Seurat function.

Cell-cell communication analysis

We analysed cell-cell communication with the CellPhoneDB (v5.0.0) package in Python (v3.12.0),[22] then integrated the results and visualised them in R with Ggalluvial (v0.12.5). We chose visualised receptors with the five highest significant means and corresponding ligands.

Cell culture

The immortalised human cerebral microvascular endothelial cell line (HCMEC/D3) and human umbilical vein endothelial cell line (PUMC-HUVEC-T1) were purchased from Pricella (Wuhan, China) and cultured in complete culture medium for ECs from Pricella in a 37°C humidified incubator with 5% CO_2. The cells were expanded through three passages and seeded in 6-well culture plates with 1,000,000 cells per well.

Lipopolysaccharide (LPS) from *Porphyromonas gingivalis* was purchased from Sigma-Aldrich (St Louis, MO, USA) and stored as a 1 mg/ml stock solution in HBSS at −20°C. ABX-1431 was purchased from Selleck (Houston, TX, USA) and stored as a 20mM stock solution in DMSO at −80°C. The cells were cultured in serum-free medium with healthy, 200ng/ml LPS, or 200ng/ml LPS + 10μM ABX-1431 for 12 hours.

Real-time quantitative polymerase chain reaction (RT-qPCR)

Total RNA was collected using an RNA quick extraction kit from GOONIE (Guangzhou, China) according to the manufacturer's instructions, and stored at −80°C. The cDNA was obtained with a PrimeScript RT reagent kit (Takara, Kusatsu, Japan) according to the manufacturer's instructions. Real-time PCR was conducted with the Taq Pro Universal SYBR qPCR Master Mix (Vazyme, Nanjing, China) and a QuantStudio 7 Flex Real-Time PCR System (Thermo Fisher Scientific, Waltham, MA, USA) according to the manufacturers' instructions. Primers were synthesised by Tsingke Biotech (Beijing, China), and the sequences are listed in the supplemental information (Table S1, provided on request).

Enzyme-linked immunosorbent assay (ELISA)

Media were collected and stored at −20°C. ELISA was conducted with an ELISA Kit (MEIMIAN, Yancheng, China) according to the manufacturer's instructions. The optical density (OD) at 450 nm was detected using a microplate reader (BioTek, Winooski, VT, USA).

Statistical analysis

Statistical analyses of the snRNA-seq data were performed in R with default parameters. A Wilcoxon test was employed to compare differences of *Mgll* expression, and an unpaired Student *t* test was used to compare differences of module score in violin plots. Differences with $P < 0.05$ were considered to indicate statistical significance. Statistical analyses of the cellular experiments were performed in GraphPad Prism (v10.1.2; Dotmatics, Boston, MA, USA) and are presented as means ± standard errors of the means (SEMs). A one-way analysis of variance (ANOVA) followed by a Tukey multiple comparisons test was used for multiple comparisons. Differences with $P < 0.05$ were considered to indicate statistical significance.

Results

Construction of the single-nucleus transcriptomic atlases of mouse brains and hippocampi

To investigate disorders in the brain and hippocampus caused by periodontitis, the present authors obtained single-nucleus transcriptomic data from the brains and hippocampi of healthy mice and those with experimental periodontitis (Fig 1a). We successfully constructed the cell atlases of the brain (Fig 1b and c) and hippocampi (Fig 1d and e) of mice with periodontitis. The present study identified cells as eight clusters according to known markers, including inhibitory neurons (In) (*Gad1*$^+$, *Gad2*$^+$), excitatory neurons (Ex) (*Slc17a7*$^+$, *Camk2a*$^+$), astrocytes (Ast) (*Aqp4*$^+$, *Gfap*$^+$), oligodendrocytes (Oli) (*Mobp*$^+$, *Mog*$^+$), oligodendrocyte progenitor cells (OPCs) (*Olig1*$^+$, *Olig2*$^+$), microglia (Mic) (*Csf1r*$^+$, *P2ry12*$^+$) and endothelial cells (ECs) (*Flt1*$^+$, *Cdh5*$^+$). The present authors also revealed that the proportions of inhibitory neurons, microglia and ECs were decreased in both the brain and hippocampus, that of excitatory neurons and astrocytes was increased, and that of the entire neural population was slightly decreased (Fig 1f and g). This finding suggests that periodontitis can affect the brain and hippocampus in a similar pattern. The atlases formed the basis of the subsequent analyses.

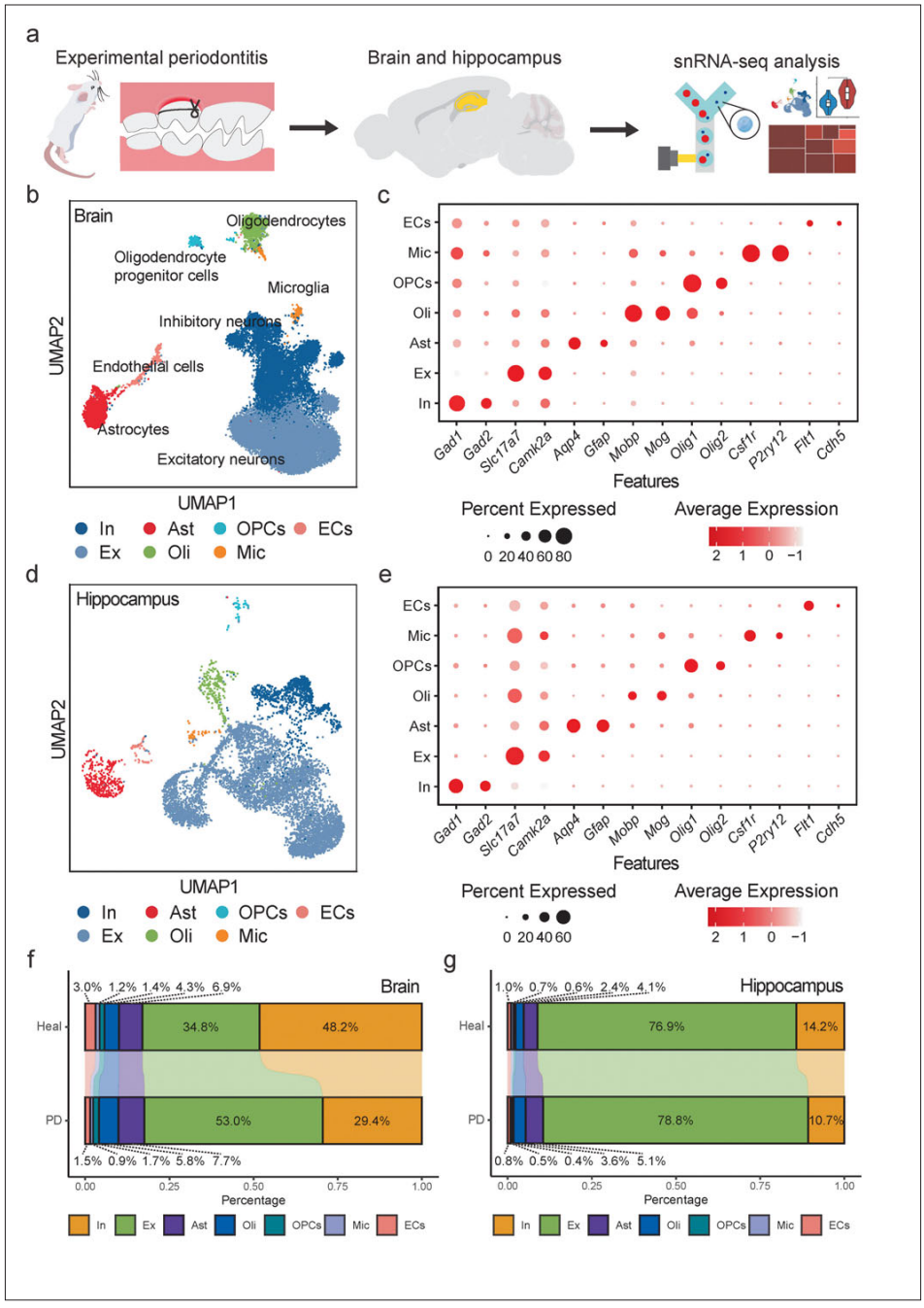

Fig 1a to g The single-nucleus transcriptomic atlases of the mouse brain and hippocampus. Overview of the processing of snRNA-seq data **(a)**; UMAP showing cell clusters in the brain **(b)**; dot plots showing marker genes of every cluster in the brain **(c)**; UMAP showing cell proportions in the hippocampus **(d)**; dot plots showing marker genes of every cluster in the hippocampus **(e)**; proportions of different cell types in the brain **(f)** and the hippocampus **(g)**.

Changes in the function of brain and hippocampal ECs and communication between the ECs and neighbouring cells in the hippocampal area

To explore the initiating mechanism of cognitive disorders in the hippocampus, the present authors compared the functions of activated ECs in both the brain and hippocampus of mice with periodontitis through functional enrichment and pathway analysis (Fig 2a and b). ECs form the BBB as the first line of defence with pericytes and fibroblasts in every area of the brain.[23] The present research revealed that ECs in the hippocampus have different gene expression patterns and functions from those in other areas of the brain when affected by periodontitis. The upregulated genes in ECs of the hippocampus were enriched mainly in the terms 'negative regulation of neurogenesis' and 'Alzheimer's disease (AD)' (Fig 2b). The present study suggests that ECs in the hippocampus may initiate the development of periodontitis-induced AD.

Fig 2a to f Changes in the function of brain and hippocampal ECs and communication between the ECs and neighbouring cells in the hippocampal area. Tree maps showing functional analyses of upregulated genes in the brain and hippocampus with periodontitis **(a and b)**; alluvial plots showing the main interactions between endothelial cells and surrounding cells, including inhibitory neurons **(c)**, excitatory neurons **(d)**, astrocytes **(e)** and microglia **(f)**, in the hippocampus of different groups.

The present authors also investigated the interactions between ECs and other significant clusters in the neurovascular unit, and observed that ECs in the hippocampus of mice with periodontitis had disrupted communication with neurons, astrocytes and microglia compared to those in healthy mice. Specifically, in ECs, *FLRT2* expression was upregulated, and expression of *FLRT2* receptor was correspondingly upregulated on neurons (Fig 2c and d). FLRT2 can regulate synapse formation, which may contribute to the imbalanced activation of neurons.[24,25] For ligands to astrocytes, ECs downregulated the expression of *CLSTN2*, *LRRTM1* and *LRRTM3*, whereas *GJA1* and *PTN* expression increased (Fig 2e). Moreover, ECs heightened the expression of *PTN* and *SLC1A3* ligands as well as matching receptors on microglia (Fig 2f). These findings suggest that periodontitis alters intercellular communication between hippocampal ECs and neighbouring cells, potentially contributing to cognitive impairment.

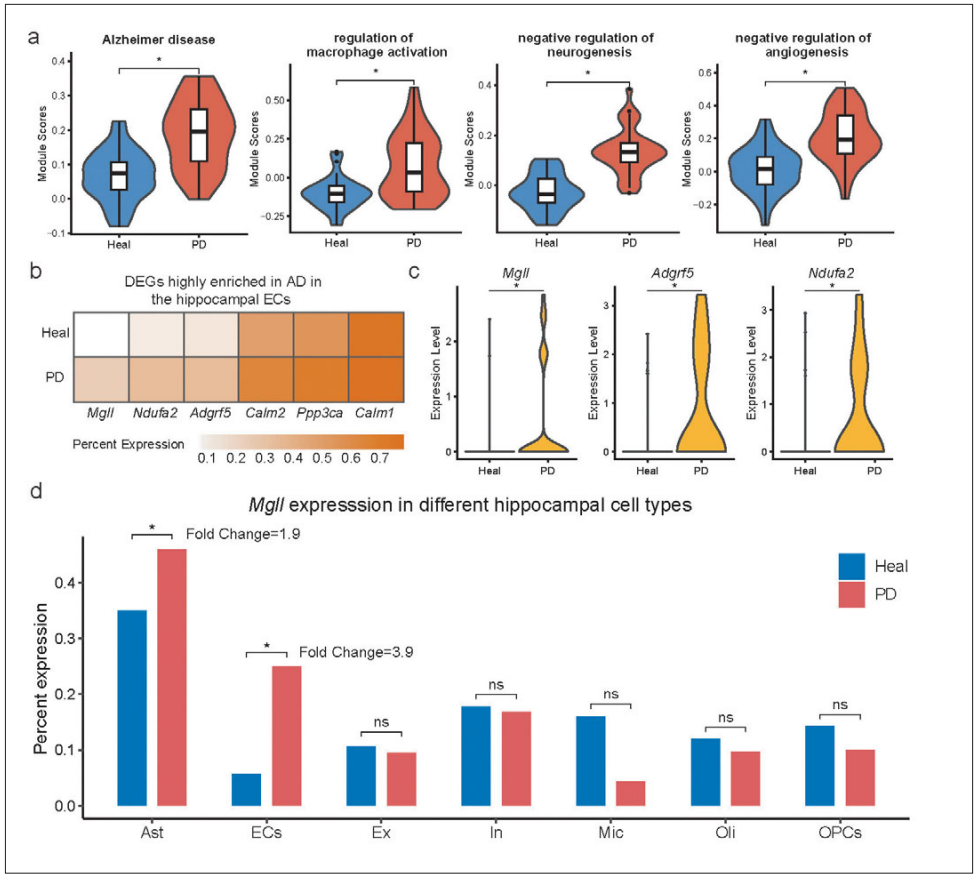

Fig 3a to d Activation of the *Mgll* in the hippocampal ECs with periodontitis. Module scores of significantly enriched pathway genes in the hippocampal endothelial cells with periodontitis **(a)**; heatmap showing DEGs highly enriched in AD in the hippocampal ECs with periodontitis **(b)**; violin plots showing the top three most highly expressed genes enriched in AD in hippocampal ECs in different groups **(c)**; bar plots of *Mgll* expression in different hippocampal cell types **(d)**. *$P < 0.05$.

Activation of Mgll in the hippocampal ECs in mice with periodontitis

The present authors then conducted a detailed analysis of the key genes involved in pathways associated with cognitive dysfunction upregulated in hippocampal ECs in response to periodontitis. The examination of these pathways revealed a significant upregulation in the AD pathway (Fig 3a). Pathways related to the negative regulation of angiogenesis, neurogenesis and macrophage activation were also upregulated in ECs affected by periodontitis. Heatmap visualisation highlighted specific genes linked to the AD pathway, such as *Mgll*, *Calm1*, *Ppp3ca*, *Calm2*, *Adgrf5* and *Ndufa2*, whereas *Mgll* exhibited the greatest increase in expression (Fig 3b and c). The analysis also indicated that *Mgll* is predominantly expressed in hippocampal astrocytes and ECs under the influence of periodontitis, whereas its upregulation in ECs was most notable (Fig 3d). Consequently, the present authors focused on the expression of *Mgll*, as its upregulation could potentially disrupt endothelial function and impact cellular communication. These findings suggest that *Mgll* is activated in the hippocampal ECs in mice with periodontitis.

Activation of Mgll exacerbates inflammation and antigen presentation in the hippocampal ECs

The present authors further investigated the impact of *Mgll* activation on the functions of ECs by comparing the gene expression profiles of ECs with high and low *Mgll* levels. Enrichment analysis of differentially expressed genes revealed that genes associated with the immune response, apoptotic signalling regulation and antigen presentation via MHC class II were upregulated in ECs with high Mgll expression, whereas genes associated with developmental growth pathways were downregulated in those cells (Fig 4a and b). Statistical analysis confirmed the significant upregulation of immune response and apoptotic signalling regulation and the downregulation of developmental growth in high *Mgll*-expressing cells (Fig 4c). Examination of immune-related genes in high *Mgll*-expressing cells identified H2-Eb1, Cd74 and H2-Aa as the top three genes with significantly increased expression compared to *Mgll*-negative cells, indicating enhanced MHCII complex regulation and inflammatory functions in ECs with high *Mgll* expression (Fig 4d and e). The activation of proinflammatory ECs was found to exacerbate neuroinflammation and cognitive dysfunc-

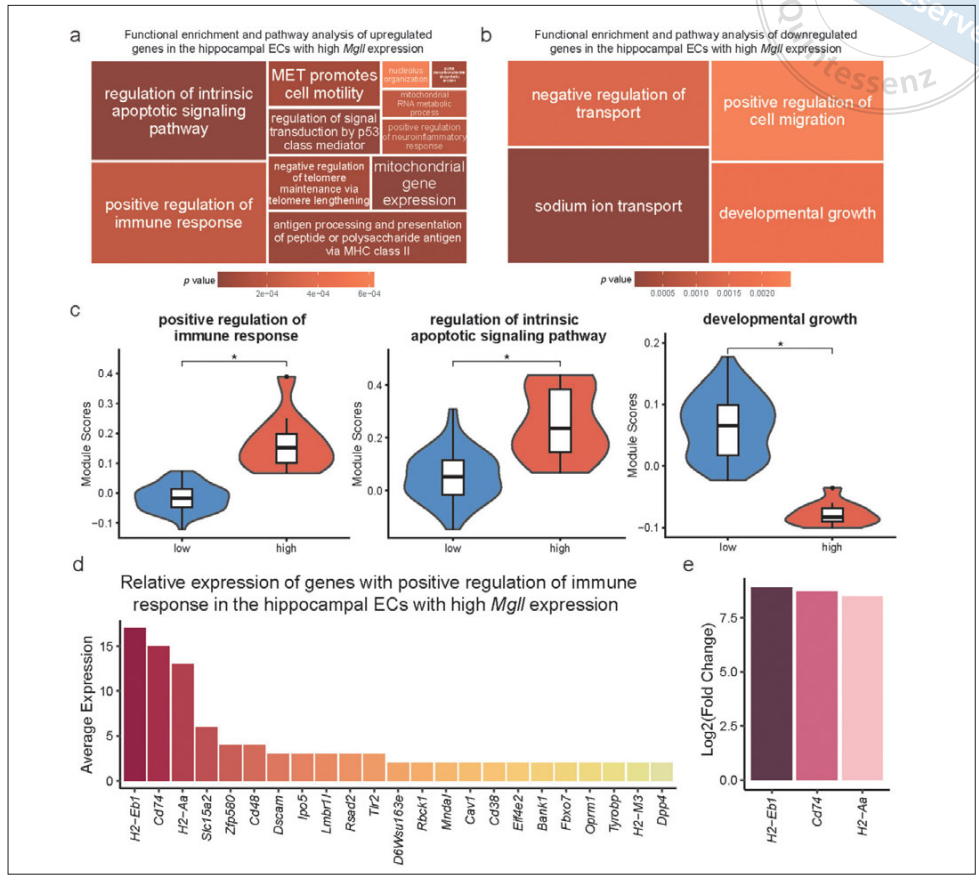

Fig 4a to e Activation of *Mgll* exacerbates inflammation and antigen presentation in the hippocampal ECs. Tree maps showing functional analyses of upregulated **(a)** and downregulated genes **(b)** in hippocampal ECs with high *Mgll* expression; module scores of significant pathway genes in functions enriched in the hippocampal ECs with high *Mgll* expression **(c)**; bar plot showing the relative expression of genes that positively regulate the immune response in hippocampal ECs with high *Mgll* expression **(d)**; bar plot showing the top three genes with the greatest changes in the expression of genes associated with positive regulation of the immune response in hippocampal ECs with high *Mgll* expression **(e)**. **P* < 0.05.

tion by stimulating T cells and microglia. These findings suggest that *Mgll* activation amplifies inflammation and antigen presentation in hippocampal ECs.

The MGLL inhibitor ABX-1431 mitigated inflammation and antigen presentation in ECs

ECs exhibiting high *Mgll* expression demonstrate heightened proinflammatory and enhanced antigen presenting properties; however, the precise mechanisms through which *Mgll* governs these EC functions remain ambiguous. Therefore, the present authors investigated the impact of LPS on simulating bacteria on HCMEC/D3 cells (Fig 5) and PUMC-HUVEC-T1 cells (Fig S3, provided on request). After LPS stimulation, elevated expression levels of type 2 cannabinoid receptors (*CB2*) were observed, as well as the proinflammatory and antigen presenting genes *HLA-DRB1* and *CIITA* (Fig 5a). *CB1* expression had no significant change, which corresponded to a previous study.[26] 2-arachidonoylglycerol (2-AG) is the ligand of cannabinoid receptors, the activation of which is known to significantly mitigate neuroinflammation and aid disease-related damage repair.[27] MGLL predominantly hydrolyses 2-AG to arachidonic acid (AA), which induces cannabinoid receptors to exert inhibitory effects.[26] AA can also attribute to neuroinflammation.[28] The present authors observed consistent results, which affirmed that MGLL played an important role in the endothelial inflammation (Fig 5b). ABX-1431 is a common MGLL inhibitor.[29] Notably, treatment with ABX-1431 suppressed 2-AG hydrolysation, decreasing the expression of *HLA-DRB1* and *CIITA* and restoring the expression of CB2 (Fig 5b). The present findings clarified that MGLL decreased the levels of 2-AG and CB2, attributing to increased CIITA and MHCII expression, leading to neuroinflammation in surrounding cells (Fig 5c). These results suggest that MGLL inhibitors can diminish the inflammatory and antigen-presenting capacities of ECs by augmenting 2-AG levels and suppressing CIITA and MHCII expression, which could be potential therapies for periodontitis-associated AD.

Discussion

By utilising single-nucleus transcriptomics of brain and hippocampal cells, the present study revealed that periodontitis exacerbates cognitive impairment by inducing endothelial inflammation and dysfunction of antigen

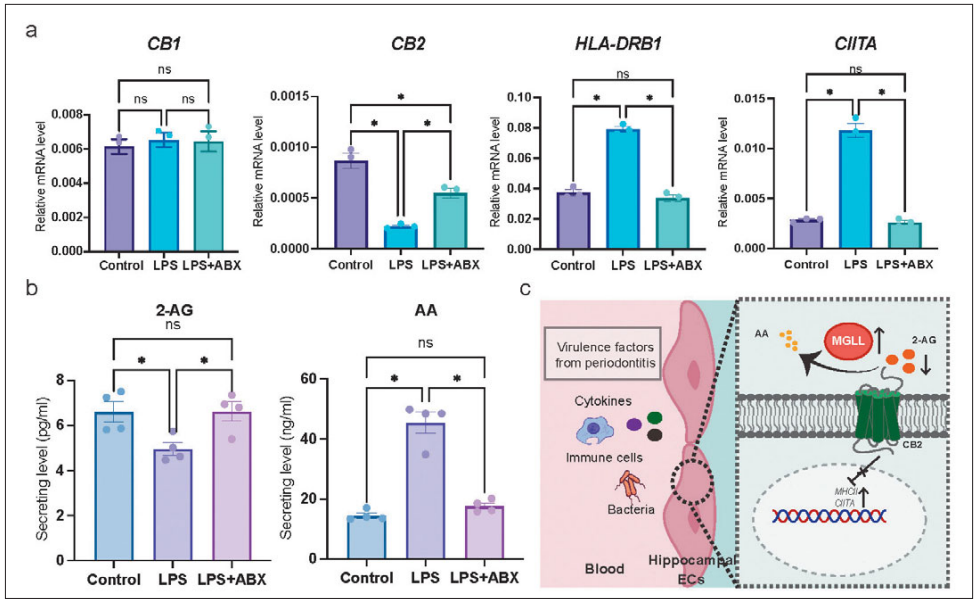

Fig 5a to c The MGLL inhibitor mitigated inflammation and antigen presentation in HCMEC/D3. RT-qPCR analyses of MGLL associated genes in different groups **(a)**; ELISA analysis of 2-AG and AA in different groups **(b)**; overview of the mechanisms by which MGLL induces neuroinflammation during the process by which periodontitis exacerbates AD **(c)**. ABX: ABX-1431. Error bars indicate the standard error of the mean (SEM). *Adjust $P < 0.05$.

presentation through upregulation of *Mgll* expression. This study offers valuable perspectives for the advancement of precise therapeutic interventions for cognitive impairment.

The present study revealed the key role of endothelial inflammation as a significant contributor to periodontitis-associated cognitive impairment. Previous research has emphasised the importance of endothelial dysfunction during the development of AD, but has not precisely explored the connection between endothelial dysfunction and periodontitis-associated AD. Abnormalities of brain ECs contributing to cognitive impairment have been observed in morphology, metabolism and immunity.[30,31] Periodontitis involves sophisticated mechanisms that can damage systemic health,[32-34] and may play a pivotal role in brain endothelial abnormalities that exacerbate neuroinflammation and cognitive decline; however, changes in brain ECs underlying periodontitis are unclear. Through the snRNA-seq of brain and hippocampal cells, the present authors identified the distinct pathways upregulated in the hippocampal ECs of mice with periodontitis that are linked to AD. Subsequent analysis of cell communication revealed aberrant interactions between ECs and surrounding cells involving neurons, astrocytes and microglia in the hippocampus, which may have intensified neuroinflammation. In summary, the present study provides a comprehensive understanding of the impact of periodontitis on hippocampal ECs and elucidates potential mechanisms that contribute to the exacerbation of neuroinflammation.

The present authors also identified the potential mechanism through which periodontitis exacerbates neuroinflammation via endothelial cell dysfunction. MGLL was identified as one of the key molecules leading to endothelial cell dysfunction. It can participate in endocannabinoid signalling, cause dysfunction of astrocytes and microglia and augment inflammatory mediators such as prostaglandin.[28] Previous studies have shown an imbalanced endocannabinoid system in gingival crevicular fluid in individuals with periodontitis.[35,36] In the central nervous system, a recent study observed elevated MGLL expression in protein extracts from the frontal cortex in cases of depression combined with periodontitis;[37] however, its contribution and underlying mechanisms in the hippocampus with periodontitis-associated AD is unclear. Thus, the present authors focused on its function by comparing cells that exhibited high and low *Mgll* expression in the hippocampal data of periodontitis-afflicted mice. Analysis of upregulated genes involved in AD-related pathways revealed the predominant expression of *Mgll* in ECs and astrocytes, and the most significant upregulation was observed in the ECs. Interestingly, the present authors observed an accompanying increase in the expression of genes associated with MHCII molecules, including a notable increase of more than sevenfold in the expression of *H2-Eb1*, *Cd74* and *H2-Aa*. MHCII molecules play a crucial role in the antigen presentation function of ECs, contributing to the activation of T cells and macrophages and the exacerbation of tissue inflammation.[38,39] The present authors infer that peri-

odontitis may aggravate neuroinflammation and cognitive impairment by activating the antigen presentation of ECs, leading to the activation of microglia, astrocytes and other cell types. Periodontitis may aggravate MGLL expression through inflammatory signalling, such as PI3K/AKT and NF-κB, as described in previous studies,[40-42] which should be studied further. Further experimental validation is imperative to substantiate the direct connection between periodontitis, MGLL activation in hippocampal ECs and upregulated antigen presentation.

Specifically, the present authors elucidated that the MGLL-2AG-CB2 pathway activates antigen presentation and inflammatory phenotypes in ECs. MGLL can hydrolyse 2-AG to AA, while the expression of the 2-AG receptor CB1 and CB2 decreases in surrounding environment.[28] CB2 has been shown to play a crucial role in regulating inflammation and neuronal modulation in the brain, including the transition of microglia and astrocytes to the M2 phenotype, and the release of excitatory and inhibitory neurotransmitters.[43] CB2 is also widely expressed on immune cells such as macrophages and dendritic cells, which suggests that it may participate in antigen presentation.[44,45] In the present authors' hypothesis based on the analyses, CB2 suppresses CIITA expression and reduces MHCII levels, while decreasing CB2 expression can augment anti-inflammatory antigen presentation in ECs, trigger tissue inflammation and worsen tissue damage. Therefore, the present authors investigated whether inhibiting MGLL could enhance CB2 expression and decrease CIITA and MHCII levels in ECs. The findings revealed that MGLL inhibition increases 2-AG levels, activates endothelial CB2 and subsequently downregulates CIITA and MHCII. Targeting MGLL to reduce the anti-inflammatory antigen presentation and inflammatory profiles of ECs could represent a potential strategy for mitigating periodontitis-induced neuroinflammation and cognitive impairment; however, the use of LPS as a model of inflammation may not fully recapitulate the complex microbial and host interactions in vivo. Further experimental validation is also necessary to confirm the efficacy and feasibility of this approach, which will be the focus of follow-up studies.

Conclusion

In summary, with analyses of snRNA-seq data from brain and hippocampal cells, this study reveals the role of the MGLL-2AG-CB2 pathway in linking periodontitis to inflammation and antigen presentation of ECs, leading to neuroinflammation and cognitive impairment. These insights offer a foundation for targeted therapeutic approaches for cognitive impairment.

Conflicts of interest

The authors declare no conflicts of interest related to this study.

Author contribution

Drs Zong Shan SHEN, Ji Chen YANG and Bin CHENG designed and directed the study; Drs Zong Shan SHEN and Ji Chen YANG contributed to the collection and analysis of the data and the manuscript draft; Drs Chuan Jiang ZHAO and Bin CHENG critically revised the manuscript. All the authors approved the final submission.

(Received Aug 14, 2024; accepted Jan 21, 2025)

References

1. Dominy SS, Lynch C, Ermini F, et al. Porphyromonas gingivalis in Alzheimer's disease brains: Evidence for disease causation and treatment with small-molecule inhibitors. Sci Adv 2019;5:eaau3333.
2. Wang RP, Huang J, Chan KWY, et al. IL-1β and TNF-α play an important role in modulating the risk of periodontitis and Alzheimer's disease. J Neuroinflammation 2023;20:71.
3. Jia L, Du Y, Chu L, et al. Prevalence, risk factors, and management of dementia and mild cognitive impairment in adults aged 60 years or older in China: A cross-sectional study. Lancet Public Health 2020;5:e661–e671.
4. Yamaguchi S, Murakami T, Satoh M, et al. Associations of dental health with the progression of hippocampal atrophy in community-dwelling individuals: The ohasama study. Neurology 2023;101:e1056–e1068.
5. Lei S, Li J, Yu J, et al. Porphyromonas gingivalis bacteremia increases the permeability of the blood-brain barrier via the Mfsd2a/caveolin-1 mediated transcytosis pathway. Int J Oral Sci 2023;15:3.
6. Li F, Ma C, Lei S, et al. Gingipains may be one of the key virulence factors of porphyromonas gingivalis to impair cognition and enhance blood-brain barrier permeability: An animal study. J Clin Periodontol 2024;51:818–839.
7. Kerkis I, da Silva ÁP, Araldi RP. The impact of interleukin-6 (IL-6) and mesenchymal stem cell-derived IL-6 on neurological conditions. Front Immunol 2024;15:1400533.
8. Shen Z, Kuang S, Zhang Y, et al. Restoring periodontal tissue homoeostasis prevents cognitive decline by reducing the number of Serpina3nhigh astrocytes in the hippocampus. Innovation (Camb) 2023;5:100547.
9. Bryant A, Li Z, Jayakumar R, et al. Endothelial cells are heterogeneous in different brain regions and are dramatically altered in Alzheimer's disease. J Neurosci 2023;43:4541–4557.
10. Custodia A, Ouro A, Romaus-Sanjurjo D, et al. Endothelial progenitor cells and vascular alterations in Alzheimer's disease. Front Aging Neurosci 2022;13:811210.

11. Waigi EW, Pernomian L, Crockett AM, et al. Vascular dysfunction occurs prior to the onset of amyloid pathology and aβ plaque deposits colocalize with endothelial cells in the hippocampus of female APPswe/PSEN1dE9 mice. Geroscience 2024;46:5517–5536.
12. Zhang P, Fu G, Xu W, et al. Up-regulation of miR-126 via DNA methylation in hypoxia-preconditioned endothelial cells may contribute to hypoxic tolerance of neuronal cells. Mol Biol Rep 2024;51:808.
13. Linnerbauer M, Wheeler MA, Quintana FJ. Astrocyte crosstalk in CNS inflammation. Neuron 2020;108:608–622.
14. Huo A, Wang J, Li Q, et al. Molecular mechanisms underlying microglial sensing and phagocytosis in synaptic pruning. Neural Regen Res 2024;19:1284–1290.
15. Hao Y, Stuart T, Kowalski MH, et al. Dictionary learning for integrative, multimodal and scalable single-cell analysis. Nat Biotechnol 2024;42:293–304.
16. Korsunsky I, Millard N, Fan J, et al. Fast, sensitive and accurate integration of single-cell data with harmony. Nat Methods 2019;16:1289–1296.
17. Xing J, Ren L, Xu H, et al. Single-cell RNA sequencing reveals cellular and transcriptional changes associated with traumatic brain injury. Front Genet 2022;13:861428.
18. Li Y, Li Z, Wang C, et al. Spatiotemporal transcriptome atlas reveals the regional specification of the developing human brain. Cell 2023;186:5892–5909.e22.
19. Khrameeva E, Kurochkin I, Han D, et al. Single-cell-resolution transcriptome map of human, chimpanzee, bonobo, and macaque brains. Genome Res 2020;30:776–789.
20. Lau SF, Cao H, Fu AKY, Ip NY. Single-nucleus transcriptome analysis reveals dysregulation of angiogenic endothelial cells and neuroprotective glia in Alzheimer's disease. Proc Natl Acad Sci U S A 2020;117:25800–25809.
21. Zhou Y, Zhou B, Pache L, et al. Metascape provides a biologist-oriented resource for the analysis of systems-level datasets. Nat Commun 2019;10:1523.
22. Troulé K, Petryszak R, Prete M, et al. CellPhoneDB v5: Inferring cell-cell communication from single-cell multiomics data. http://arxiv.org/abs/2311.04567. Accessed 23 July 2024.
23. Yang Q, Wei X, Deng B, et al. Cerebral small vessel disease alters neurovascular unit regulation of microcirculation integrity involved in vascular cognitive impairment. Neurobiol Dis 2022;170:105750.
24. Pederick DT, Lui JH, Gingrich EC, et al. Reciprocal repulsions instruct the precise assembly of parallel hippocampal networks. Science 2021;372:1068–1073.
25. Maestú F, de Haan W, Busche MA, DeFelipe J. Neuronal excitation/inhibition imbalance: Core element of a translational perspective on Alzheimer pathophysiology. Ageing Res Rev 2021;69:101372.
26. Zhou S, Ling X, Zhu J, et al. MAGL protects against renal fibrosis through inhibiting tubular cell lipotoxicity. Theranostics 2024;14:1583–1601.
27. Moe A, Rayasam A, Sauber G, et al. Type 2 cannabinoid receptor expression on microglial cells regulates neuroinflammation during graft-versus-host disease. J Clin Invest 2024;134:e175205.
28. Bajaj S, Jain S, Vyas P, Bawa S, Vohora D. The role of endocannabinoid pathway in the neuropathology of Alzheimer's disease: Can the inhibitors of MAGL and FAAH prove to be potential therapeutic targets against the cognitive impairment associated with Alzheimer's disease? Brain Res Bull 2021;174:305–322.
29. Müller-Vahl KR, Fremer C, Beals C, Ivkovic J, Loft H, Schindler C. Endocannabinoid modulation using monoacylglycerol lipase inhibition in tourette syndrome: A phase 1 randomized, placebo-controlled study. Pharmacopsychiatry 2022;55:148–156.
30. Leira Y, Vivancos J, Diz P, Martín Á, Carasol M, Frank A. The association between periodontitis and cerebrovascular disease, and dementia. Scientific report of the working group of the Spanish society of periodontology and the Spanish society of neurology. Neurologia (Engl Ed) 2024;39:302–311.
31. İş Ö, Wang X, Reddy JS, et al. Gliovascular transcriptional perturbations in Alzheimer's disease reveal molecular mechanisms of blood brain barrier dysfunction. Nat Commun 2024;15:4758.
32. Shen Z, Zhang R, Huang Y, et al. The spatial transcriptomic landscape of human gingiva in health and periodontitis. Sci China Life Sci 2024;67:720–732.
33. Lu J, Zhang S, Huang Y, et al. Periodontitis-related salivary microbiota aggravates Alzheimer's disease via gut-brain axis crosstalk. Gut Microbes 2022;14:2126272.
34. Herrera D, Molina A, Buhlin K, Klinge B. Periodontal diseases and association with atherosclerotic disease. Periodontol 2000 2020;83:66–89.
35. Nakajima Y, Furuichi Y, Biswas KK, et al. Endocannabinoid, anandamide in gingival tissue regulates the periodontal inflammation through NF-kappaB pathway inhibition. FEBS Lett 2006;580:613–619.
36. Özdemir B, Shi B, Bantleon HP, Moritz A, Rausch-Fan X, Andrukhov O. Endocannabinoids and inflammatory response in periodontal ligament cells. PloS One 2014;9:e107407.
37. Robledo-Montaña J, Díaz-García C, Martínez M, et al. Microglial morphological/inflammatory phenotypes and endocannabinoid signaling in a preclinical model of periodontitis and depression. J Neuroinflammation 2024;21:219.
38. Rodor J, Chen SH, Scanlon JP, et al. Single-cell RNA sequencing profiling of mouse endothelial cells in response to pulmonary arterial hypertension. Cardiovasc Res 2022;118:2519–2534.
39. Rustenhoven J, Drieu A, Mamuladze T, et al. Functional characterization of the dural sinuses as a neuroimmune interface. Cell 2021;184:1000–1016.e27.
40. Zhu W, Zhao Y, Zhou J, et al. Monoacylglycerol lipase promotes progression of hepatocellular carcinoma via NF-κB-mediated epithelial-mesenchymal transition. J Hematol Oncol 2016;9:127.
41. Gandhi AY, Yu J, Gupta A, Guo T, Iyengar P, Infante RE. Cytokine-mediated STAT3 transcription supports ATGL/CGI-58-dependent adipocyte lipolysis in cancer cachexia. Front Oncol 2022;12:841758.
42. Shen S, Fu B, Deng L, et al. Paeoniflorin protects chicken against APEC-induced acute lung injury by affecting the endocannabinoid system and inhibiting the PI3K/AKT and NF-κB signaling pathways. Poult Sci 2024;103:103866.
43. Grabon W, Rheims S, Smith J, Bodennec J, Belmeguenai A, Bezin L. CB2 receptor in the CNS: From immune and neuronal modulation to behavior. Neurosci Biobehav Rev 2023;150:105226.
44. Xiang W, Shi R, Kang X, et al. Monoacylglycerol lipase regulates cannabinoid receptor 2-dependent macrophage activation and cancer progression. Nat Commun 2018;9:2574.
45. Cabral GA, Ferreira GA, Jamerson MJ. Endocannabinoids and the immune system in health and disease. Handb Exp Pharmacol 2015;231:185–211.

Impact of Nanofiller Fractions on Selected Properties of Microfilled Composite Resin

Enni PARPO[1], Lippo LASSILA[1], Pekka K VALLITTU[1,2], Sufyan GAROUSHI[1]

Objective: *To assess the impact of incorporating various weight fractions of nanometre-sized particulate fillers on specific properties of microfilled composite resin.*

Methods: *Microfilled composite resin was prepared by mixing 29 wt.% of resin matrix (Bis-GMA/TEGDMA) with the 71 wt.% of silane treated particulate fillers (Ø 0.4 µm). Then, various fractions of nanometre-sized (180 nm) fillers (0, 5, 10, 15, 20, 25, 30 and 35 wt.%) were added gradually using a high-speed mixing machine. For each composite resin, flexural properties (n = 8) were evaluated using a three-point bending test on a universal testing machine (ISO standard 4049). Fourier transform infrared (FTIR)-spectrometry was used to calculate the degree of monomer conversion (DC%). Surface microhardess (Vickers) was also determined. Surface gloss was measured before and after polishing (4,000-grit paper). A two-body wear test was performed in a ball-on-flat configuration using a chewing simulator with 15,000 cycles. A non-contact 3D optical profilometer was utilised to measure wear depth. An analysis of variance (ANOVA) was applied to interpret the results statistically, then a post hoc Tukey analysis was performed.*

Results: *ANOVA revealed that the fraction of nanofillers had a significant effect ($P < 0.05$) on flexural modulus, DC%, microhardness, gloss and wear depth. The group without nanofillers showed the highest DC% (56.6%), gloss after polishing (76.2 GU) and wear resistance (24.2 µm) values, whereas the group with 35 wt.% of nanofillers had the highest flexural modulus (9 GPa) and microhardness (70 VH).*

Conclusion: *It is beneficial to add nanofillers to microfilled composite resin; however, it is essential to assess the proportion ratio carefully. Optimising all the properties of composite resin at once with just one formulation is challenging.*

Keywords: *microfilled composite resin, nanofiller fractions, properties*

Chin J Dent Res 2025;28(2):115–122; doi: 10.3290/j.cjdr.b6260583

Composites resins have become essential in restorative dentistry due to their versatility and the continuous improvement of their material properties. They typically consist of a polymeric matrix reinforced with fillers, where the filler–matrix interface, often mediated by silane coupling agents, plays a crucial role in the overall performance of the material.[1] By manipulating the proportion, size and shape of these fillers, significant enhancements in mechanical, physical and aesthetic properties can be achieved, allowing composite resins to meet the demands of a wide array of dental applications.[2]

Despite their widespread use, composite resins have not yet reached their full potential, and research efforts continue to focus on improving their clinical performance.[2,3] Innovations in the resin matrix predominantly involve the development of new monomer systems,[4-6] whereas advancements in fillers focus on optimising loading capacity, particle size and surface treatment, and exploring novel particulate or fibre technologies.[7-10] These areas of study are particularly important, as the filler content and particle size significantly influence many properties of dental composites.[7,8]

1 Department of Biomaterials Science and Turku Clinical Biomaterial Center-TCBC, Institute of Dentistry, University of Turku, Turku, Finland
2 Wellbeing Services County of South-West Finland, Turku, Finland

Corresponding author: Dr Sufyan GAROUSHI, Department of Biomaterials Science and Turku Clinical Biomaterials Center-TCBC, Institute of Dentistry, University of Turku, Itäinen Pitkäkatu 4 B, FI-20520 Turku, Finland. Tel: 358 2033308379. Email: sufgar@utu.fi

One of the most promising advancements in this field is the integration of nanotechnology. Nanotechnology involves manipulating materials on a nanoscale (5 to 200 nm) to enhance specific properties through various physical and chemical approaches.[11] The incorporation of nanometre-sized fillers into microfilled composite resins has garnered significant attention, as these nanofillers occupy voids between larger microfillers, increasing the overall filler content and improving material performance.[12] Given that the resin matrix typically exhibits lower mechanical strength compared to the fillers, reducing the inter-filler voids is essential to improve the strength, hardness and wear resistance of the composite.[7,13] Furthermore, nanofillers offer additional benefits in dental composites, particularly by enhancing optical properties, which are critical for achieving highly aesthetic restorations.[14,15]

Despite these advancements, significant challenges remain with regard to optimising the mechanical and surface properties of composite resins, especially in high-stress areas. The relationship between filler size, shape, distribution and composite performance remains a critical focus of ongoing research.[2] Gaining a deeper understanding of how these variables influence material behaviour is essential for developing next-generation composite resins that combine superior aesthetics with long-lasting durability. Thus, this study aims to explore the optimal weight fraction of nanometre-sized particulate fillers that can significantly enhance the physical, mechanical and aesthetic properties of microfilled composite resins.

Materials and methods

Materials

The dimethacrylate (BisGMA 50% [bisphenol A-glycidyl dimethacrylate] and TEGDMA 50% [triethylenglycol dimethacrylate]) monomer resin system and radiopaque fillers of $BaAlSiO_2$ (0.4 µm in size) (UltraFine, Schott, Landshut, Germany) were used. Nanofillers (SiO_2, 180 nm in size) with various weight fractions (NanoFine, Schott) were incorporated into the resin system. Both types of fillers were received silanated from the manufacturer.

Preparation of the experimental composite resins

Experimental composite resins were prepared by mixing 29 wt.% of resin matrix with 71 wt.% of $BaAlSiO_2$ radiopaque fillers. Then, various weight fractions of nanofillers (0, 10, 15, 20, 25, 30 and 35 wt.%) were added gradually to the mixture. Mixing was carried out using a high-speed mixing machine for 4 minutes at 3,500 rpm (SpeedMixer DAC, Hauschild, Hamm, Germany).

All groups had the same resin matrix and a consistent fraction of microfillers but varied in their nanofiller fractions (resulting in different total filler fractions). Composite resins were transferred from mixing cups to syringes and mixed in a centrifuge (SPR centrifuge, Beckman Coulter, Brea, CA, USA) until all entrapped air was eliminated.

Flexural strength and modulus

Specimens of specific dimension ($2 \times 2 \times 25$ mm^3) were prepared for a three-point bending test from all evaluated composites. By using a half-split stainless-steel mould and transparent Mylar sheets, bar-shaped specimens were prepared. Light curing of dental composite was performed using a hand light-curing unit (Elipar DeepCure-L, 3M, St Paul, MN, USA) for a duration of 20 seconds in four different parts through metal moulds on both sides. The light tip of the curing device was 1 mm away from the composite. The light intensity was 1600 mW/cm^2, with a wavelength ranging from 400 to 480 nm (Marc Resin Calibrator; BlueLight Analytics, Halifax, NS, Canada). Before testing, the specimens of each group (n = 8) were kept dry for 2 days in an incubator (37°C). According to ISO 4049, a three-point bending test was performed (test span 20 mm, crosshead speed 1 mm/min, indenter 2 mm diameter, load cell 2500 N). Using a material-testing machine (model LRX, Lloyd Instruments, Fareham, UK), all specimens were loaded, and software was used to record the load-deflection curves (Nexygenf4.0, Lloyd Instruments).

Flexural strength (σf) as well as flexural modulus (Ef) were measured according to equations:

$\sigma f = 3FmI /(2bh^2)$

$Ef = SI^3 /(4bh^3)$

Where Fm is the load applied (N) at the maximum point of the load-extension curve, I is the length of span (20 mm), b is the width of the test specimens and h represents the thickness of the test specimens. S is the stiffness (N/m) S = F/d where d represents the deflection that corresponds to load F at a particular point along the straight-line portion of the trace.

Degree of monomer conversion

Fourier transform infrared (FTIR)-spectroscopy was employed using an attenuated total reflectance (ATR) accessory (Spectrum One, Perkin-Elmer, Beaconsfield,

UK) for the quantification of carbon-carbon double bond conversion (DC%) both before and after photoinitiation of the polymerisation process. The assessment was conducted within a mould with a thickness of 1.5 mm and a diameter of 4.5 mm, encompassing the analysis of composite resins. The initial step involved the measurement of the spectrum of the non-polymerised specimen. Subsequently, the composite resin underwent polymerisation using a manual light-curing unit (Elipar DeepCure-L), with irradiation conducted through an upper glass slide for 40 seconds. Following the irradiation process, the FTIR spectrum of the specimen was subjected to scanning, then DC% was measured from the aliphaticfC = C peak at 1638 cm^{-1} and normalised against the aromaticfC = C peak at 1608 cm^{-1} following this formula:

$$DC\ \% = (1 - \frac{C_{aliphatic}\ /C_{aromatic}}{U_{aliphatic}\ /U_{aromatic}})$$

Where the C aliphatic is the absorption peak at 1638 cm^{-1} and C aromatic the reference peak of the polymerised specimen, whereas U aliphatic represents the absorption peak at 1638 cm^{-1} and U aromatic the reference peak of the unpolymerised specimen. Five trials were run for each experimental composite resin.

Surface gloss

Disk-shaped specimens (15 mm diameter and 2 mm thickness) were fabricated from each material using a metal mould (n = 5). One side of the specimen surface facing the mould was polished with 4,000-grit paper, and this side was named the polished side. The other side of the specimen facing the glass slide and mylar strip remained unpolished and was named the unpolished side. After polishing, specimens were rinsed with water and stored in dry conditions at room temperature before testing. The surface gloss was measured at an incidence angle of 60 degrees, using a calibrated infrared Glossmeter (Zehntner Testing Instruments, Germany) with a square measurement area of 6 x 40 mm. The mean of four measurements was recorded per surface.

Surface microhardness

The surface microhardness of each group was measured using the same polished disk-shaped specimens (n = 5) and a Duramin hardness microscope (Struers, Copenhagen, Denmark) equipped with a 40x objective lens. A load of 1.96 N was applied for 15 seconds to each specimen, with five indentations made on the surface of each one. The diagonal lengths of the impressions were measured, and the Vickers hardness values were automatically converted into microhardness values by the machine. Microhardness was calculated using the following equation:

$$H = \frac{1854.4 \times P}{d^2}$$

where H is Vickers hardness in kg/mm^2, P is the load in grams and d is the length of the diagonals in μm.

Two-body wear

The two-body wear test was applied according to previous studies[16,17] to demonstrate the wear resistance of each composite. Two polished specimens (20 mm length × 10 mm width × 3 mm depth) of each composite were prepared in acrylic resin block. All specimens were immersed in distilled water at a temperature of 37°C for 24 hours prior to testing. Wear assessments were conducted using a chewing simulator (CS-4.2, SD-Mechatronik, Feldkirchen-Westerham, Germany), consisting of two distinct chambers designed to replicate vertical and horizontal masticatory movements sequentially, while operating within an aqueous environment. Each chamber composed of a lower sample holder for specimen insertion and an upper loading tip serving as the counteracting element to the specimens under examination. An upper antagonist, in the form of a steatite ball with a diameter of 6 mm, was employed. For each specimen, a total of 15,000 simulated chewing cycles were executed at a frequency of 1.5 Hz, employing a vertical load of 2 kg to emulate a chewing force of 20 N. Subsequent to the simulations, wear patterns were assessed via a 3D optical profilometer (ContourGT-I, Bruker Nano, Tucson, AZ, USA). The mean wear depth (in μm) was calculated based on the examination of the deepest points among six wear profiles from each group, representing a comprehensive measure of wear resistance (Fig 1).

Microstructure analysis

To evaluate the microstructure of the investigated composites, a scanning electron microscopy (SEM) (LEO, Oberkochen, Germany) was used. Polished specimens (n = 2) from the experimental composites (0 and 35 wt.%) were kept dry in a desiccator for 24 hours. After that, specimens were gold coated in a vacuum evaporator utilising a sputter coater (SCD 050 Sputter Coater, BAL-TEC, Balzers, Liechtenstein) prior to SEM inspection.

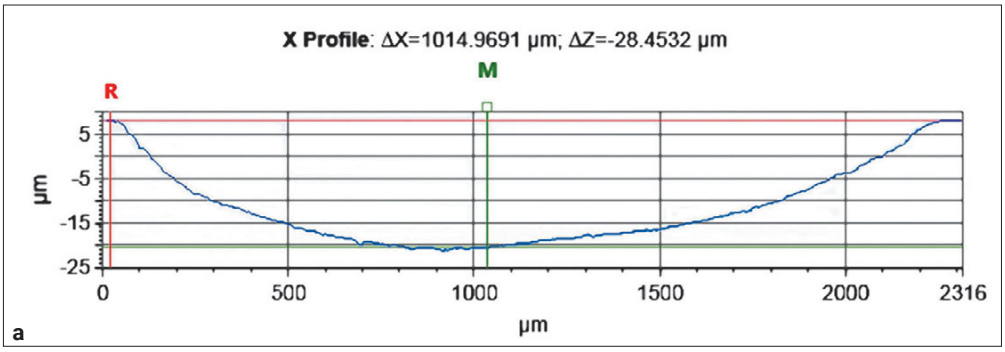

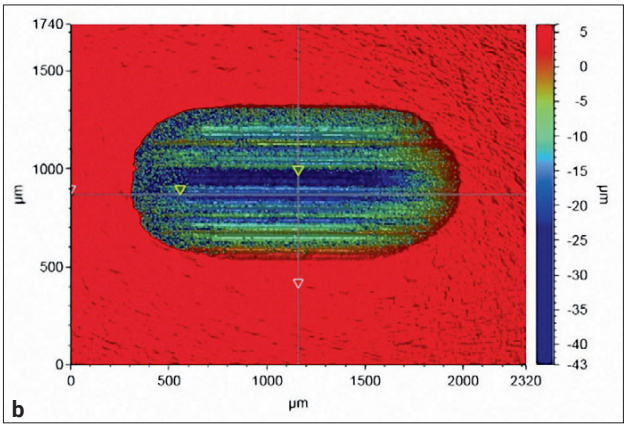

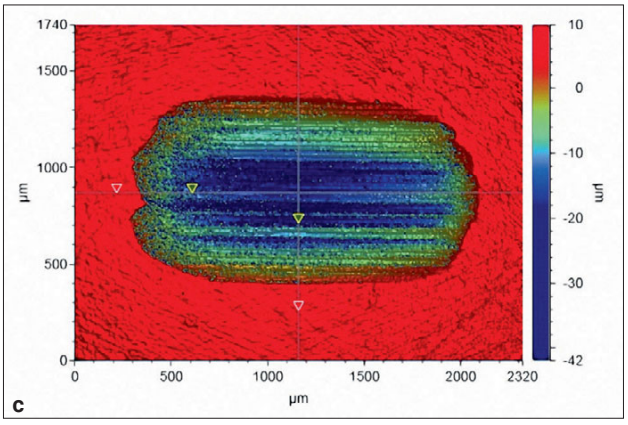

Fig 1a to c The mean wear depth was calculated based on the examination of the deepest points among six wear profiles from each group (a). Example of 2D surface profiles of the wear facet of a specimen without **(a)** and with nanofillers **(c)**.

Statistical analysis

Analysis of variance (ANOVA) with the level of significance set at 0.05 was employed to statistically analyse the data with SPSS version 23 (IBM, Armonk, NY, USA). The results were primarily assessed using a Levene test to evaluate equality of variances. Tukey HSD post hoc analysis was used to ascertain the variations between tested groups. The Pearson correlation coefficient was calculated to examine the relationship between the investigated material properties and the nanofiller weight percentage.

Results

The results presented in Table 1 indicate that the fraction of nanofillers had a significant effect ($P < 0.05$) on flexural modulus (positive correlation, $R^2 = 0.8$), degree of conversion (DC%) (negative correlation, $R^2 = 0.9$), microhardness (positive correlation, $R^2 = 0.9$), gloss (negative correlation, $R^2 = 0.8$) and wear depth (negative correlation, $R^2 = 0.9$). However, the addition of nanofillers did not correlate with flexural strength values ($R^2 = 0.2$).

The group without nanofillers exhibited the highest DC% (56.6%), gloss after polishing (76.2 GU) and wear resistance (24.2 µm). In contrast, the group with 35 wt.% nanofillers showed the highest flexural modulus (9 GPa) and microhardness (70 VH).

The polishing protocol used in this study (4,000 grit) reduced the surface gloss of the composite surfaces compared to the unpolished surfaces polymerised against a mylar matrix strip ($P < 0.05$). Nanofillers had no effect on the gloss values of the unpolished specimens.

Figure 1 illustrates a typical wear facet profile of specimens with and without nanofillers. The addition of nanofillers increased both the wear depth values and the size of the wear facet area. Moreover, SEM images (Fig 2) provide further insight into the structural differences, showing that nanofillers effectively filled the spaces between micro-sized fillers, resulting in a more uniform material. Specimens without nanofillers, on the other hand, exhibited greater porosity, suggesting that these unfilled gaps could negatively impact certain material properties.

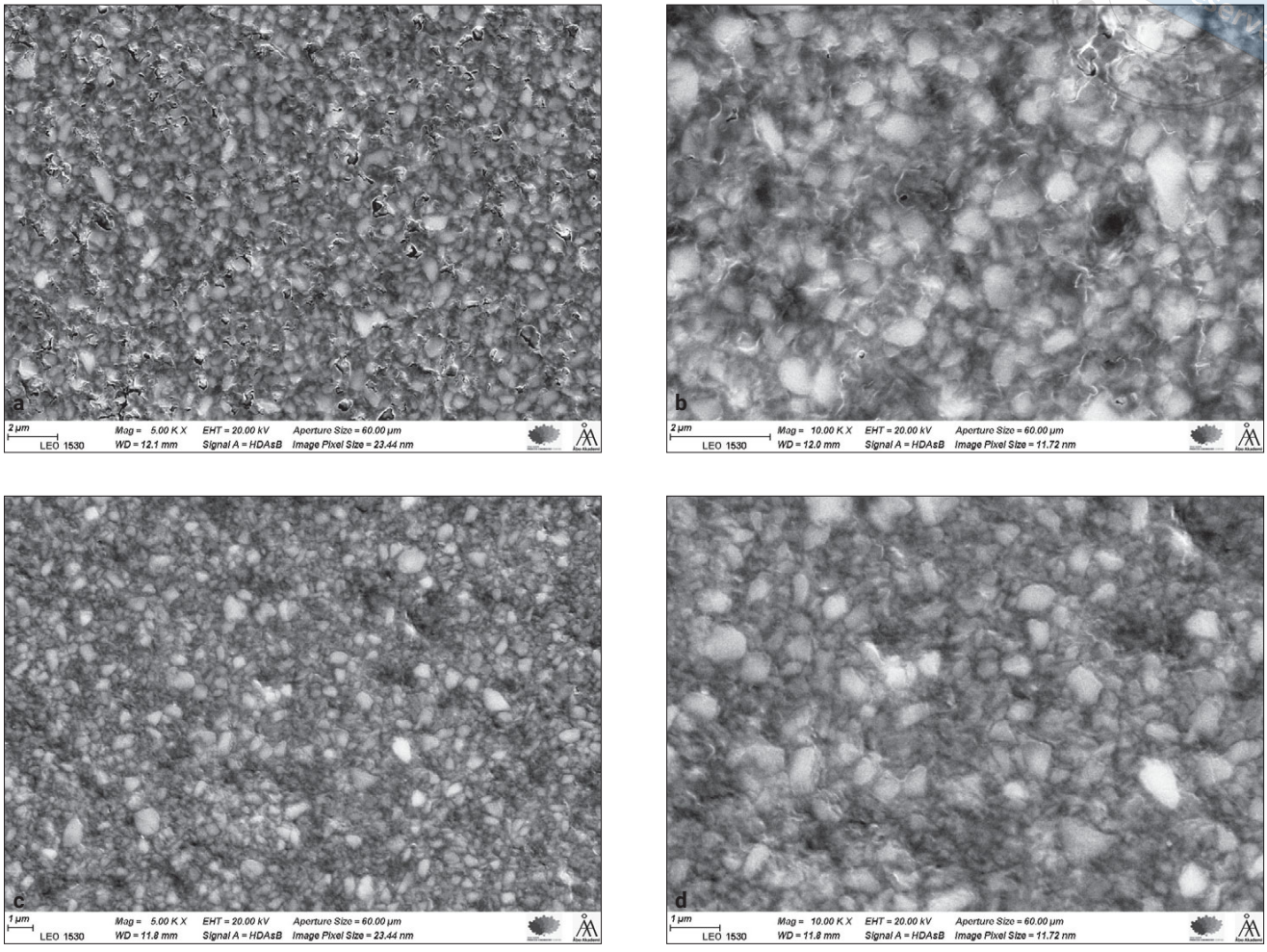

Fig 2a to d SEM images at different magnifications of the group without nanofillers **(a and b)**, showing some porosity, and the group with 30 wt.% nanofillers **(c and d)**, where the nanofillers are filling the spaces between the micro-sized fillers.

Discussion

The use of inorganic particles as a reinforcement method for polymer-based materials is well-documented, with various studies showing that incorporating nanofillers into polymer matrices enhances multiple properties of the resulting composites.[18] In the present study, the effect of adding nanofillers on the properties of microfilled composite resin was explored by testing eight experimental composite groups, each containing varying amounts of nanofillers. The parameters were assessed in accordance with the dental standard ISO 4094 or other reliable testing methods.[19-21] Despite the experimental resin-based materials not being fully optimised, the results indicated that the selected formulations fell within the property range of standard commercial products.[21-23]

The findings demonstrate the significant influence of nanofiller content on the mechanical and surface properties of the microfilled composite resins tested. Specifically, the positive correlation between the fraction of nanofillers and the flexural modulus (R^2 = 0.8) and microhardness (R^2 = 0.9) suggests that increasing the nanofiller content enhances the stiffness and surface hardness of the microfilled composite resin. Consistent with previous studies, the combination of micro- and nano-sized fillers allows for denser packing, which in turn increases the filler volume fraction of the composite resins.[7,24,25]

The flexural strength results (R^2 = 0.2) indicate that there is no significant correlation between the addition of nanofillers and the flexural strength of the composite. Although an initial increase in strength was observed at low nanofiller loadings (5 wt.%), a significant decrease in strength occurred at higher filler loadings (Table 1). This suggests that while small amounts of nanofiller may enhance flexural strength, further increasing the filler content beyond a certain threshold

Table 1 Results, mean ± standard deviation (SD).

Group	Flexural strength (MPa)	Flexural modulus (GPa)	DC%	Surface gloss (GU)		Hardness (VH)	Wear (µm)
				Unpolished	Polished		
0 wt.%	135 ± 19^{a}	7.7 ± 0.6^{a}	56.6 ± 0.6^{a}	90.8 ± 0.5^{a}	76.2 ± 2.3^{a}	56.1 ± 5.0^{a}	24.2 ± 1.4^{a}
5 wt.%	158 ± 20^{b}	8.2 ± 0.3^{a}	56.4 ± 0.4^{a}	90.9 ± 2.0^{a}	74.9 ± 2.6^{a}	61.0 ± 3.0^{a}	25.9 ± 1.8^{b}
10 wt.%	139 ± 18^{a}	8.2 ± 0.1^{a}	55.0 ± 0.5^{b}	90.7 ± 1.2^{a}	75.8 ± 3.5^{a}	61.2 ± 3.0^{b}	26.4 ± 1.9^{c}
15 wt.%	144 ± 19^{c}	8.6 ± 0.2^{b}	54.1 ± 0.6^{b}	90.0 ± 1.5^{a}	75.6 ± 3.4^{a}	61.2 ± 2.0^{a}	27.4 ± 1.8^{d}
20 wt.%	149 ± 25^{d}	9.0 ± 0.5^{c}	54.4 ± 0.2^{b}	89.1 ± 0.6^{a}	68.5 ± 1.3^{b}	65.2 ± 2.6^{c}	27.5 ± 1.3^{d}
25 wt.%	146 ± 22^{e}	8.6 ± 0.5^{c}	53.8 ± 0.3^{c}	90.6 ± 1.4^{a}	68.2 ± 1.2^{b}	67.0 ± 2.4^{c}	30.0 ± 2.1^{e}
30 wt.%	130 ± 11^{f}	8.9 ± 0.5^{d}	52.2 ± 0.8^{d}	91.0 ± 0.7^{a}	68.9 ± 2.2^{b}	67.9 ± 4.4^{d}	28.9 ± 1.6^{f}
35 wt.%	121 ± 12^{g}	9.0 ± 0.4^{d}	51.4 ± 0.5^{d}	89.1 ± 0.9^{a}	65.5 ± 0.1^{c}	70.4 ± 3.5^{d}	31.0 ± 1.7^{g}

The same superscript letter after the values indicates groups that were statistically similar ($P > 0.05$).

negatively impacts this property. This finding aligns with reports in the literature on particulate-filled composite resins, where increasing nanofiller loading can counteract the expected reinforcement due to a higher concentration of particles.[25,26] The observed decrease in strength is likely due to increased mechanical failure at the interface between the resin matrix and the inorganic fillers.[27] In other words, the wettability of the nanofillers is reduced. Conversely, the negative correlation between nanofiller content and DC% (R^2 = 0.9), gloss (R^2 = 0.8) and wear depth (R^2 = 0.9) indicates that higher concentrations of nanofiller may hinder the polymerisation process, reduce the surface gloss and increase the susceptibility to wear. The reduction in DC% observed in groups with higher nanofiller content may be attributed to the increased viscosity of the composite resin, which restricts monomer mobility and diminishes the efficiency of the curing process. The inclusion of nanofillers can increase the refractive index and reduce the extinction coefficient, which could hinder the polymerisation of monomers.[28] Additionally, the formation of a dense or highly filled structure (Fig 2) might impede light penetration or cause light scattering, particularly when the filler particle size is close to the wavelength of the light from the curing unit.[29,30] As a result, increased scattering reduces light intensity, further impacting the curing process.

Gloss refers to a surface's ability to reflect light, with high gloss typically indicating a smooth restoration surface.[31] In the present study, the gloss values of the composite surface polymerised against a Mylar strip (unpolished surface) were higher than those obtained after polishing. Similar findings have been reported in other studies.[32,33] Although light curing against a Mylar sheet produces a smoother surface, restorations usually require finishing to remove excess material and recontour the surface, which decreases smoothness and necessitates further polishing. The observed reduction in gloss, particularly after polishing, suggests that composites with higher nanofiller content may exhibit less reflectivity, likely due to increased surface roughness and the loss of filler particles during the polishing process.[33]

These results contrast with the findings of Valente et al,[34] who reported that nanofilled composites (mean particle size Ø 175 nm) retained higher surface gloss both before and after brushing, suggesting that smaller inorganic fillers can better maintain aesthetic properties under oral conditions. However, Kaizer et al[35] noted that there is no in vitro evidence to favour nanofilled composite resins over traditional microfilled composites in terms of superior surface smoothness or gloss.

The wear facet profiles shown in Fig 1 provide further insight into the effect of nanofillers on wear performance. The increased wear depth and facet area observed in the specimens containing nanofillers suggest that, despite enhancing certain mechanical properties, nanofillers can also make the composite more vulnerable to wear under specific conditions. This outcome is not unexpected, as previous studies have shown that flowable composite resins with lower filler content often exhibit better wear resistance than packable, highly filled composites.[36,37] This may be partly attributed to the elastic deformation of the low-viscosity composite matrix, which offers some shock-absorbing properties.[23,36] The literature presents mixed results: some studies report a positive[38,39] or negative correlation[23,37] between surface hardness and wear resistance, whereas others found no relationship.[21,40] Bayne et al[41] emphasise that filler quantity is less critical than how it is distributed, with inter-particle spacing being a key factor in protecting the composite surface. However, the wear of composite materials remains a complex process, and no definitive conclusions have been reached in the literature so far.

It is important to highlight that the nanofillers in the present study were well distributed throughout the matrix, as no agglomeration was observed in the SEM images (Fig 2). This uniform distribution is most likely attributable to the silane treatment.

Conclusion

In summary, the incorporation of nanofillers into composite materials presents a complex balance of benefits and drawbacks. While nanofillers enhance flexural modulus and microhardness, they may also reduce the DC%, gloss and wear resistance. These findings emphasise the importance of carefully optimising nanofiller content in composite formulations to achieve the desired combination of mechanical strength, surface quality and durability for specific applications. Further studies are needed to explore the mechanisms underlying these effects and to identify strategies for mitigating the negative impacts of nanofillers on composite performance.

Conflicts of interest

The authors declare no conflicts of interest related to this study.

Author contribution

Dr Enni PARPO contributed to the data collection/analysis and manuscript draft; Dr Lippo LASSILA contributed to the study design, data analysis/interpretation and manuscript revision; Dr contributed to the manuscript editing and revision; Dr Sufyan GAROUSHI contributed to the study design, manuscript writing and revision.

(Received Sep 29, 2024; accepted Nov 18, 2024)

References

1. Ferracane JL. Resin composite—State of the art. Dent Mater 2011;27:29–38.
2. Ferracane JL. A historical perspective on dental composite restorative materials. J Funct Biomater 2024;15:173.
3. Paolone G, Diana C, Cantatore G. 2023 state-of-the-art in resin-based composites and future trends. Compend Contin Educ Dent 2023;44:98–100.
4. He J, Lassila L, Garoushi S, Vallittu P. Tailoring the monomers to overcome the shortcomings of current dental resin composites - Review. Biomater Investig Dent 2023;10:2191621.
5. Lone SB, Zeeshan R, Khadim H, Khan MA, Khan AS, Asif A. Synthesis, monomer conversion, and mechanical properties of polylysine based dental composites. J Mech Behav Biomed Mater 2024;151:106398.
6. Ma X, Zhang X, Huang X, Liu F, He J, Mai S. Performance of low shrinkage Bis-EFMA based bulk-fill dental resin composites. Dent Mater 2024:40:1378–1389.
7. Garoushi S, Lassila LV, Vallittu PK. Influence of nanometer scale particulate fillers on some properties of microfilled composite resin. J Mater Sci Mater Med 2011;22:1645–1651.
8. Kontou E, Christopoulos A, Koralli P, Mouzakis DE. The effect of silica particle size on the mechanical enhancement of polymer nanocomposites. Nanomaterials (Basel) 2023;13:1095.
9. Rozza BY, El-Refai DA, Essawy HA, Alian GA. Effect of silanization of poly (urea-formaldehyde) microcapsules on the flexural strength and self-healing efficiency of an experimental self-healing dental resin composite (An in-vitro study). J Mech Behav Biomed Mater 2024;151:106372.
10. Chen H, Luo J, Yang J, Zeng C, Jiang X. Synthesis of pore-size-tunable porous silica particles and their effects on dental resin composites. Biomolecules 2023;13:1290.
11. Schmalz G, Hickel R, van Landuyt KL, Reichl FX. Scientific update on nanoparticles in dentistry. Int Dent J 2018;68: 299–305.
12. Pavanello L, Cortês IT, de Carvalho RDP, et al. Physicochemical and biological properties of dental materials and formulations with silica nanoparticles: A narrative review. Dent Mater 2024:40:1729–1741.
13. Torno V, Soares P. Tribological behavior and wear mechanisms of dental resin composites with different polymeric matrices. J Mech Behav Biomed Mater 2023;144:105962.
14. Cavalcante LM, Masouras K, Watts DC, Pimenta LA, Silikas N. Effect of nanofillers' size on surface properties after toothbrush abrasion. Am J Dent 2009;22:60–64.
15. Lassila LV, Nagas E, Vallittu PK, Garoushi S. Translucency of flowable bulk-filling composites of various thicknesses. Chin J Dent Res 2012;15:31–35.
16. Mangoush E, Garoushi S, Vallittu P, Lassila L. Load-bearing capacity and wear characteristics of short fiber-reinforced composite and glass ceramic fixed partial dentures. Eur J Oral Sci 2023;131:e12951.
17. Lassila L, Mangoush E, He J, Vallittu PK, Garoushi S. Effect of post-printing conditions on the mechanical and optical properties of 3D-printed dental resin. Polymers (Basel) 2024;16:1713.
18. Kutvonen A, Rossi G, Puisto SR, Rostedt NK, Ala-Nissila T. Influence of nanoparticle size, loading, and shape on the mechanical properties of polymer nanocomposites. J Chem Phys 2012;137:214901.
19. International Standardization Organization ISO 4049. Dentistry- Polymer based filling, restorative and luting materials. Geneva, Switzerland: International Standardization Organization; 2000.
20. Ilie N, Hilton TJ, Heintze SD, et al. Academy of Dental Materials guidance-Resin composites: Part I-Mechanical properties. Dent Mater 2017;33:880–894.
21. Garoushi S, Lassila L, Vallittu PK. Impact of fast high-intensity versus conventional light-curing protocol on selected properties of dental composites. Materials (Basel) 2021;14:1381.
22. Ilie N, Hickel R. Investigations on mechanical behaviour of dental composites. Clin Oral Investig 2009;13:427–438 [erratum 2009;13:485–487].
23. Oja J, Lassila L, Vallittu PK, Garoushi S. Effect of accelerated aging on some mechanical properties and wear of different commercial dental resin composites. Materials (Basel) 2021;14:2769.

24. Masouras K, Silikas N, Watts DC. Correlation of filler content and elastic properties of resin-composites. Dent Mater 2008;24:932–939.
25. Rodríguez HA, Kriven WM, Casanova H. Development of mechanical properties in dental resin composite: Effect of filler size and filler aggregation state. Mater Sci Eng C Mater Biol Appl 2019;101:274–282.
26. Fu SY, Feng XQ, Lauke B, Mai Y. Effects of particle size, particle/matrix interface adhesion and particle loading on mechanical properties of particulate–polymer composites. Compos B Eng 2008;39:933–961.
27. Wang R, Habib E, Zhu XX. Synthesis of wrinkled mesoporous silica and its reinforcing effect for dental resin composites. Dent Mater 2017;33:1139–1148.
28. Turssi CP, Ferracane JL, Vogel K. Filler features and their effects on wear and degree of conversion of particulate dental resin composites. Biomaterials 2005;26:4932–4937.
29. Lehtinen J, Laurila T, Lassila LV, et al. Optical characterization of bisphenol-A-glycidyldimethacrylate-triethyleneglycoldimethacrylate (BisGMA/TEGDMA) monomers and copolymer. Dent Mater 2008;24:1324–1328.
30. Garoushi S, Vallittu PK, Watts DC, Lassila LV. Effect of nanofiller fractions and temperature on polymerization shrinkage on glass fiber reinforced filling material. Dent Mater 2008;24:606–610.
31. de Melo TP, Delgado A, Martins R, et al. Can specular gloss measurements predict the effectiveness of finishing/polishing protocols in dental polymers? A systematic review and linear mixed-effects prediction model. Oper Dent 2022;47: E131–E151.
32. Cazzaniga G, Ottobelli M, Ionescu AC, et al. In vitro biofilm formation on resin-based composites after different finishing and polishing procedures. J Dent 2017;67:43–52.
33. Lassila L, Dupont A, Lahtinen K, Vallittu PK, Garoushi S. Effects of different polishing protocols and curing time on surface properties of a bulk-fill composite resin. Chin J Dent Res 2020;23:63–69.
34. Valente LL, Peralta SL, Ogliari FA, Cavalcante LM, Moraes RR. Comparative evaluation of dental resin composites based on micron- and submicron-sized monomodal glass filler particles. Dent Mater 2013;29:1182–1187.
35. Kaizer MR, de Oliveira-Ogliari A, Cenci MS, Opdam NJ, Moraes RR. Do nanofill or submicron composites show improved smoothness and gloss? A systematic review of in vitro studies. Dent Mater 2014;30:e41–e78.
36. Lassila L, Novotny R, Säilynoja E, Vallittu PK, Garoushi S. Wear behavior at margins of direct composite with CAD/CAM composite and enamel. Clin Oral Investig 2023;27:2419–2426.
37. Hahnel S, Schultz S, Trempler C, Ach B, Handel G, Rosentritt M. Two-body wear of dental restorative materials. J Mech Behav Biomed Mater 2011;4:237–244.
38. Nagarajan VS, Jahanmir S, Thompson VP. In vitro contact wear of dental composites. Dent Mater 2004;20:63–71.
39. He J, Garoushi S, Säilynoja E, Vallittu P, Lassila L. Surface integrity of dimethacrylate composite resins with low shrinkage comonomers. Materials (Basel) 2021;14:1614.
40. Lazaridou D, Belli R, Petschelt A, Lohbauer U. Are resin composites suitable replacements for amalgam? A study of two-body wear. Clin Oral Investig 2015;19:1485–1492.
41. Bayne SC, Taylor DF, Heymann HO. Protection hypothesis for composite wear. Dent Mater 1992;8:305–309.

A New Classification System for Alveolar Bone Morphology around Maxillary Incisors in Adult Patients with Maxillary Protrusion

Qian Yi QIN[1], Yun Fei ZHENG[1], Yi Ping HUANG[1], Yi Fan LIN[2], Run Zhi GUO[1], Wei Ran LI[1]

Objective: *To develop a new alveolar bone morphology classification for maxillary incisors in patients with maxillary protrusion, and to investigate the association of alveolar morphology with skeletal patterns and alveolar bone defects following retraction.*

Methods: *A retrospective study of CBCT scans was performed for 250 patients with maxillary protrusion. The morphology of alveolar bone around maxillary incisors was classified into four types: A1 (upright maxillary incisor in thin alveolar bone), A2 (lingually inclined maxillary incisor in thin alveolar bone), B1 (upright maxillary incisor in thick alveolar bone) and B2 (lingually inclined maxillary incisor in thick alveolar bone). The association of alveolar types with different skeletal patterns and the incidence of post-treatment alveolar bone defects were analysed.*

Results: *For maxillary incisors in patients with maxillary protrusion, A1 was the most common alveolar type (33.4%), followed by A2 (28.5%), B1 (22.1%) and B2 (16.0%). Types B1 (34.4%) and A2 (42.2%) were the most common in maxillary central and lateral incisors, respectively. In high angle patients, A2 and A1 were the most common types for maxillary lateral (49.6%) and central incisors (41.2%), respectively. Additionally, types A1 and A2 were at greater risk of severe lingual dehiscence.*

Conclusion: *This is the first alveolar bone morphology classification for maxillary incisors in patients with maxillary protrusion. The alveolar types exhibited a significant association with skeletal patterns and the incidence of alveolar bone defects after retraction.*

Keywords: *alveolar bone morphology, classification, maxillary incisor*

Chin J Dent Res 2025;28(2):123–129; doi: 10.3290/j.cjdr.b6260618

For patients with maxillary protrusion, extraction of the maxillary premolars followed by maxillary incisor retraction may improve facial harmony and aesthetics. The sagittal position of the maxillary incisors is considered crucial for treatment planning and facial profile evaluation. There are several methods for determining the ideal sagittal position of the maxillary incisors.[1-3] For example, Andrews[1] proposed six elements of orofacial harmony, and suggested the facial-axis point of the maxillary central incisor should be located at the forehead anterior limit line; however, these methods often neglect the alveolar bone morphology surrounding the maxillary incisors, which limits tooth movement. Exceeding these limits during maxillary incisor retraction can lead to alveolar bone defects, such as labial fenestration and lingual dehiscence, as reported by several studies using CBCT.[4,5] Thus, it is important to evaluate the alveolar bone morphology before initiating orthodontic treatment.

Current classification systems for assessing alveolar bone morphology surrounding the maxillary incisors

1 Department of Orthodontics, Peking University School and Hospital of Stomatology, Beijing, P.R. China

2 Division of Paediatric Dentistry and Orthodontics, Faculty of Dentistry, the University of Hong Kong, Hong Kong SAR, P.R. China

Corresponding authors: Dr Run Zhi GUO and Dr Wei Ran LI, Department of Orthodontics, Peking University School and Hospital of Stomatology, #22 Zhongguancun Avenue South, Haidian District, Beijing 100081, P.R. China. Tel: 86-10-82195338. Email: runzhiguo2017@163.com; weiranli@bjmu.edu.cn

This study was supported by grants from Peking University Medicine Sailing Program for Young Scholars' Scientific & Technological Innovation (BMU2023YFJHPY005), the National Key Research and Development Program of China (2023YFC2413604), and Haidian Original Innovation Joint Foundation of Beijing Natural Science (L232026).

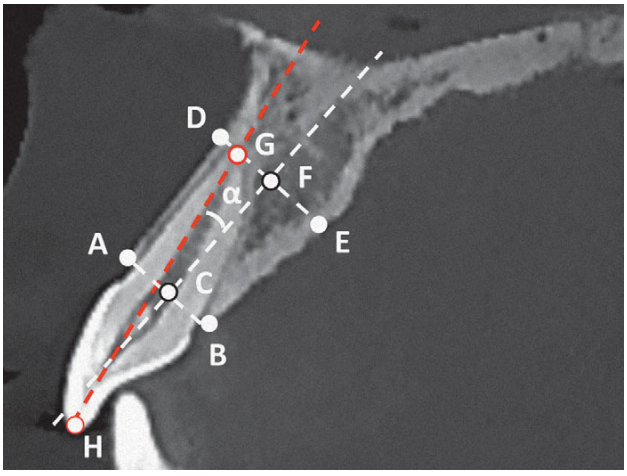

Fig 1 Measurement of alveolar bone thickness (AB, cervical alveolar bone thickness; DE, apical alveolar bone thickness) and maxillary incisor to alveolar bone inclination (angle α, angle between the line HG and the line CF).

are primarily focused on implant treatment. Kan et al[6] and Lau et al[7] classified alveolar bone morphology based on the labial and lingual bone thicknesses and tooth position and angulation for immediate implantation. However, there is a lack of studies regarding the classification of alveolar bone morphology within the context of maxillary incisor retraction in patients with maxillary protrusion.

The present study analysed the maxillary incisor position relative to the corresponding alveolar bone and introduced a new classification system for evaluating alveolar bone morphology in patients with maxillary protrusion. Due to the strong correlation of alveolar bone morphology, including alveolar thickness and tooth inclination, with sagittal and vertical skeletal patterns,[8,9] the present authors further evaluated the distribution of alveolar types across different skeletal patterns and analysed the prevalence of alveolar bone defects following retraction in each alveolar type.

Materials and methods

Participants

This study was approved by the Ethics Committee of Peking University School and Hospital of Stomatology (PKUSSIRB-202168141). Written informed consent was obtained from all participants. The inclusion criteria were age > 18 years, skeletal Class I/II (0° < ANB angle < 8°), maxillary jaw protrusion (SNA angle > 81°),[10] upper lip in front of the E-line (> 1 mm), orthodontic extraction treatment with maxillary incisor retraction (> 3 mm) and available pre- and post-treatment CBCT images. The exclusion criteria were maxillary incisors with obvious crowding (≥ 3 mm), root canal treatment or crowns, moderate to severe root resorption, periodontitis, trauma, tumours, cleft lip and/or palate, systemic disease, smoking and use of medication related to bone metabolism.

A total of 250 patients with maxillary protrusion from the Department of Orthodontics, Peking University School and Hospital of Stomatology were included retrospectively. Three orthodontists (Li WR, Huang YP and Guo RZ) performed the orthodontic treatment using MBT brackets with a 0.022” × 0.028” slot (3M Unitek, Monrovia, CA, USA). Sliding mechanics and one-step retraction were used to retract the maxillary incisors with 0.019” × 0.025” stainless steel. The four maxillary incisors in one patient were analysed separately, resulting in a total of 1,000 maxillary incisors.

CBCT imaging

The CBCT images were generated using a CBCT unit (NewTom VGi, Quantitative Radiology, Verona, Italy) with axial slice thickness 0.25 mm, field of view 16 × 16 cm and scan time 15 s. Raw DICOM data were then imported into Dolphin 3D Imaging software (Dolphin Imaging and Management Solutions, version 11.95 Premium, Chatsworth, CA, USA). The CBCT images of maxillary incisors were orientated by adjusting the axial slice to pass through the cementoenamel junction, with the sagittal slice passing through the long axis of the maxillary incisor (a line connecting the midpoint of the incisal edge and the root apex). The sagittal view of the maxillary incisor acquired in this way was used for further analysis.

Evaluation of alveolar bone morphology

To assess the pre-treatment sagittal root position of maxillary incisors relative to the surrounding alveolar bone, maxillary incisor to alveolar bone inclination and alveolar bone thickness (ABT) at the cervical and apical levels were assessed (Fig 1). The angle between the long axis of the tooth (a line connecting the midpoint of incisal edge and the root apex) and the alveolar bone axis (a line connecting the midpoints of the alveolar bone at the crest and apical levels) was selected as maxillary incisor to alveolar bone inclination.

Alveolar bone defects of the maxillary incisor after retraction, including labial fenestration and lingual dehiscence, were analysed. Labial fenestration was defined as a bone defect involving exposure of the

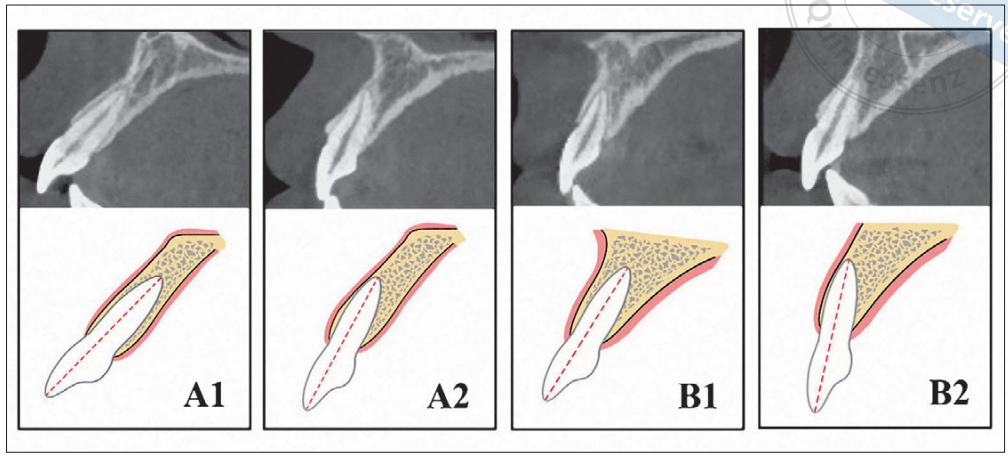

Fig 2 CBCT images and schematic diagrams of four alveolar types (A1, A2, B1 and B2).

labial root surface, lacking a cortical covering, but without involving the alveolar crest.[11] Lingual dehiscence was defined as a defect where the crest of the labial alveolar bone was at least 4 mm apical to that of the interproximal alveolar bone, and was further classified into no or mild, moderate and severe categories (lingual alveolar crest within the cervical, middle and apical thirds of the root, respectively).[12]

New alveolar bone morphology classification

Based on the ABT, alveolar bone morphology of maxillary incisors was initially classified into types A and B, having thin (ABT at apical level less than that at cervical level) and thick alveolar bone (ABT at apical level greater than that at cervical level), respectively. Subtype classification was based on the maxillary incisor to alveolar bone inclination, as reported by Jin et al[13] and Petaibunlue et al.[14] Subtype 1 included maxillary incisors that were upright above the alveolar bone (maxillary incisor to alveolar bone inclination < 20°), whereas subtype 2 included lingually inclined maxillary incisors relative to the alveolar bone (maxillary incisor to alveolar bone inclination ≥ 20°). According to the clinical findings, there were no labially inclined maxillary incisors relative to the alveolar bone (maxillary incisor to alveolar bone inclination < 0°). Altogether, the classification system for alveolar bone morphology of maxillary incisors comprised four alveolar types (A1, A2, B1 and B2) (Fig 2).

Subgroup analysis

To analyse the distribution of the four alveolar types with different sagittal and vertical skeletal patterns, the 250 patients were divided into subgroups according to ANB and SN-MP values. Skeletal Classes I and II were defined as 0° < ANB < 5° and ANB ≥ 5°, respectively. Average, low and high angle skeletal patterns were defined as 28° < SN-MP < 37°, SN-MP ≤ 28° and SN-MP ≥ 37°, respectively. Additionally, the prevalence of post-treatment alveolar bone defects among the four alveolar types was analysed.

Statistical analysis

Twenty patients were randomly selected for reproducibility analysis. The pre-treatment alveolar bone morphology classification and post-treatment alveolar bone defect diagnosis were assessed independently by two examiners (Guo RZ and Qin QY) and repeated after 2 weeks. The intra- and inter-examiner agreements were assessed using a weighted Cohen kappa test. The new classification system showed excellent intra- and inter-examiner agreement (0.962 and 0.974, respectively). For the diagnosis of post-treatment alveolar bone defects, the intra- and inter-examiner agreement was also satisfactory (0.924 and 0.939, respectively). A chi-square test was applied to compare the distribution of alveolar types among groups. Statistical analyses were conducted using SPSS Statistics software (version 26; IBM, Armonk, NY, USA). The level of statistical significance was set at 0.05.

Results

Distribution of alveolar types among maxillary incisors

The basic characteristics of the participants are shown in Table 1. The alveolar bone morphology surrounding the maxillary incisors was predominantly characterised as type A (61.9%), whereas type B accounted for 38.1% (Table 2). Among the four types, A1 (33.4%) was

Table 1 Demographic information of patients included in the study.

Measurements	Mean ± SD
Age (y)	25.30 ± 5.70
Sex (male/female)	29/221
Angle classification (Class I/Class II)	191/59
Vertical overlap (mm)	1.35 ± 1.20
Horizontal overlap (mm)	4.19 ± 1.82
SNA (°)	86.26 ± 2.89
ANB (°)	5.96 ± 2.19
SN-MP (°)	37.00 ± 6.37
U1-SN (°)	110.19 ± 6.40
Nasolabial angle (°)	93.96 ± 10.57

the most common, followed by A2 (28.5%), B1 (22.1%) and B2 (16.0%). The distribution of alveolar types varied significantly between the maxillary central and lateral incisors. Types A1 (33.6%) and B1 (34.4%) were most common around maxillary central incisors, whereas A2 (42.2%) and A1 (33.2%) were most common around maxillary lateral incisors.

Alveolar type distribution in different skeletal patterns

As shown in Table 3, the distribution of the four alveolar types differed significantly between skeletal Class I and Class II patients for both the maxillary central incisor ($P = 0.038$) and lateral incisor subgroups ($P = 0.002$). Skeletal Class II participants had a higher proportion of type 2 alveolar bone (maxillary central incisor 35.3%; maxillary lateral incisor 58.7%) compared to Class I patients (maxillary central incisor 23.2%; maxillary lateral incisor 52.3%). For maxillary lateral incisors, type A1 was more common in skeletal Class I patients (37.3%), whereas type A2 was the most common alveolar type in skeletal Class II patients (46.7%).

Significant differences were also observed in alveolar type distribution among the vertical skeletal patterns ($P < 0.001$ for both maxillary central and lateral incisors). For maxillary central incisors, type B accounted for 56.3%, 78.5% and 44.4% of the average, low and high angle patients, respectively. Regarding the subtypes, B1 was the most common alveolar type in average (41.0%) and low angle (67.9%) patients, whereas A1 was the most common in high angle patients (41.2%). For maxillary lateral incisors, type A was the most common alveolar type in all vertical skeletal patterns. Types A2 (49.6%) and A1 (36.8%) accounted for the majority of high angle patients. Type B was more common in low angle patients (46.4%) compared to average (34.2%) and high angle (13.6%) patients.

Prevalence of alveolar bone defects among alveolar bone morphological types

Following maxillary incisor retraction, the "no or mild lingual dehiscence" category accounted for the majority of type B1 (maxillary central incisor 72.7%; maxillary lateral incisor 61.2%) and B2 cases (maxillary central incisor 62.8%; maxillary lateral incisor 41.9%) (Table 4). Compared to other types, A1 and A2 were at greater risk of severe lingual dehiscence (maxillary central incisor 25.0% and 24.3%; maxillary lateral incisor 31.9% and 40.8%, respectively). Type B1 had the lowest prevalence of labial fenestrations (maxillary central incisor 4.6%; maxillary lateral incisor 14.3%), whereas type B2 in maxillary lateral incisors had the highest prevalence of 27.0%.

Discussion

For patients with maxillary protrusion, maxillary incisor retraction can enhance aesthetics, but it poses a risk of alveolar bone defects. Several CBCT studies have reported a high incidence of alveolar bone defects following maxillary incisor retraction.[15,16] The present authors' previous research demonstrated that the lingual cortical bone was a critical boundary for maxillary incisor retraction, with lingual dehiscence occurring once teeth breached this boundary.[5] Consequently, there is an increasing emphasis on the use of CBCT for evaluating the pre-treatment alveolar bone morphology to minimise the occurrence of alveolar bone defects.[17,18]

Existing classification criteria for alveolar bone morphology of maxillary incisors focus primarily on implant treatment, often taking ABT and tooth position into consideration. Kan et al[6] previously proposed four types of alveolar bone morphology based on the labial and lingual ABT. The present classification system simplified ABT into thin (type A) and thick (type B) types. A previous study reported predominantly thin labial alveolar bone in patients with maxillary protrusion, consistent with the present findings.[19] The labial ABT was thin in both types A and B, whereas the lingual ABT in types A and B was thin and thick, respectively. Due to alveolar bone remodelling, the labial ABT remained relatively stable and the lingual ABT significantly decreased during maxillary incisor retraction. Regarding tooth position, Zhang et al[20] classified it as the root being positioned against the labial cortex, against the lingual cortex or in the centre of the alveolar housing. Orthodontic treatment aims to maintain an upright position of the maxillary incisors within the alveolar bone during retraction. Therefore, the present

Table 2 Distribution of alveolar types among maxillary incisors.

Tooth	Type A1	Type A2	Type B1	Type B2	*P* value
Maxillary incisor	33.4% (334/1,000)	28.5% (285/1,000)	22.1% (221/1,000)	16.0% (160/1,000)	
Maxillary central incisor	33.6% (168/500)	14.8% (74/500)	34.0% (172/500)	17.2% (86/500)	< 0.001
Maxillary lateral incisor	33.2% (166/500)	42.2% (211/500)	9.8% (49/500)	14.8% (74/500)	

Table 3 Distribution of alveolar type in different skeletal patterns.

Skeletal pattern		Maxillary central incisor					Maxillary lateral incisor				
		Type A1	Type A2	Type B1	Type B2	*P* value	Type A1	Type A2	Type B1	Type B2	*P* value
Sagittal skeletal type	Skeletal Class I	34.3% (46/134)	11.9% (16/134)	42.5% (57/134)	11.3% (15/134)	0.038*	37.3% (50/134)	29.9% (40/134)	10.4% (14/134)	22.4% (30/134)	0.002*
	Skeletal Class II	33.3% (122/366)	15.9% (58/366)	31.4% (115/366)	19.4% (71/366)		31.7% (116/366)	46.7% (171/366)	9.6% (35/366)	12.0% (44/366)	
Vertical skeletal type	Average angle	27.0% (60/222)	16.7% (37/222)	41.0% (91/222)	15.3% (34/222)	< 0.001**	30.2% (67/222)	35.6% (79/222)	14.0% (31/222)	20.2% (45/222)	< 0.001**
	Low angle	17.9% (5/28)	3.6% (1/28)	67.9% (19/28)	10.6% (3/28)		25.0% (7/28)	28.6% (8/28)	25.0% (7/28)	21.4% (6/28)	
	High angle	41.2% (103/250)	14.4% (36/250)	24.8% (62/250)	19.6% (49/250)		36.8% (92/250)	49.6% (124/250)	4.4% (11/250)	9.2% (23/250)	

*$P < 0.05$, **$P < 0.001$.

Table 4 Prevalence of alveolar bone defects among alveolar bone morphological types.

Alveolar type		No or mild lingual dehiscence	Moderate lingual dehiscence	Severe lingual dehiscence	Labial fenestration	*P* value
Maxillary central incisor	Type A1	48.8% (82/168)	13.7% (23/168)	25.0% (42/168)	12.5% (21/168)	< 0.001
	Type A2	32.4% (24/74)	31.1% (23/74)	24.3% (18/74)	12.2% (9/74)	
	Type B1	72.7% (125/172)	16.9% (29/172)	5.8% (10/172)	4.6% (8/172)	
	Type B2	62.8% (54/86)	12.8% (11/86)	12.8% (11/86)	11.6% (10/86)	
Maxillary lateral incisor	Type A1	27.1% (45/166)	19.3% (32/166)	31.9% (53/166)	21.7% (36/166)	< 0.001
	Type A2	21.8% (46/211)	19.4% (41/211)	40.8% (86/211)	18.0% (38/211)	
	Type B1	61.2% (30/49)	18.4% (9/49)	6.1% (3/49)	14.3% (7/49)	
	Type B2	41.9% (31/74)	17.6% (13/74)	13.5% (10/74)	27.0% (20/74)	

authors first used the alveolar bone axis as a reference and classified the alveolar bone into two subtypes, i.e., upright maxillary incisors (subtype 1) and lingually inclined maxillary incisors (subtype 2), based on the angle between the long axis of the tooth and the alveolar bone axis. To the best of the present authors' knowledge, this is the first classification system for alveolar bone morphology around maxillary incisors in patients with maxillary protrusion.

According to the present authors' new classification system, significant differences in alveolar bone morphology were observed between maxillary central and lateral incisors. Studies have reported that maxillary lateral incisors typically exhibit narrower alveolar bone widths compared with maxillary central incisors, particularly in the apical region, consistent with the present findings.[20,21] The prevalence of type A was 48.4% in maxillary central incisors and 75.4% in maxillary lateral incisors. Jin et al[13] reported that maxillary central incisors were positioned upright within the alveolar bone in 74.67% of men and 84.66% of women. The present results indicated that types B1 and A1 were more common in maxillary central incisors, whereas type A2 was more common in maxillary lateral incisors. Aside from the thinner alveolar bone, maxillary lateral incisors also exhibited a lingual inclination relative to the alveolar bone axis.

Differences in alveolar bone morphology among different skeletal patterns have been reported. Dalaie et al[8] reported that high angle individuals often presented with thinner alveolar bone around maxillary central incisors. Similarly, Son et al[22] demonstrated that Class II malocclusions with a high angle and normal maxillary incisor inclination were a risk factor for lin-

gual bone loss. In line with these findings, the present study demonstrated that type A was more common in high angle patients, whereas type B was more common in those with average and low angle patterns. In high angle patients, A1 and A2 were the most common types in the maxillary central and lateral incisors, respectively. Regarding the sagittal skeletal patterns, Class II patients had a higher proportion of type 2 alveolar bone compared to Class I patients because of the compensatory lingual inclination of maxillary incisors in Class II patients. Thus, the vertical skeletal pattern primarily influenced the ABT, whereas the sagittal skeletal pattern influenced the maxillary incisor position.

The incidences of alveolar bone defects, including lingual dehiscence and labial fenestration, among the four types were further evaluated. Compared to maxillary incisors with type B alveolar bone, those with type A bone were at a greater risk of lingual dehiscence following retraction. In particular, the incidence rates of severe lingual dehiscence in maxillary lateral incisors with type A1 and A2 bone were 31.9% and 40.8%, respectively. Sheng et al[4] demonstrated that the apex to labiolingual ABT before orthodontic treatment was inversely related with the risk of bone defect occurrence. Hence, excessive retraction of maxillary incisors with type A bone should be performed cautiously. Labial fenestration is another common alveolar bone defect during maxillary incisor retraction. The present authors found that the incidence of labial fenestration in maxillary lateral incisors was higher than that in maxillary central incisors. In addition, labial fenestration was more common in maxillary incisors with subtype 2 compared to those with subtype 1. Subtype 2 often requires torque control in maxillary incisors to mitigate the risk of labial fenestration during long-distance retraction. Thus, a clear association was present between the original alveolar bone morphology and the occurrence of alveolar bone defects after treatment. It is therefore essential to evaluate the initial condition of the alveolar bone using CBCT scans before proceeding with orthodontic treatment. This classification system could enhance the predictability of alveolar bone defects following maxillary incisor retraction and facilitate clinical decision-making.

Several considerations require emphasis during the application of this classification. The retraction distance of maxillary incisors was not considered. Hence, the reported predictability of alveolar bone defects following maxillary incisor retraction was preliminary. Additionally, there were no cases of labial bone dehiscence or lingual bone fenestrations in this study. Consequently, these defects could not be analysed. In these 250 patients, there were no cases with labially inclined maxillary incisors relative to the alveolar bone. Further studies with larger sample sizes are needed to verify the present results and improve the classification. Meanwhile, analysis of the association between the classification system and other factors, such as age and sex, will also be performed in further studies.

Conclusion

A new classification of alveolar bone morphology around maxillary incisors for patients with maxillary protrusion was proposed in this study. A1 was the most frequently observed type, with A1 and B1 being common in maxillary central incisors, and A2 being more common in maxillary lateral incisors. The alveolar type surrounding the maxillary incisors was significantly associated with the skeletal patterns. Type A was the main alveolar type in high angle patients, whereas type B was more common in average and low angle patients. Skeletal Class II patients had a higher proportion of subtype 2 compared to skeletal Class I patients. Pre-treatment alveolar type was significantly associated with the occurrence of alveolar bone defects after treatment. Maxillary incisors with type A bone, particularly lateral incisors with type A2 bone, had a higher risk of lingual dehiscence following retraction.

Conflicts of interest

The authors declare no conflicts of interest related to this study.

Author contribution

Dr Qian Yi QIN contributed to the data analysis and manuscript draft; Drs Yun Fei ZHENG, Yi Ping HUANG, and Yi Fan LIN contributed to the CBCT data collection and statistical analysis; Dr Run Zhi GUO contributed to the study design and manuscript draft; Dr Wei Ran LI contributed to the study conception and manuscript revision.

(Received Sep 4, 2024; accepted Dec 21, 2024)

References

1. Andrews WA. AP relationship of the maxillary central incisors to the forehead in adult white females. Angle Orthod 2008;78:662–669.
2. Cao L, Zhang K, Bai D, Jing Y, Tian Y, Guo Y. Effect of maxillary incisor labiolingual inclination and anteroposterior position on smiling profile esthetics. Angle Orthod 2011;81:121–129.

3. Naini FB, Manouchehri S, Al-Bitar ZB, Gill DS, Garagiola U, Wertheim D. The maxillary incisor labial face tangent: Clinical evaluation of maxillary incisor inclination in profile smiling view and idealized aesthetics. Maxillofac Plast Reconstr Surg 2019;41:31.
4. Sheng Y, Guo HM, Bai YX, Li S. Dehiscence and fenestration in anterior teeth : Comparison before and after orthodontic treatment. J Orofac Orthop 2020;81:1–9.
5. Guo R, Li L, Lin Y, et al. Long-term bone remodeling of maxillary anterior teeth with post-treatment alveolar bone defect in adult patients with maxillary protrusion: A prospective follow-up study. Prog Orthod 2023;24:36.
6. Kan JY, Roe P, Rungcharassaeng K, et al. Classification of sagittal root position in relation to the anterior maxillary osseous housing for immediate implant placement: A cone beam computed tomography study. Int J Oral Maxillofac Implants 2011;26:873–876.
7. Lau SL, Chow J, Li W, Chow LK. Classification of maxillary central incisors-implications for immediate implant in the esthetic zone. J Oral Maxillofac Surg 2011;69:142–153.
8. Dalaie K, Hajimiresmail YS, Safi Y, Baghban AA, Behnaz M, Rafsanjan KT. Correlation of alveolar bone thickness and central incisor inclination in skeletal Class I and II malocclusions with different vertical skeletal patterns: A CBCT study. Am J Orthod Dentofacial Orthop 2023;164:537–544.
9. Yagci A, Veli I, Uysal T, Ucar FI, Ozer T, Enhos S. Dehiscence and fenestration in skeletal Class I, II, and III malocclusions assessed with cone-beam computed tomography. Angle Orthod 2012;82:67–74.
10. El H, Palomo JM. An airway study of different maxillary and mandibular sagittal positions. Eur J Orthod 2013;35:262–270.
11. Evangelista K, Vasconcelos Kde F, Bumann A, Hirsch E, Nitka M, Silva MA. Dehiscence and fenestration in patients with Class I and Class II division 1 malocclusion assessed with cone-beam computed tomography. Am J Orthod Dentofacial Orthop 2010;138:133.e1–e7.
12. Davies RM, Downer MC, Hull PS, Lennon MA. Alveolar defects in human skulls. J Clin Periodontol 1974;1:107–111.
13. Jin L, Bishuang P, Yulan X, Chengze W, Gang W, Jing L. The influence of angulation of maxillary anterior teeth on treatment design of dental implants [in Chinese]. Hua Xi Kou Qiang Yi Xue Za Zhi 2016;34:611–616.
14. Petaibunlue S, Serichetaphongse P, Pimkhaokham A. Influence of the anterior arch shape and root position on root angulation in the maxillary esthetic area. Imaging Sci Dent 2019;49:123–130.
15. Ahn HW, Moon SC, Baek SH. Morphometric evaluation of changes in the alveolar bone and roots of the maxillary anterior teeth before and after en masse retraction using cone-beam computed tomography. Angle Orthod 2013;83:212–221.
16. Yang CYM, Atsawasuwan P, Viana G, et al. Cone-beam computed tomography assessment of maxillary anterior alveolar bone remodelling in extraction and non-extraction orthodontic cases using stable extra-alveolar reference. Orthod Craniofac Res 2023;26:265–276.
17. Leung CC, Palomo L, Griffith R, Hans MG. Accuracy and reliability of cone-beam computed tomography for measuring alveolar bone height and detecting bony dehiscences and fenestrations. Am J Orthod Dentofacial Orthop 2010;137: S109–S119.
18. Kapila SD, Nervina JM. CBCT in orthodontics: assessment of treatment outcomes and indications for its use. Dentomaxillofac Radiol 2015;44:20140282.
19. Tsigarida A, Toscano J, de Brito Bezerra B, et al. Buccal bone thickness of maxillary anterior teeth: A systematic review and meta-analysis. J Clin Periodontol 2020;47:1326–1343.
20. Zhang LQ, Zhao YN, Zhang YQ, Zhang Y, Liu DG. Morphologic analysis of alveolar bone in maxillary and mandibular incisors on sagittal views. Surg Radiol Anat 2021;43:1009–1018.
21. Zhang W, Skrypczak A, Weltman R. Anterior maxilla alveolar ridge dimension and morphology measurement by cone beam computerized tomography (CBCT) for immediate implant treatment planning. BMC Oral Health 2015;15:65.
22. Son EJ, Kim SJ, Hong C, et al. A study on the morphologic change of palatal alveolar bone shape after intrusion and retraction of maxillary incisors. Sci Rep 2020;10:14454.

THE WHOLE PICTURE

NEW

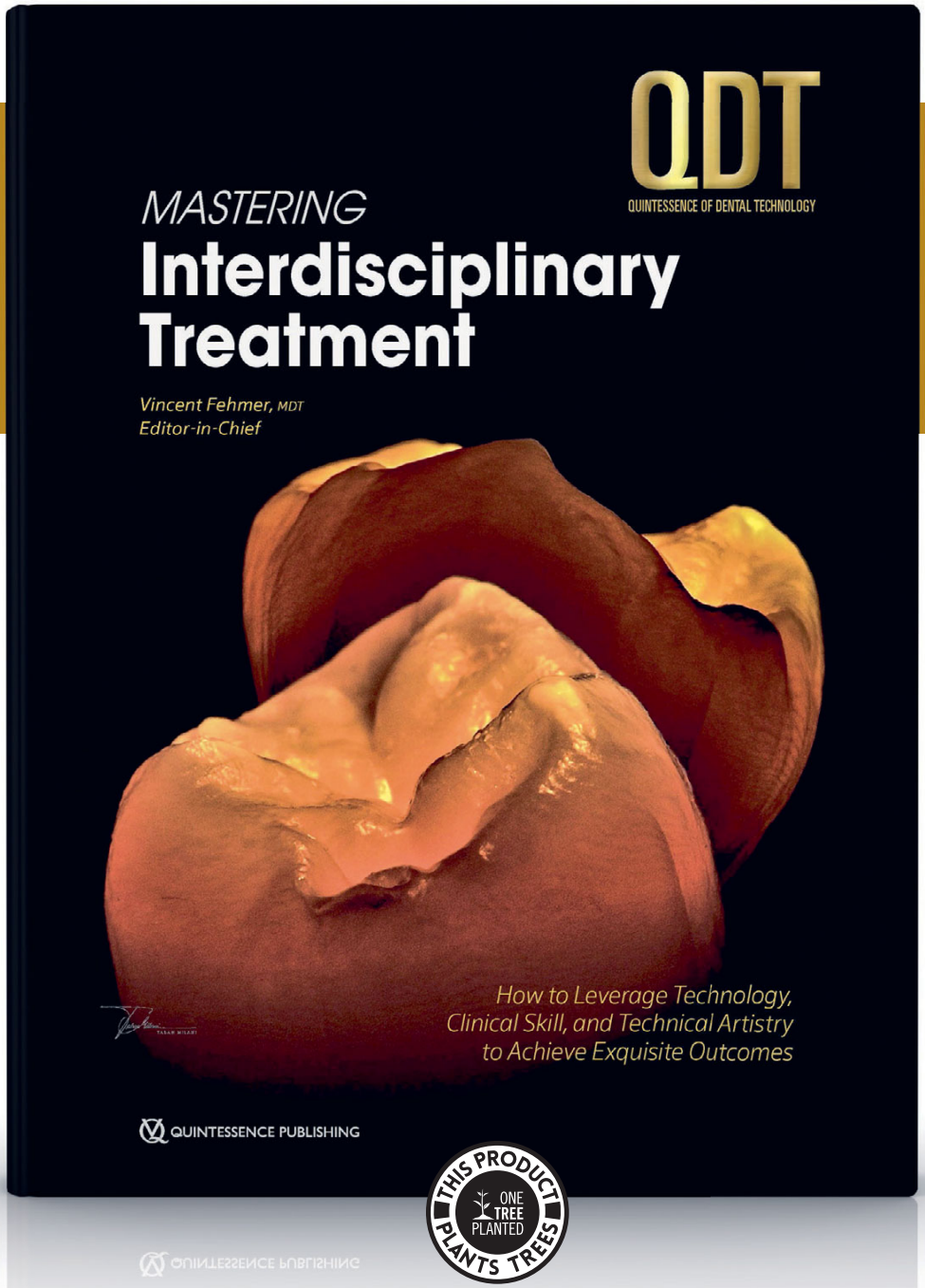

Vincent Fehmer (Ed)

Mastering Interdisciplinary Treatment

How to Leverage Technology, Clinical Skill, and Technical Artistry to Achieve Exquisite Outcomes

276 pages, 742 illus
ISBN 978-1-64724-201-5, €168

QDT has always served dental technicians with the best of the best work being done in the field. But technical artistry is only half of the equation, which is why QDT 2025 focuses on the whole picture of interdisciplinary dentistry, highlighting how clinician and technician work together to achieve predictable and esthetic outcomes. This year's issue is stacked with several articles on FP1 prostheses and the digital workflows and procedures required for their planning and delivery, as well as multiple articles on minimally invasive laminate veneers and other topics relevant to daily practice, such as the fabrication of digital complete dentures, shade matching zirconia crowns, and managing the single central incisor. Throughout the issue, the latest technologies and their capabilities are emphasized, truly reflecting this era of digital dentistry while always relying on the foundation of manual skills and artistry, which can never fully be replaced by digital tools. With such a stellar group of contributing authors, this may just be the best issue of QDT yet.

www.quint.link/qdt25
books@quintessenz.de
+49 (0)30 761 80 667

QUINTESSENCE PUBLISHING

Assessment of the Canalis Sinuosus Using CBCT in Pathological Lesions

Numan DEDEOĞLU[1], Oğuzhan ALTUN[1]

Objective: *To assess the canalis sinuosus (CS) in pathological lesions located in the anterior maxilla using CBCT.*

Methods: *In total, 104 lesions in the anterior maxilla were assessed. The localisation of CS termination points on the alveolar crest was evaluated. Subsequently, the consistency of the CS and CS–lesion relationships were determined based on the maximal diameter of the lesion and the presence of a cortical perforation.*

Results: *Of the 104 lesions, 82 (78.8%) exhibited at least one CS. The presence of CS was statistically significantly different based on the diameter of the lesion ($P < 0.001$). When the presence of CS was investigated in relation to cortical perforation status, a significant difference was observed ($P < 0.05$). Anatomically, CS was most common in the central incisor and ended most frequently near the crest apex vertically and in the palatal region horizontally. Among the instances of CS, 55.3% were lesion-related, 22.3% were in contact and 23 (22.3%) were unrelated to the lesion.*

Conclusion: *The incidence of CS was high in anterior maxillary pathological lesions and even higher in small-sized pathological lesions. Most CSs were located within or next to the surgical margin of the pathological lesion.*

Keywords: *canalis sinuosus, CBCT, maxilla, oral surgery, pathological lesion*

Chin J Dent Res 2025;28(2):131–137; doi: 10.3290/j.cjdr.b6260624

The nasopalatine canal in the anterior maxilla is considered highly important by dental clinicians because of its potential clinical impacts.[1] Nevertheless, most clinicians are unaware of the canalis sinuous (CS) and lack knowledge regarding its diagnosis.[2] The CS is a branch of the infraorbital canal enclosing the anterior superior alveolar neurovascular structure, and the termination point of this intraosseous canal is in the anterior maxilla.[3-5] The neurovascular bundle within the CS innervates the anterior maxillary teeth, the floor of the nasal cavity and the maxillary sinuses. In the anterior maxilla, several procedures are conducted, including dental implant surgery, orthognathic surgery, extraction of impacted or supernumerary teeth, periodontal and endodontic surgery and cyst treatments.[6] A lack of anatomical knowledge about CS can cause pain, local infection and even paraesthesia.[4] Thus, preventing injury during local anaesthesia and maxillofacial surgery requires a comprehensive understanding of key anatomical reference points and areas in the oral and maxillofacial regions, particularly regarding the CS.[7]

Individuals diagnosed with anterior maxillary intraosseous pathological lesions (IPLs) are likely to require surgical intervention, and the surgical risks related to the CS apply to these patients as well. Multiple studies on the prevalence of CS conducted in different countries using CBCT have acknowledged the clinical significance of the CS; however, none have assessed IPLs in the anterior maxilla as yet.[1,6,8-14] Thus, adequate anatomical and clinical information regarding the CS in the anterior maxilla with pathological lesions is lacking. The present study aimed to determine the clinical importance of the CS through CBCT images of patients diagnosed with anterior maxillary IPLs. Moreover, using the collected clinical data, the present authors aimed to identify and mitigate potential risks and complications before surgery for pathological lesions in the anterior maxilla.

1 Inonu University, Faculty of Dentistry, Department of Oral and Maxillofacial Radiology, Malatya, Turkey

Corresponding author: Dr Numan DEDEOĞLU, Department of Oral and Maxillofacial Radiology, Faculty of Dentistry, Inonu University, 44280, Malatya, Turkey. Tel: 90-535-4808325; 90-422-3411106. Email: dedenu@gmail.com

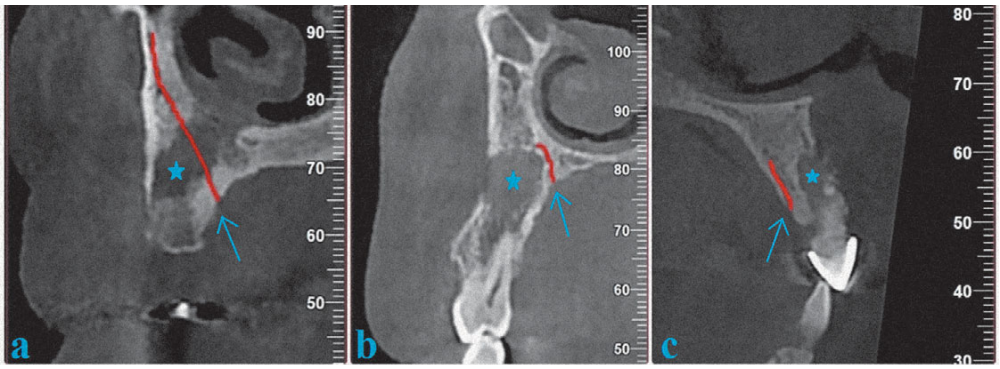

Fig 1a to c CSs that were related to **(a)**, in contact with **(b)** and not associated with the bony tissue lesion **(c)** (star, IPL; arrow, ending of CS).

Materials and methods

This study was approved by the university's scientific research and publication ethics committee (2023/4846).

Study population

A total of 104 IPLs in the anterior maxilla of 83 patients were evaluated cross-sectionally. IPLs in the anterior maxilla were assessed using CBCT. In the images of the patient's anterior maxilla, when the normal bone tissue was disrupted and replaced by a hypodense appearance, it was considered an intraosseous pathology. The inclusion criteria were as follows:

- intraosseous lesions between the maxillary right and left premolar regions;
- extensive intraosseous lesions between the anterior and posterior maxilla;
- intraosseous pathologies presenting a lesion centred in the posterior maxilla and extending to the anterior premolar region.

The exclusion criteria were as follows:

- individuals with cleft lip and palate;
- individuals with plates or miniscrews in the anterior maxilla resulting from trauma or other factors;
- individuals with dental implants in the anterior maxilla;
- individuals having undergone grafting procedures or surgical operations;
- individuals with low quality CBCT records (caused by beam hardening and movement);
- individuals with conditions and medications that impact bone metabolism.

CBCT technique

Images acquired using a NewTom 5G CBCT device (Verona, Italy) were used in this study, and NNT software (NewTom) was employed for evaluation. The patients were placed in a supine position while being scanned on the device, which incorporates a gantry. The exposure parameters were 110 kv, 1-20 mA, with a scan time of 18 seconds and exposure time of 3.6 seconds.

Image assessment

The presence of CS was analysed in axial, coronal and sagittal sections in multiplanar reformat (MPR) images with voxel values of 0.3, 0.25 and 0.2 mm and cross-sections with a thickness of 0.3, 0.25 and 0.20 mm. Subsequently, measurements were taken and other evaluations were conducted on cross-sections with a thickness of 0.3, 0.25 and 0.2 mm. All evaluations were performed by a clinician (ND) with 12 years of experience in CBCT.

The CS begins at the infraorbital foramen and orbital base, extending medially and inferiorly. It then proceeds from the front of the maxillary sinus to the lateral and inferior border of the nasal cavity, before reaching the anterior maxilla and ending at the accessory foramen (AF), continuing from the lateral aspect of the nasal septum and the front of the incisive canal.[1]

In the present study, when a pathological lesion was situated on the right or left side, the CS was assessed between the midline and the second premolar. The presence of CS was assessed between the right and left second premolars in patients with bilaterally extending pathological lesions. In scenarios with more than one lesion on one side of the anterior maxilla, CS was investigated between the midpoint of the intact bone and the second premolar and midline between the two lesions. The presence of CS was recorded separately for men and women. CSs were categorised into three groups based on their relationship with the pathologic lesion: CS in direct relation with the pathology, CS in contact with the lesion but with cortical bone separating the CS and the lesion, and CS not associated with the le-

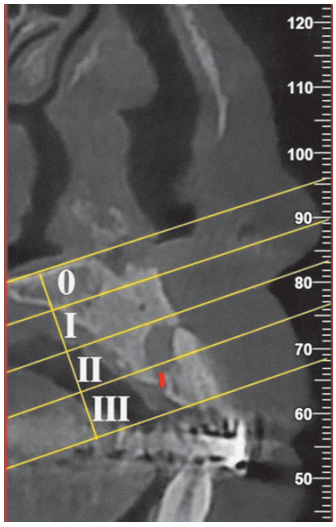

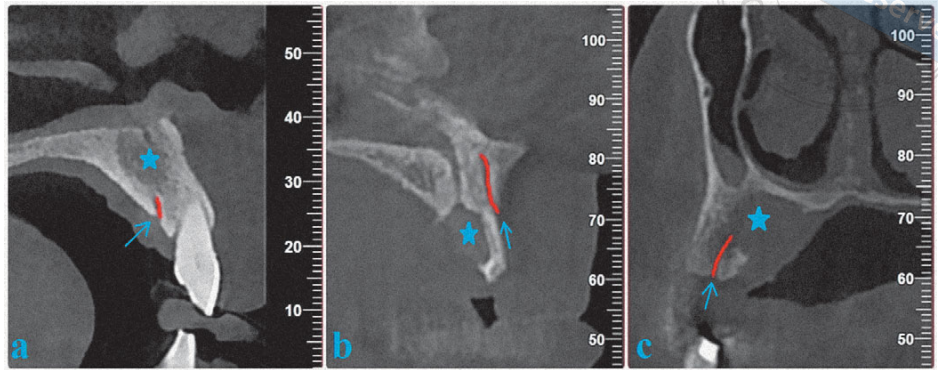

Fig 2 (left) Vertical orientation of the CS from the base of the nasal cavity to the apex of the crest apex was shown with a numerical value ranging from 0 to III.

Fig 3a to c (top) On the alveolar ridge, horizontal localisation of CS termination was shown as palatinal **(a)**, buccal **(b)** and crest apex **(c)** (star, IPL; arrow, ending of CS).

sion with bony tissue between the CS and the lesion (Fig 1). The termination point of the CS was considered to be the AF and its diameter was measured. This value was recorded as less than or greater than 1 mm. The anatomical points along the dental arch where the CS termination point was present were categorised based on the Oliveria Santos classification (central incisor, between central and lateral teeth, lateral incisor region, canine region, first premolar, adjacent to the incisive foramen; posterior/anterior/lateral).[8] Nonetheless, CSs in the second premolars were also deemed as premolars because of the lesion expansion phenomenon. The vertical position of CS termination in the alveolar crest was categorised using the classification developed by Khojastepour and Akbarizadeh.[12] The alveolar ridge was divided into four equal parts, extending from its highest point at the crest to the floor of the nasal cavity. Each section, from the base of the nasal cavity to the apex of the crest, was labelled with a numerical value from 0 to III (Fig 2). The section that contained the CS opening was recorded. Additionally, the palatal, buccal and crest apex termination of the CS in the alveolar ridge in the horizontal direction were recorded (Fig 3).[6]

The maximum diameters of the pathological lesions were measured. Moreover, lesions were sorted into 0 to 10, 10 to 20, 20 to 30, 30 to 40 and > 40 mm groups based on their maximum diameter, and CS presence was assessed according to these groupings. Subsequently, cortical perforation in pathological lesions was examined, and CS presence was assessed based on the perforation status.

Statistical analysis

Descriptive analysis and chi-square tests were used to compare categorical independent variables across groups. A Bonferroni corrected Z test was used to analyse multiple comparisons of proportions. Maximum diameters of pathological lesions and CS termination diameters were remeasured for 40% of the data 2 weeks later to analyse intraobserver agreement using a Kappa test. The level of statistical significance was set at $P < 0.05$.

Results

This study assessed 104 pathological lesions in the maxilla of 83 patients. In total, 66 patients had one lesion, 13 had two lesions and 4 had three lesions. Of these 83 patients, 49 (59%) were male and 34 (41%) were female (Table 1). Of the 104 pathological lesions assessed, 60 (57.7%) were observed in men and 44 (42.3%) in women. Regarding the distribution of pathological lesions, 33 (31.7%) were present on the right side, 44 (42.3%) on the left, and 27 (26%) on both sides (Table 1). At least one CS was detected in 82 (78.8%) of the 104 lesions, and in 47 (57.3%) men and 35 (42.7%) women (Table 1). Additionally, the presence of at least one CS did not reveal a statistically significant difference between sexes ($P = 0.881$). Overall, 63 pathological lesions had one CS, 17 had two and two had three, to give 103 CSs in total (Table 1). The Kappa values for intraobserver agreement on the maximum diameter of the pathological lesion and CS diameter were 0.96 and 0.88, respectively.

Table 1 Number of IPLs and CSs according to patient, sex and side.

Variable	Number			Total
	1	2	3	
Patient	66	13	4	83
IPL	66	13	4	104
CS	63	17	2	103
Sex	Female	Male		Total
Patient	34	49		83
IPL	44	60		104
At least one CS	47	35		82
Side	Right	Left	Bilateral	Total
IPL	33	44	27	104

Table 2 Comparison of CS presence according to perforation of pathological lesions (chi-square test).

Cortical status of IPL	CS		*P* value
	Presence	Absence	
Cortical perforated lesion	51 (72.9%)	19 (27.1%)	0.032
Cortical intact lesion	31 (91.2%)	3 (8.8%)	

Cortical perforation was confirmed in 70 (67.3%) pathological lesions, whereas intact cortical borders were detected in 34 (32.7%) lesions. Cortical perforation was associated with CS in 51 (72.9%) pathological lesions, whereas CS without cortical perforation was observed in 31 (91.2%) lesions. A statistically significant difference ($P = 0.032$) was observed when the presence of cortical perforation in pathological lesions was compared based on the presence of CS (Table 2).

The pathological lesions were categorised according to their maximal diameters: 0 to 10, 10 to 20, 20 to 30, 30 to 40 and > 40 mm. CS was identified in all 29 lesions (100%) in the 0 to 10 mm group, 32 (84.2%) of 38 lesions in the 10 to 20 mm group, 11 (61.1%) of 18 lesions in the 20 to 30 mm group, 8 (80%) of 10 lesions in the 30 to 40 mm group, and 2 (22.2%) of 9 lesions in the > 40 mm group. The groups, categorised based on lesion diameter, exhibited statistically significant differences in terms of CS presence ($P < 0.001$). Significant differences were observed between the 0 to 10 mm and 20 to 30 mm, 30 to 40 mm and > 40 mm, 10 to 20 mm and > 40 mm groups (Table 3).

The mean diameter of the AF was 0.667 mm with a minimum of 0.2 mm, a maximum of 1.6 mm and standard deviation of ± 0.298 mm. Eleven patients (10.7%) had an AF diameter > 1 mm. CS termination regions were present in the central incisor for 36 (35%) patients, between the central and lateral incisor for 8 (7.8%), lateral incisor for 18 (17.5%), canine for 17 (16.5%) and premolar for 24 (23.3%).

The localisation evaluation in the vertical orientation and apical-incisal direction revealed that the termination occurred in 9 (8.7%) cases of Type 0, 14 (13.6%) of Type I, 32 (31.1%) of Type II, and 48 (46.4%) of Type III. In the horizontal orientation, 87 (84.5%) of the CSs ended in the palatal direction, 6 (5.8%) in the buccal direction and 10 (9.7%) transversely.

In the present study, 57 (55.3%) of the CSs were related to the lesion, 23 (22.3%) were in contact and 23 (22.3%) were not related.

Discussion

Differentiating the CS using conventional, two-dimensional, panoramic and periapical radiography techniques commonly employed in dentistry is highly challenging. CBCT is highly effective in assessing the CS and enables 3D evaluation of the path of the canal in the anterior maxilla across axial, coronal and sagittal sections.[15] In the present study, CBCT was used to assess the CS. Furthermore, thin cross-sections aside from axial, coronal and sagittal sections were examined. The recommended slice thickness for CBCT evaluation of the CS is 0.5 to 1 mm.[11] The present authors employed a more meticulous evaluation method by examining CBCT values with lower voxel sizes, namely 0.3 to 0.25 and 0.2 mm.

The presence of CS in the anterior maxilla is common; however, its proximity to surgical sites may cause pain and bleeding during and after surgical proced-

Table 3 Comparison of CS presence according to maximum diameter of IPLs (chi-square test).

Lesion max diameter, mm	CS		*P* value
	Presence number (%)	Absence number (%)	
0–10	29 (100%)[a]	0 (0.0)	< 0.001
10–20	32 (84.2%)[ab]	6 (15.8)	
20–30	11 (61.1%)[bc]	7 (38.9)	
30–40	8 (80.0%)[abc]	2 (20.0)	
> 40	2 (22.2%)[c]	7 (77.8)	

a-c, there was no difference between diameters with the same letter.

ures.[1] Thus, the use of CBCT for identifying CSs prior to surgical procedures is crucial in preventing accidents and complications, such as dental implant failure, sensory disturbances and bleeding.[16,17] Moreover, nerve injury can be avoided by accurately determining the location of CSs through CBCT prior to implant surgery.[4] Research employing CBCT technology in patients with impacted canines scheduled for surgical intervention found the mean distance between the CS and the impacted teeth to be approximately 5.27 mm, with the shortest measured distance being 0.75 mm.[14] In the present study, 55.3% of the CSs were directly related to pathological lesions, whereas 22.3% were in close contact; thus, most CSs were located within or near the surgical margins of the pathological lesions. However, no clinical studies discussing whether these pathological lesions can lead to bleeding or paraesthesia during or after surgery were found in the literature.

According to CBCT studies conducted on maxillae with no pathological lesions, the occurrence of CS ranges from 15.7% to 100%.[1,8-15,18,19] The present study, the first in the literature in this field, examined anterior maxillae with IPLs, including those < 1 mm in diameter. The frequency of CS was determined to be 78.8%, which aligned with the results reported in previous studies. Moreover, the present study showed that the frequency of CS was 100% in lesions < 10 mm in diameter, but this frequency decreased to 22% in lesions > 40 mm in diameter. Based on this, it can be inferred that a CS may be resorbed and subsequently lost once the lesion diameter reaches a considerable size. To the best of the present authors' knowledge, the present study is the first to reveal that there is a higher likelihood of CSs in small anterior maxillary pathological lesions. Additionally, although the frequency of CSs was found to be higher in patients with cortical perforation than in those without, the underlying reason could not be elucidated. Thus, further studies on this subject are needed.

A study conducted to assess CS terminations in a vertically orientated apical-incisal direction reported that type 0 near the nasal cavity floor accounted for 3.94%, type I for 38.15%, type II for 52.63%, and type III near the crest apex for 5.26%.[12] The vertical terminations of CS in the present study were determined as types III, II, I and 0, in decreasing order, from the crest apex to the nasal cavity floor. Unlike in the previous study,[12] the present authors evaluated CSs in the maxilla with IPLs. The vertical position of the CS must be understood to facilitate surgical intervention and avoid potential complications. Because most CSs open close to the crest, they should be considered during surgical planning for patients with IPLs.

A study reported CS terminations as 91% palatal, 5.1% buccal, and 3.8% transversal.[7] Yeap et al[1] found that the palatal region was the most common CS endpoint. Another study reported that all CSs ended in the palatal region.[10] In the present study, most CSs (84.5%) ended in the palatal region, aligning with previous literature.

A previous study reported that the mean (minimum–maximum) diameter of the CS was 1.30 ± 0.44 (0.57–2.88) mm.[9] In the present study, the mean diameter was 0.667 ± 0.298 (0.2–1.6) mm. The prevalence of CS with a diameter > 1 mm was reported as 20% by Machado et al,[7] 15.7% by Oliveira-Santos et al[8] and 3.4% by Aoki et al.[15] The present results show a prevalence rate of 10.7% for CS with a diameter > 1 mm. Although the exact correlation between the diameter of the CS and the occurrence of clinical complications is unclear, an increase in diameter is expected to exacerbate bleeding because of the correlation between canal and vessel diameters.[1] Regardless of the fact that CSs measuring > 1 mm in diameter can cause noteworthy complications, vessels with smaller diameters can also contribute to substantial bleeding.[8]

The distribution of CSs based on sex was investigated by Tomrukçu and Köse,[9] Aoki et al[15] and Machado et al,[7] and all concluded that CSs were more prevalent in men. According to Şekerci et al[20] and Anatoly et al,[11] however, the prevalence of CS was higher among women. Studies conducted by Beyzade et al,[10] Von Arx et al[6]

and Oliveria Santos et al[8] did not yield statistical significance based on sex. In the present study, although more CSs were observed in men, this difference was not statistically significant.

With regard to the termination points of CSs in the dental arch, 35% were in the central incisor, 23.3% in the premolar, 17.5% in the lateral, 16.5% in the canine and 7.8% in the central-lateral incisor region. Aoki et al[15] observed the highest prevalence of CSs in the central incisor region, whereas the premolar region showed no CSs. Tomrukçu and Köse[9] and Beyzade et al[10] observed the most significant number of CSs in the central incisor region, with the premolar region having the lowest number of CSs. In the present study, the central incisor region exhibited the highest percentage of CS terminations, followed by the premolar region. Considering the potential anatomical displacement of the CSs caused by pathological lesions, the present study could have detected an increased prevalence of CSs in the premolar region.

Sun et al[21] found 502 CSs among 1,002 patients in their study. Of these patients, 259 had one CS, 147 had two, 80 had three, 10 had four, 2 had five, 2 had six, 1 had seven and 1 had eight.[21] Conversely, most of the lesions in the present study had a single CS and none of the pathological lesions had > 3 CSs.

The present study has the limitation of lacking clinical data support. It is imperative to conduct controlled clinical studies to determine whether CSs diagnosed with preoperative CBCT lead to intra- or postoperative complications. A further limitation is the absence of histopathological confirmation to determine whether the lesions were malignant or benign for the definitive diagnosis of the analysed IPLs.

Conclusion

Considering the extensive utilisation of preoperative CBCT in maxillofacial pathological lesions, it is essential to conduct a CS assessment of the obtained images because CSs are prevalent in anterior maxillary IPLs. A higher incidence of CSs was observed when the anterior maxillary pathological lesion was small, whereas the incidence was notably diminished in larger lesions, particularly in cases with pathological lesions > 40 mm in diameter. Moreover, a significant number of CSs were identified within or close to the surgical margin. Thus, more clinical studies are necessary to determine whether these characteristics contribute to complications during or after surgery.

Conflicts of interest

The authors declare no conflicts of interest related to this study.

Author contribution

Both authors participated in the data collection process, statistical analysis and writing of this article.

(Received Jun 11, 2024, accepted Jan 21, 2025)

References

1. Yeap CW, Danh D, Chan J, Parashos P. Examination of canalis sinuosus using cone beam computed tomography in an Australian population. Aust Dent J 2022;67:249–261.
2. Lopes-Santos G, Salzedas LMP, Bernabé DG, Ikuta CRS, Miyahara GI, Tjioe KC. Assessment of the knowledge of canalis sinuosus amongst dentists and dental students: An online-based cross-sectional study. Eur J Dent Educ 2022;26:488–498.
3. Jones FW. The anterior superior alveolar nerve and vessels. J Anat 1939;73:583–591.
4. Neves FS, Crusoé-Souza M, Franco LC, Caria PH, Bonfim-Almeida P, Crusoé-Rebello I. Canalis sinuosus: A rare anatomical variation. Surg Radiol Anat 2012;34:563–566.
5. Ferlin R, Pagin BSC, Yaedú RYF. Canalis sinuosus: A systematic review of the literature. Oral Surg Oral Med Oral Pathol Oral Radiol 2019;127:545–551.
6. von Arx T, Lozanoff S, Sendi P, Bornstein MM. Assessment of bone channels other than the nasopalatine canal in the anterior maxilla using limited cone beam computed tomography. Surg Radiol Anat 2013;35:783–790.
7. Machado VC, Chrcanovic BR, Felippe MB, Manhães Júnior LR, de Carvalho PS. Assessment of accessory canals of the canalis sinuosus: A study of 1000 cone beam computed tomography examinations. Int J Oral Maxillofac Surg 2016;45:1586–1591.
8. de Oliveira-Santos C, Rubira-Bullen IR, Monteiro SA, León JE, Jacobs R. Neurovascular anatomical variations in the anterior palate observed on CBCT images. Clin Oral Implants Res 2013;24:1044–1048.
9. Tomrukçu DN, Köse TE. Assesment of accessory branches of canalis sinuosus on CBCT images. Med Oral Patol Oral Cir Bucal 2020;25:e124–e130.
10. Beyzade Z, Yılmaz HG, Ünsal G, Çaygür-Yoran A. Prevalence, radiographic features and clinical relevancy of accessory canals of the canalis sinuosus in Cypriot population: A retrospective cone-beam computed tomography (CBCT) study. Medicina (Kaunas) 2022;58:930.
11. Anatoly A, Sedov Y, Gvozdikova E, et al. Radiological and morphometric features of canalis sinuosus in Russian population: Cone-beam computed tomography study. Int J Dent 2019;19:2453469.
12. Khojastepour L, Akbarizadeh F. Evaluation of extension type of canalis sinuosus in the maxillary anterior region: A CBCT study. Chin J Dent Res 2023;26:29–34.
13. Sedov YG, Avanesov AM, Mordanov OS, Zurnacheva DD, Mustafaeva RS, Blokhina AV. Visualization features of canalis sinuosus with cone beam computed tomography. Indian J Dent Res 2019;30:656–660.

14. Gurler G, Delilbasi C, Ogut EE, Aydin K, Sakul U. Evaluation of the morphology of the canalis sinuosus using cone-beam computed tomography in patients with maxillary impacted canines. Imaging Sci Dent 2017;47:69–74.
15. Aoki R, Massuda M, Zenni LTV, Fernandes KS. Canalis sinuosus: Anatomical variation or structure? Surg Radiol Anat 2020;42:69–74.
16. de Oliveira-Neto OB, Barbosa FT, Lima FJC, de Sousa-Rodrigues CF. Prevalence of canalis sinuosus and accessory canals of canalis sinuosus on cone beam computed tomography: A systematic review and meta-analysis. Int J Oral Maxillofac Surg 2023;52:118–131.
17. Lopes Dos Santos G, Ikuta CRS, Salzedas LMP, Miyahara GI, Tjioe KC. Canalis sinuosus: An anatomic repair that may prevent success of dental implants in anterior maxilla. J Prosthodont 2020;29:751–755.
18. Beckenstrater MA, Gamieldien MY, Smit C, Buchanan GD. A cone-beam computed tomography study of canalis sinuosus and its accessory canals in a South African population. Oral Radiol 2024;40:367–374.
19. Ferlin R, Pagin BSC, Yaedú RYF. Evaluation of canalis sinuosus in individuals with cleft lip and palate: A cross-sectional study using cone beam computed tomography. Oral Maxillofac Surg 2021;25:337–343.
20. Sekerci AE, Cantekin K, Aydinbelge M. Cone beam computed tomographic analysis of neurovascular anatomical variations other than the nasopalatine canal in the anterior maxilla in a pediatric population. Surg Radiol Anat 2015;37:181–186.
21. Sun Z, Li D, Zhang X, Zhang J, Li H, He C. Cone-beam computed tomography of accessory canals of the canalis sinuosus and analysis of the related risk factors. Surg Radiol Anat 2024;46:635–643.

A CALL FOR PERSONALIZED ORAL MEDICINE

NEW

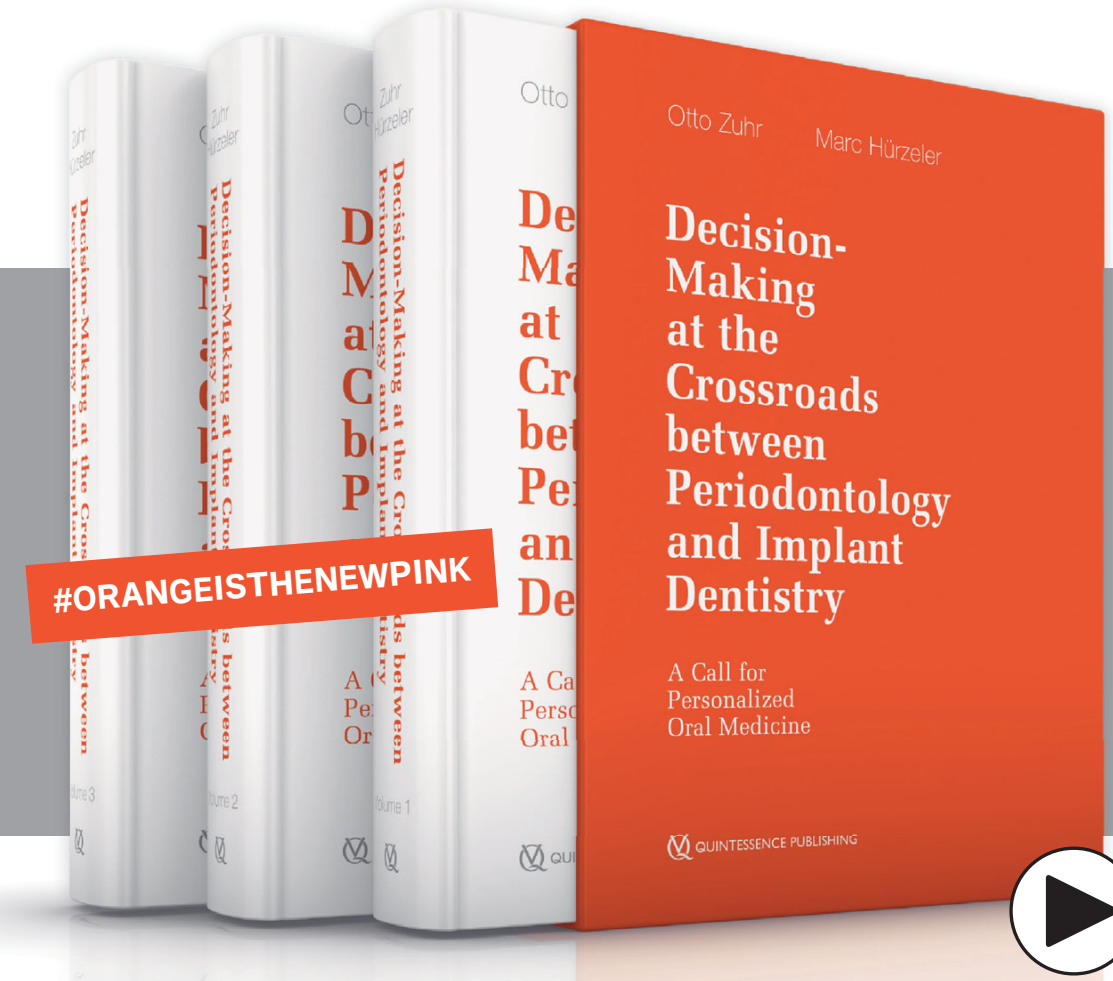

#ORANGEISTHENEWPINK

Otto Zuhr | Marc Hürzeler

Decision-Making at the Crossroads between Periodontology and Implant Dentistry

A Call for Personalized Oral Medicine

1st Edition 2025
Three-volume book in a slipcase; Hardcover
1,900 pages, 4,900 illus.
ISBN 978-3-86867-625-9

€498

Including 19 videos with 34 minutes total runtime!

With their book *Plastic-Esthetic Periodontal and Implant Surgery – A Microsurgical Approach*, these two nationally and internationally renowned authors have already written one of the most important works on oral surgery. They now present their patient-oriented treatment approach for implantology and periodontal surgery.

In this groundbreaking three-volume compendium, they demonstrate, among other things, how to achieve healthy and stable gingival and peri-implant soft tissue, considering the latest evidence and the individual risk profiles and needs of patients.

Due to extensive current scientific evidence available in dental medicine, it is no longer appropriate for dentists to be for or against preserving severely damaged teeth or to be for or against implants. The time has come to break away from dogma and combine both worlds – tooth preservation and implant therapy – into a coherent approach for the benefit of patients.

The work contains a wealth of information, providing all the necessary biologic and technical principles (Volume 1) as well as the surgical techniques (Volumes 2 and 3) required for practitioners in the fields of implantology, periodontology, and oral surgery. The in-depth work comprises a user-friendly format, including numerous detailed case studies with step-by-step procedures and extensive lists of materials. It is brilliantly illustrated with top-quality photographs and radiographs as well as other illustrative material, and is supplemented by a number of videos. This compendium is without doubt a real breakthrough and should be included in every dental library!

www.quint.link/new-pink
books@quintessenz.de
+49 (0)30 761 80 667
QUINTESSENCE PUBLISHING

Evaluation of Periapical Healing Outcomes of Single-visit Non-surgical Endodontic Retreatment of Teeth with Apical Periodontitis in Patients with Type 2 Diabetes Mellitus: a Retrospective Study

Merve IŞIK[1], Tülin DOĞAN ÇANKAYA[2], Zeliha UĞUR AYDIN[3]

Objective: *To compare the results of non-surgical endodontic retreatment (NSER) applied in a single visit between type 2 diabetes mellitus (DM) patients with teeth with apical periodontitis (AP) and healthy individuals.*

Methods: *The subjects enrolled were divided into two groups. The type 2 DM group was composed of 26 single-rooted mandibular teeth belonging to 26 patients (aged 45.04 ± 10.13 years; 19 women and 7 men) who did not have any other systemic disease. The control group, meanwhile, consisted of 27 single-rooted mandibular teeth from 27 patients (aged 37.78 ± 12.61 years; 15 women and 12 men) with no systemic disease. Both groups received single-visit non-surgical endodontic retreatment. Periapical radiographs were taken with a parallel technique before NSER and at least 6 months after treatment. Periapical index scores (PAI) for the relevant teeth were recorded. The data obtained were analysed statistically. P < 0.05 was considered significant.*

Results: *In both groups, postoperative PAI values decreased compared to the initial values after NSER treatment applied in a single visit (P < 0.05); however, there was no significant difference in the change in PAI values over time between the control and type 2 DM groups (P > 0.05). There was also no significant difference in healing between men and women in both groups (P > 0.05).*

Conclusion: *Following single-visit NSER in teeth with apical periodontitis, similar treatment outcomes were achieved in patients with type 2 DM and healthy individuals.*

Keywords: *diabetes mellitus, endodontic treatment, periapical index*
Chin J Dent Res 2025;28(2):139–146; doi: 10.3290/j.cjdr.b6260628

The biological mechanisms involved in the repair of periapical tissues after endodontic treatment are significantly affected by genetic and systemic factors with regard to the patient's health status (for example age, nutrition, stress, hormones, vitamin intake, hydration status and diabetes, cardiovascular diseases, osteoporosis and smoking habit).[1,2] Diabetes mellitus (DM) is a chronic metabolic disease characterised by impaired insulin secretion or utilisation, leading to a state of chronic hyperglycaemia.[3] DM affects various functions of the immune system, making the patient more vulnerable to chronic inflammation, progressive tissue damage and reduced tissue repair, and type 2 DM constitutes 85% to 90% of DM cases.[4] Apical periodontitis (AP) is a chronic inflammatory lesion that originates from the pulp and affects the periapical tissues. It has been reported that AP occurs as a result of missed root canals, the presence of persistent microorganisms in the canal, low radiographic quality of existing root canal treatment, low quality of the existing coronal restoration,

1 Department of Endodontics, Faculty of Dentistry, Bolu Abant Izzet Baysal University, Bolu, Turkey
2 Department of Endodontics, Faculty of Dentistry, Alanya Alaaddin Keykubat University, Antalya, Turkey
3 Department of Endodontics, Gulhane Faculty of Dentistry, University of Health Sciences, Ankara, Turkey

Corresponding author: Dr Tülin DOĞAN ÇANKAYA, Department of Endodontics, Faculty of Dentistry, Alanya Alaaddin Keykubat University, Antalya, Turkey. Tel: 90-506 6951106. Email: tdogancankaya@gmail.com

low-grade systemic inflammation and the impairment of the systemic health of the patient.[5,6] In addition, it is stated in the literature that the incidence of AP is higher in DM patients than in healthy individuals.[7] The high incidence of apical periodontitis in patients with DM and the increased need for endodontic treatment indicate that DM is a potential modulator of endodontic pathologies. Thus, it is important to evaluate the results of endodontic treatment in teeth with AP in patients with type 2 DM.[8]

In cases where endodontic treatment fails, the first preferred treatment option is non-surgical endodontic retreatment (NSER) as it is a conservative method,[9] with a success rate that has been reported to vary between 62% and 89%.[10,11] Today, endodontic treatment can be completed in a single visit thanks to magnification systems, rubber dam isolation, electronic apex locator, endodontic motor and NiTi rotary file systems used during treatment. This offers increased convenience for the patient and the physician in terms of time. In addition, the possibility of reinfection of the canal due to leakage between visits is eliminated.[12,13]

Following a comprehensive literature review, no studies were found comparing healing of AP after NSER in a single visit between patients with type 2 DM and systemically healthy patients. The aim of this study is to evaluate the condition of periapical tissues using periapical index (PAI) scores in periapical radiographs after single-visit NSER in systemically healthy patients and type 2 DM, and to compare the treatment success.

Materials and methods

Ethical considerations

This study is a single-centre, retrospective case-control study using periapical radiographs of patients gathered from the archives of Bolu Abant Izzet Baysal University Faculty of Dentistry. The protocol was conducted according to the principles described in the Declaration of Helsinki, including all changes and revisions. Ethical approval was obtained from the Clinical Research Ethics Committee of Bolu Abant Izzet Baysal University (decision no. 2023/205).

Sample size calculation

The sample size was based on a previous study of similar design,[14] with a power calculation performed to determine the required sample size (G*Power 3.1 software; Heinrich Heine University, Düsseldorf, Germany), with a = 0.05 and b = 0.80. It was determined that 23 teeth per group was statistically sufficient for the present study.

Inclusion criteria

The inclusion criteria were as follows:

- teeth with a single root and a single canal;
- teeth with adequate quality root canal filling after NSER and ending in the apical 2 mm[15];
- teeth without instrument fractures and calcified canals;
- teeth without compatibility problems in permanent restorations[16];
- teeth with standard periapical radiographs taken using the parallel technique with the same intraoral X-ray device (Kodak 2100 230V; Carestream Health, Rochester, NY, USA) and parameters (60 KVp, 6 mAs), and of sufficient quality that the tooth and surrounding tissues be clearly displayed without artefacts, superposition or image distortion;
- teeth with follow-up periapical radiographs taken at least 6 months after NSER;
- teeth with a periapical lesion diameter of less than 5 mm.

Teeth that met abovementioned conditions[17] could be included in the study. Patients needed to be periodontally healthy and non-smokers, generally healthy or have no systemic disease other than controlled type 2 DM characterised by an HbA1c level below 7%.[18]

Subjects were divided into two groups. The type 2 DM group was composed of 26 mandibular teeth from 26 type 2 DM patients (45.04 ± 10.13 years; 19 women and 7 men), whereas the control group included 27 mandibular teeth from 27 patients (37.78 ± 12.61 years; 15 women and 12 men).

Clinical procedure

All teeth were treated by the same endodontist and following the same protocol outlined below. Local anaesthesia (Ultracain DS Ampoule; Sanofi Aventis, Paris, France) was applied, and after rubber dam insulation, the entrance space was prepared. Previous root canal fillings were removed using an endodontic motor (WDV Gold, VDW, Munich, Germany) and ProTaper Retreatment Universal files (Dentsply Sirona, Charlotte, NC, USA). Apical patency was checked with a #10 K-type hand file (Dentsply Sirona), and working length was determined with an electronic apex locator (DTE III, Woodpecker, Guangxi, China), then confirmed by periapical radiographs. All root canals were prepared using ProTaper Next files (Dentsply Sirona) and the endo-

Table 1 Follow-up period and demographic data of control and DM groups.

Group	n	Age (y)			Follow-up period (mo)			Sex	
		Minimum	Maximum	Mean ± SD	Minimum	Maximum	Mean ± SD	Female	Male
Control	27	18	63	37.78 ± 12.61	6	48	16.85 ± 10.98	15	12
DM	26	29	65	45.04 ± 10.13	6	48	23.57 ± 25.55	19	7

SD, standard deviation.

Table 2 Preoperative PAI values in control and DM groups.

Group	PAI 1	PAI 2	PAI 3	PAI 4	PAI 5
Control	0	0	3 (33.3%)	10 (58.8%)	14 (51.9%)
DM	0	0	6 (66.7%)	7 (41.2%)	13 (48.1%)

dontic motor according to the manufacturer's instructions. The size of the master apical file was determined specifically for each root canal based on the initial canal size. After each file change, the canals were irrigated with 2 ml 2.5% NaOCl (Mikrovem, Istanbul, Turkey). For final irrigation of the root canals, 5 ml 17% ethylenediaminetetraacetic acid (EDTA; Imicryl, Konya, Turkey), 5 ml distilled water and 5 ml 2.5% NaOCl were used, respectively. All irrigation procedures were performed with a 30 G lateral vented needle (NaviTip; Ultradent, South Jordan, UT, USA). The root canals were dried and filled using the cold lateral compaction technique with gutta-percha cones (Dentsply Sironar) compatible with the file system used and epoxy resin–based root canal sealer (AH Plus; Dentsply Sirona). The permanent restoration was completed using the one-step self-etch adhesive G-Premio Bond (GC Corporation, Tokyo, Japan) and composite resin (3M ESPE, Seefeld, Germany).

Periapical conditions were scored with the PAI by awarding points from 1 to 5 to the periapical radiographs of the relevant teeth of the patients who were followed for at least 6 months before and after NSER.[19] PAI scoring was performed by two independent endodontist observers for each group. In cases where there was inconsistency between the observers' scores, a consensus was reached by reevaluation (overall correlation coefficients for inter- and intra-observer reliability were 0.854 and 0.802). Treatment results were classified as "healing" (PAI < 3) or "not healing" (PAI ≥ 3) according to periapical radiographic criteria.[11]

Statistical analysis

Data from the current study were analysed with SPSS v. 23 (IBM, Armonk, NY, USA). The suitability of the data for normal distribution was examined with ae Shapiro-Wilk test. A Wilcoxon test was used to evaluate PAI change within the groups, and a chi-square test was employed to compare PAI change between groups. Chi-squared and McNemar-Bowker tests were used to evaluate intra- and inter-group PAI changes according to sex. The level of statistical significance was set at $P < 0.05$.

Results

The demographic data and follow-up period for the patients included in the study are shown in Table 1.

There was no significant difference in the distribution of PAI values before the NSER procedure in the control and type 2 DM groups ($P > 0.05$) (Table 2). Postoperative PAI values were found to decrease compared to baseline after NSER applied in a single visit in both groups ($P < 0.05$) (Table 3 and Fig 1). There was no significant difference in the change in PAI values over time between the control and type 2 DM groups ($P > 0.05$).

No significant difference was detected between men and women in the change in PAI values after NSER in a single visit in either of the groups ($P > 0.05$) (Table 4). No significant difference was detected in the time-dependent change in PAI values in both men and women after NSER in a single visit between the control and type 2 DM groups ($P > 0.05$) (Table 5).

Discussion

The relationship between the patient's general health status and the aetiology of apical periodontitis and the periapical healing process in endodontically treated teeth has long been discussed in the literature.[20-22] It is reported that DM, which affects patients' general health status and is becoming increasingly common all over the world, is an important factor in both the success and aetiology of root canal treatment.[20] According to the results of the present study, the null hypothesis was accepted because there was no difference in the healing status of periapical tissues and treatment success after NSER applied in a single visit between individuals with type 2 DM and systemically healthy individuals.

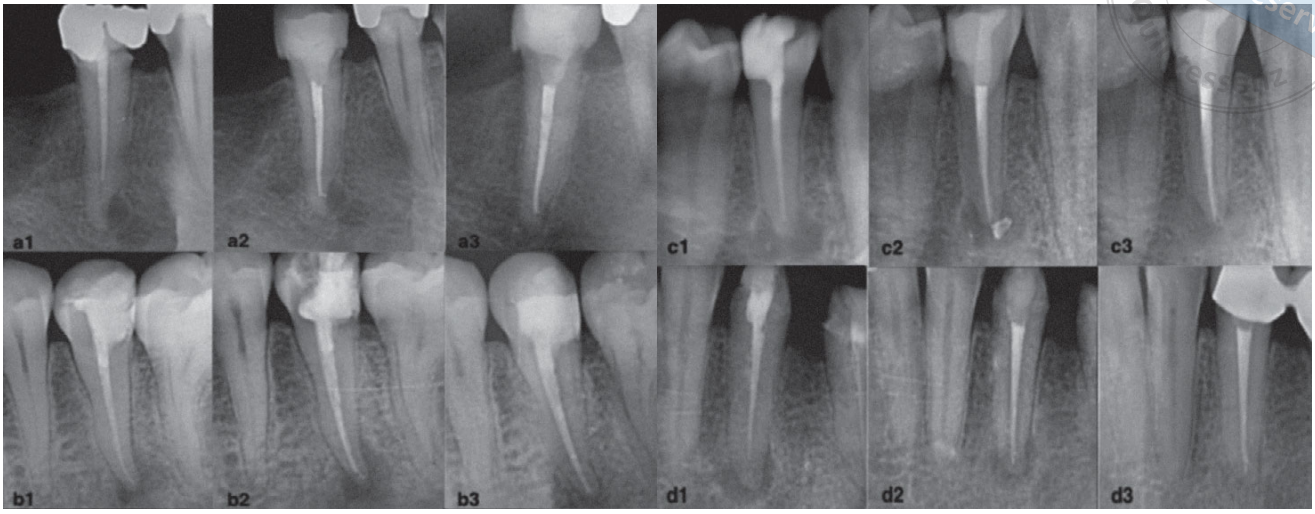

Fig 1 Four cases of radiographic follow-up of periapical status before and after NSER in type 2 DM patients (a and b) and healthy individuals (c and d). Preoperative (a1, b1, c1, d1); postoperative (a2, b2, c2, d2); 12-month follow-up after NSER (a3, c3); 24-month follow-up after NSER (b3); 18-month follow-up after NSER (d3).

Table 3 Postoperative PAI values in control and DM groups.

Group	PAI 1	PAI 2	PAI 3	PAI 4	PAI 5
Control	17 (51.5%)	3 (37.5%)	3 (50.0%)	4 (66.7%)	0
DM	16 (48.5%)	5 (62.5%)	3 (50.0%)	2 (33.3%)	0

Table 4 Time-dependent change in PAI values according to sex in the control and DM groups.

Group		Sex			*P* value
		Male	Female	Total	
Control	Healed	7 (70%)	13 (76.5%)	20 (74.1%)	0.525
	Not healed	3 (30%)	4 (23.5%)	7 (25.9%)	
DM	Healed	7 (100%)	14 (73.7%)	21 (80.8%)	0.177
	Not healed	0	5 (26.3%)	5 (19.2%)	

Table 5 Time-dependent change in PAI values according to sex between the control and DM groups.

Variable		PAI		*P* value
		PAI 1–2	PAI 3–5	
Sex	Female	27 (65.9%)	9 (75%)	0.621
	Male	14 (34.1%)	3 (25%)	

Short- and long-term success results of endodontic treatment were evaluated, and the age, sex and general health conditions of the patients included in the study affected the study results.[23-25] The healing process of endodontic treatment may slow down due to patients' age, malnutrition and the increased incidence of systemic diseases such as age-related diabetes.[26,27] Considering all these factors, patients between the ages of 18 and 65 years were included in the present study, and as a result of the statistical analysis, it was determined that there were similarities between the groups in terms of sex distribution and mean age.

It has been reported in the literature that factors such as tooth type, preoperative lesion size and number of visits also affect endodontic treatment results.[12,28] Ng et al[29] reported that success rates were higher in teeth with a lesion size smaller than 5 mm than in those with a lesion size larger than 5 mm. In contrast, another study reported that there was no significant difference between lesion sizes and success rates.[30] In the present study, teeth with a lesion size of less than 5 mm were included to ensure standardisation and that the study results were not affected by the lesion size. Another factor that is said to affect the outcome of endodontic treatment is tooth

type. Periapical radiographs provide two-dimensional imaging; thus, superimpositions of molar tooth roots in the evaluation of endodontic treatment results may affect the study results.[31] For this reason, the present study was conducted on single-canal mandibular teeth to ensure standardisation and that the results were not affected by changes in the root canal anatomy.

Over time, it has been reported that endodontic treatment can be completed successfully in a single visit, with the development of techniques that facilitate and accelerate treatment for physicians and patients, the use of irrigation activation methods and the production of new instruments. For this reason, endodontic treatment performed in a single visit has become popular in recent years.[32] Some studies report that there is no difference in complications occurring during treatment, postoperative pain level or success rates when endodontic treatment applied in a single visit is compared with treatment applied in multiple visits.[33,34] In line with this information, the NSER procedure was performed in a single visit in the present study; however, it is important for patients to attend a control appointment at least 6 and 12 months after the end of treatment. Clinical and radiographic follow-ups performed within the reported period make it possible to evaluate the obturation quality, coronal seal and tissue response in the periapical region.[35] Thus, patients with a minimum of 6-month follow-up radiographs were included in the present study.

As a result of this study, it was determined that PAI values decreased compared to initial values after NSER performed in a single visit in both the control and type 2 DM groups. This shows that healing occurred in the periradicular tissues in both groups after treatment. In contrast, Wang et al[36] evaluated the long-term prognosis of NSER treatment in patients with DM and reported that DM was an effective factor in related tooth loss. According to this study, type 2 DM was determined to be an important risk factor for tooth extraction due to negatively affecting NSER results. Supporting the present findings, Uğur Aydın et al[37] evaluated the results of endodontic treatment applied to the molars of healthy patients and those with type 2 DM using fractal analysis. They reported that the size of the apical lesion decreased after root canal treatment in both the type 2 DM and control groups, and the fractal size in the lesion area increased due to healing.[37] Similarly, Rudranaik et al[38] reported that there was no difference in time-dependent change in PAI after primary endodontic treatment applied in a single visit in controlled and uncontrolled type 2 DM patients with teeth with AP whose HbA1c values were measured. Based on the results of this study, the clinical and radiographic healing results of single-visit endodontic treatment were delayed in patients with uncontrolled type 2 DM.[38] In the present study, healing rates were found to be 74.1% in the control group, 80.8% in the type 2 DM group and 77.4% in total at the end of the follow-up periods. Similar success rates may have been observed in the type 2 DM group as a result of the effective application of the chemomechanical preparation technique, ensuring rubber dam isolation, eliminating microorganisms by applying the same irrigation protocol, and achieving coronal and apical sealing.

No difference was found between the type 2 DM and control groups in terms of time-dependent change in PAI scores. In contrast to these findings, Arya et al[39] reported that periapical healing after endodontic treatment in mandibular teeth with periapical lesions (size ≥ 2 mm × 2 mm) was less in individuals with type 2 DM (43%) than in healthy individuals (80%) over a 1-year period. Fouad and Burleson[40] reported that the success of primary endodontic treatment in individuals with type 2 DM was lower than in healthy individuals after a 2-year follow-up. The present authors believe that the differences in the study results are due to differences in factors such as lesion size, tooth group and treatment procedure, which are among the factors affecting the success of endodontic treatment. In contrast to these findings, Ferreira et al[14] reported that the success rate of endodontic treatment is similar in healthy individuals (80%) and individuals with type 2 DM (62%), which also supports the present results. In a retrospective study, Uğur Aydın et al[37] reported that there was no difference in the time-dependent change in PAI in mandibular molars between healthy individuals and individuals with type 2 DM after primary endodontic treatment. Cheraskin and Ringsdorf[41] evaluated the primary endodontic treatment results for patients with low and high plasma glucose levels and reported that periapical lesions healed at a higher rate in the group with low plasma glucose levels over the 30-week follow-up period. Since type 2 DM patients whose plasma glucose levels were regulated by drug treatment were included in the present study, the present authors do not think there is any difference between the control group and the type 2 DM group; however, advanced glycation end products and metabolic conditions were associated with larger periapical lesion sizes and more severe alveolar bone resorption in patients with type 2 DM.[42,43] In order to ensure standardisation, however, patients with lesions smaller than 5 mm were included in the present study. This may have been effective in patients with type 2 DM, whose NSER success rate was

similar to that of healthy individuals.

In the present study, no difference was found between sexes in terms of time-dependent changes in PAI values both within and between groups. Similarly, Arya et al[39] reported that there was no difference between sexes in terms of healing of AP in type 2 DM patients with AP after 1 year of follow-up. In contrast, Smith et al[44] reported that the healing rate was higher in male patients after endodontic treatment applied to the anterior and posterior teeth after 5 years of follow-up, whereas Swartz et al[45] reported that the healing rate was higher in female patients after 20 years of follow-up after primary endodontic treatment applied to the anterior and posterior teeth. Britto et al[46] reported that male patients with type 2 DM had less healing in their periapical lesions after primary endodontic treatment than female patients. Variations in research results may be due to differences in factors such as sex distribution, population and age.

The success of endodontic therapy in individuals with DM has been an area of interest due to the systemic implications of the disease on tissue repair and healing processes. Regulated DM, characterised by controlled glycaemic levels (HbA1c < 7%), is associated with reduced systemic inflammation and improved immune function compared to uncontrolled DM.[18] These factors contribute positively to the healing process following endodontic therapy.

In the present study, the inclusion of patients with well-regulated type 2 DM (HbA1c < 7%) facilitated a more precise evaluation of endodontic treatment outcomes. The results showed that the periapical healing rates in the type 2 DM group were comparable to those of systemically healthy individuals, suggesting that effective glycaemic control may mitigate the adverse effects of DM on tissue repair and inflammatory responses. This aligns with previous findings indicating that glycaemic regulation significantly enhances the success of both primary and secondary endodontic treatments.[37,39]

In contrast, studies have reported delayed healing and lower success rates in patients with uncontrolled DM due to persistent hyperglycaemia, which exacerbates vascular damage, impairs collagen synthesis and increases the risk of infections.[38,40] The present findings highlight the critical role of glycaemic regulation in optimising the outcomes of endodontic therapy, emphasising the need for dental practitioners to collaborate with physicians in managing the systemic health of DM patients undergoing dental treatments.

Future studies could explore the impact of varying levels of glycaemic control on the success of endodontic therapy, considering factors such as lesion size, tooth type and long-term follow-up. Additionally, advancements in regenerative endodontics targeting angiogenesis and immune modulation might provide promising avenues for improving treatment outcomes in patients with DM.

In patients with DM, decreased tissue repair capacity due to low angiogenic potential may predispose to chronic inflammation. In addition, increased susceptibility to infections due to an altered immune response may delay the healing process and alter bone turnover, potentially affecting the success of root canal treatment in diabetic patients. These observations are supported by studies in the literature.[38,47] Moreover, type 2 DM is one of the most common systemic diseases encountered by dental practitioners in clinical practice.[48] Thus, it is critical for dental practitioners to be aware of their patients' general health status to optimise the treatment process. Root canal–treated teeth should be monitored more frequently and over longer periods in patients with type 2 DM compared to healthy individuals.

This study is based on the comparison of the success of endodontic treatment results between type 2 DM patients and healthy individuals using periapical radiographs. Since it does not include clinical evaluation and is a retrospective study, the abovementioned conditions represent its limitations. Further retrospective and prospective clinical studies with larger sample sizes, and including both clinical and radiographic evaluations, are needed.

Conclusion

NSER applied in a single visit to teeth in patients with type 2 DM and AP resulted in periapical healing similar to in healthy individuals.

Conflicts of interest

The authors declare no conflicts of interest related to this study.

Author contribution

Dr Merve IŞIK contributed to the study design, data collection, analysis and manuscript draft and revision; Dr Tülin DOĞAN ÇANKAYA contributed to the data analysis, manuscript draft and manuscript revision; Dr Zeliha UĞUR AYDIN contributed to the study design and manuscript revision.

(Received Aug 29, 2024; accepted Jan 21, 2025)

References

1. Morsani JM, Aminoshariae A, Han YW, Montagnese TA, Mickel A. Genetic predisposition to persistent apical periodontitis. J Endod 2011;37:455–459.
2. Holland R, Gomes JE Filho, Cintra LTA, Queiroz ÍOA, Estrela C. Factors affecting the periapical healing process of endodontically treated teeth. J Appl Oral Sci 2017;25:465–476.
3. Tibúrcio-Machado CD, Bello MC, Maier J, Wolle CF, Bier CA. Influence of diabetes in the development of apical periodontitis: A critical literature review of human studies. J Endod 2017;43:370–376.
4. López-López J, Jané-Salas E, Estrugo-Devesa A, Velasco-Ortega E, Martín-González J, Segura-Egea JJ. Periapical and endodontic status of type 2 diabetic patients in Catalonia, Spain: A cross-sectional study. J Endod 2011;37:598–601.
5. Jakovljevic A, Nikolic N, Jacimovic J, et al. Prevalence of apical periodontitis and conventional nonsurgical root canal treatment in general adult population: An updated systematic review and meta-analysis of cross-sectional studies published between 2012 and 2020. J Endod 2020;46:1371–1386.e8 [erratum 2021;47:336].
6. Nistor CC, Suciu I, Ionescu E, Dragomirescu A, Coculescu E, Băluță A. Apical periodontitis in maxillary molars with missed second mesio-buccal root canal: A cbct study. Rom J Oral Rehabil 2024;16:100–107.
7. Segura-Egea JJ, Martín-González J, Castellanos-Cosano L. Endodontic medicine: Connections between apical periodontitis and systemic diseases. Int Endod J 2015;48:933–951.
8. Marotta PS, Fontes TV, Armada L, Lima KC, Rôças IN, Siqueira JF Jr. Type 2 diabetes mellitus and the prevalence of apical periodontitis and endodontic treatment in an adult Brazilian population. J Endod 2012;38:297–300.
9. Rodríguez G, Patel S, Durán-Sindreu F, Roig M, Abella F. Influence of cone-beam computed tomography on endodontic retreatment strategies among general dental practitioners and endodontists. J Endod 2017;43:1433–1437.
10. Salehrabi R, Rotstein I. Epidemiologic evaluation of the outcomes of orthograde endodontic retreatment. J Endod 2010;36:790–792.
11. Zandi H, Petronijevic N, Mdala I, et al. Outcome of endodontic retreatment using 2 root canal irrigants and influence of infection on healing as determined by a molecular method: A randomized clinical trial. J Endod 2019;45:1089–1098.e5.
12. Eyuboglu TF, Olcay K, Özcan M. A clinical study on single-visit root canal retreatments on consecutive 173 patients: Frequency of periapical complications and clinical success rate. Clin Oral Investig 2017;21:1761–1768.
13. Gill GS, Bhuyan AC, Kalita C, Das L, Kataki R, Bhuyan D. Single versus multi-visit endodontic treatment of teeth with apical periodontitis: An in vivo study with 1-year evaluation. Ann Med Health Sci Res 2016;6:19–26.
14. Ferreira MM, Carrilho E, Carrilho F. Diabetes mellitus and its influence on the success of endodontic treatment: a retrospective clinical study [in Portuguese]. Acta Med Port 2014;27:15–22.
15. Schaeffer MA, White RR, Walton RE. Determining the optimal obturation length: A meta-analysis of literature. J Endod 2005;31:271–274.
16. Laukkanen E, Vehkalahti MM, Kotiranta AK. Impact of systemic diseases and tooth-based factors on outcome of root canal treatment. Int Endod J 2019;52:1417–1426.
17. Rubinstein RA, Kim S. Long-term follow-up of cases considered healed one year after apical microsurgery. J Endod 2002;28:378–383.
18. ElSayed NA, Aleppo G, Aroda VR, et al, on behalf of the American Diabetes Association. 6. Glycemic Targets: Standards of Care in Diabetes-2023. Diabetes Care 2023;46(suppl 1):S97–S110.
19. Orstavik D, Kerekes K, Eriksen HM. The periapical index: A scoring system for radiographic assessment of apical periodontitis. Endod Dent Traumatol 1986;2:20–34.
20. Gupta A, Aggarwal V, Mehta N, Abraham D, Singh A. Diabetes mellitus and the healing of periapical lesions in root filled teeth: A systematic review and meta-analysis. Int Endod J 2020;53:1472–1484.
21. Nagendrababu V, Segura-Egea JJ, Fouad AF, Pulikkotil SJ, Dummer PMH. Association between diabetes and the outcome of root canal treatment in adults: An umbrella review. Int Endod J 2020;53:455–466.
22. Segura-Egea JJ, Cabanillas-Balsera D, Martín-González J, Cintra LTA. Impact of systemic health on treatment outcomes in endodontics. Int Endod J 2023;56(suppl 2):219–235.
23. Mattscheck DJ, Law AS, Noblett WC. Retreatment versus initial root canal treatment: Factors affecting posttreatment pain. Oral Surg Oral Med Oral Pathol Oral Radiol Endod 2001;92:321–324.
24. Topçuoğlu HS, Topçuoğlu G. Postoperative pain after the removal of root canal filling material using different techniques in teeth with failed root canal therapy: A randomized clinical trial. Acta Odontol Scand 2017;75:249–254.
25. Yoldas O, Topuz A, Isçi AS, Oztunc H. Postoperative pain after endodontic retreatment: Single- versus two-visit treatment. Oral Surg Oral Med Oral Pathol Oral Radiol Endod 2004;98:483–487.
26. de-Figueiredo FED, Lima LF, Lima GS, et al. Apical periodontitis healing and postoperative pain following endodontic treatment with a reciprocating single-file, single-cone approach: A randomized controlled pragmatic clinical trial. PLoS One 2020;15:e0227347.
27. Sadaf D, Ahmad MZ. Factors associated with postoperative pain in endodontic therapy. Int J Biomed Sci 2014;10:243–247.
28. Magat G, Ozcan Sener S. Evaluation of trabecular pattern of mandible using fractal dimension, bone area fraction, and gray scale value: Comparison of cone-beam computed tomography and panoramic radiography. Oral Radiol 2019;35:35–42.
29. Ng YL, Mann V, Gulabivala K. Outcome of secondary root canal treatment: A systematic review of the literature. Int Endod J 2008;41:1026–1046.
30. Sjogren U, Hagglund B, Sundqvist G, Wing K. Factors affecting the long-term results of endodontic treatment. J Endod 1990;16:498–504.
31. Olcay K, Ataoglu H, Belli S. Evaluation of related factors in the failure of endodontically treated teeth: A cross-sectional study. J Endod 2018;44:38–45.
32. Wong AW, Zhang C, Chu CH. A systematic review of nonsurgical single-visit versus multiple-visit endodontic treatment. Clin Cosmet Investig Dent 2014;6:45–56.
33. Eleazer PD, Eleazer KR. Flare-up rate in pulpally necrotic molars in one-visit versus two-visit endodontic treatment. J Endod 1998;24:614–616.
34. Roane JB, Dryden JA, Grimes EW. Incidence of postoperative pain after single- and multiple-visit endodontic procedures. Oral Surg Oral Med Oral Pathol 1983;55:68–72.
35. Ross C, Scheetz J, Crim G, Caicedo R, Morelli J, Clark S. Variables affecting endodontic recall. Int Endod J 2009;42:214–219.
36. Wang CH, Chueh LH, Chen SC, Feng YC, Hsiao CK, Chiang CP. Impact of diabetes mellitus, hypertension, and coronary artery disease on tooth extraction after nonsurgical endodontic treatment. J Endod 2011;37:1–5.

37. Uğur Aydın Z, Ocak MG, Bayrak S, Göller Bulut D, Orhan K. The effect of type 2 diabetes mellitus on changes in the fractal dimension of periapical lesion in teeth after root canal treatment: A fractal analysis study. Int Endod J 2021;54:181–189.
38. Rudranaik S, Nayak M, Babshet M. Periapical healing outcome following single visit endodontic treatment in patients with type 2 diabetes mellitus. J Clin Exp Dent 2016;8: e498–e504.
39. Arya S, Duhan J, Tewari S, Sangwan P, Ghalaut V, Aggarwal S. Healing of apical periodontitis after nonsurgical treatment in patients with type 2 diabetes. J Endod 2017;43:1623–1627.
40. Fouad AF, Burleson J. The effect of diabetes mellitus on endodontic treatment outcome: data from an electronic patient record. J Am Dent Assoc 2003;134:43–51.
41. Cheraskin E, Ringsdorf WM, Jr. The biology of the endodontic patient. 3. Variability in periapical healing and blood glucose. J Oral Med 1968;23:87–90.
42. Kohsaka T, Kumazawa M, Yamasaki M, Nakamura H. Periapical lesions in rats with streptozotocin-induced diabetes. J Endod 1996;22:418–421.
43. Iwama A, Nishigaki N, Nakamura K, et al. The effect of high sugar intake on the development of periradicular lesions in rats with type 2 diabetes. J Dent Res 2003;82:322–325.
44. Smith CS, Setchell DJ, Harty FJ. Factors influencing the success of conventional root canal therapy--A five-year retrospective study. Int Endod J 1993;26:321–333.
45. Swartz DB, Skidmore AE, Griffin JA Jr. Twenty years of endodontic success and failure. J Endod 1983;9:198–202.
46. Britto LR, Katz J, Guelmann M, Heft M. Periradicular radiographic assessment in diabetic and control individuals. Oral Surg Oral Med Oral Pathol Oral Radiol Endod 2003;96:449–452.
47. Segura-Egea JJ, Martín-González J, Cabanillas-Balsera D, Fouad AF, Velasco-Ortega E, López-López J. Association between diabetes and the prevalence of radiolucent periapical lesions in root-filled teeth: Systematic review and meta-analysis. Clin Oral Investig 2016;20:1133–1141.
48. Ghoneim M, Saber SE, El-Badry T, Obeid M, Hassib N. The use of different irrigation techniques to decrease bacterial loads in healthy and diabetic patients with asymptomatic apical periodontitis. Open Access Maced J Med Sci 2016;4:714–719.

Mandibular Osteonecrosis Involving Tooth Germ in Children: a Rare Case Report with a 6-year Follow-up

Yue FEI[1,2], Guang Yun LAI[1,2], Jun WANG[1,2]

Osteonecrosis involving the permanent tooth germ in primary dentition is a rare condition that can affect dental and maxillofacial development without correct intervention. This case report presents the successful recovery from drug-induced mandibular osteonecrosis involving the permanent tooth germ in a child. A healthy 4-year-old Chinese girl visited the clinic with an unhealed gingival wound and alveolar bone exposure of the missing primary molar area after 1-day arsenic trioxide sealing during pulp therapy. Radiographic examinations indicated inflammation and sequestrum formation in the jaw. The diagnosis was mandibular osteonecrosis. The treatment plans involved sequestrectomy without extended curettage and removal of the affected permanent tooth germ with systemic antibiotic therapy. A 6-year follow-up revealed no recurrence of the lesion or complications, a gradual increase in bone density of the osteonecrosis area and the development of adjacent permanent tooth germs. A conservative treatment regimen without extended curettage may be an option for young patients with jaw osteonecrosis.

Keywords: *arsenic trioxide, deciduous teeth, osteonecrosis, sequestrectomy, tooth germ*
Chin J Dent Res 2025;28(2):147–151; doi: 10.3290/j.cjdr.b6260631

Osteonecrosis in children is commonly associated with infection, trauma, radiotherapy, metastatic disease or drugs.[1,2] Due to its low incidence, there is a paucity of data on the long-term effects of osteonecrosis on dental and maxillofacial development in children.[3] It is also important to note that paediatric skeletons not only possess a thicker overlying periosteum and greater osteogenic remodelling potential than adult bone, but also contain a unique structure of permanent tooth germs in the jaws.[4] These physiological differences between paediatric and adult skeletons prevent the direct application of treatment options for adults in children.[5]

Involvement of permanent tooth germ in paediatric jaw osteonecrosis is rare. There has been only one report of Mycobacterium abscessus-induced osteonecrosis, in a 3-year-old American patient.[6] To the best of the present authors' knowledge, this is the first case of drug-induced mandibular osteonecrosis involving the permanent tooth germ in a child. This case is presented following the CAse REport (CARE) Reporting Checklist.

Case presentation

A 4-year-old Chinese girl with an unhealed wound affecting the primary mandibular right first molar visited the Department of Pediatric Dentistry, Shanghai Ninth People's Hospital affiliated with Shanghai Jiao Tong University School of Medicine in 2016. Five months prior, arsenic trioxide had been sealed into the chamber of the affected tooth during pulp therapy in a private clinic. The patient experienced severe gingival pain and swelling 1 day after sealing, so the private dental practitioner removed the substance, perfored resealing with calcium hydroxide and prescribed cefaclor postoperatively. Al-

1 Department of Pediatric Dentistry, Shanghai Ninth People's Hospital, Shanghai Jiao Tong University School of Medicine, Shanghai, P.R. China
2 College of Stomatology, Shanghai Jiao Tong University, National Center for Stomatology, National Clinical Research Center for Oral Diseases, Shanghai Key Laboratory of Stomatology, Shanghai Engineering Research Center of Advanced Dental Technology and Materials, Shanghai, P.R. China

Corresponding author: Dr Jun WANG, Department of Pediatric Dentistry, Shanghai Ninth People's Hospital, Shanghai Jiao Tong University School of Medicine, No.639 Zhizaoju Road, Shanghai 200011, P.R. China. Tel: 86-21-53315890. Email: wangjun202@126.com.

This research was funded by the Biomaterials and Regenerative Medicine Institute Cooperative Research Project, Shanghai Jiao Tong University School of Medicine (2022LHB06), Consensus, Standards and Guidelines cultivation project of Shanghai Ninth People's Hospital, Shanghai Jiao Tong University School of Medicine (CSG202410), and Biological Clinical Sample Project of Shanghai Ninth People's Hospital (YBKB202222).

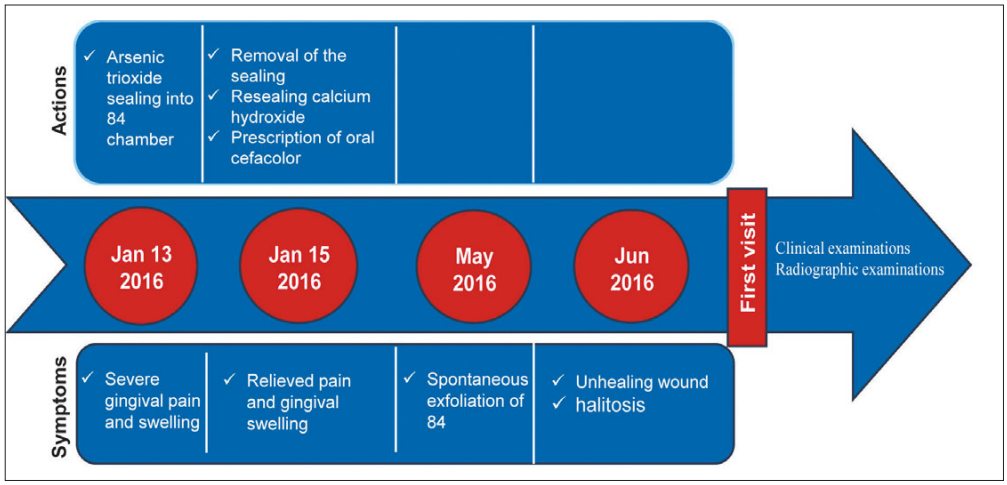

Fig 1 Timeline illustrating the progression of the case.

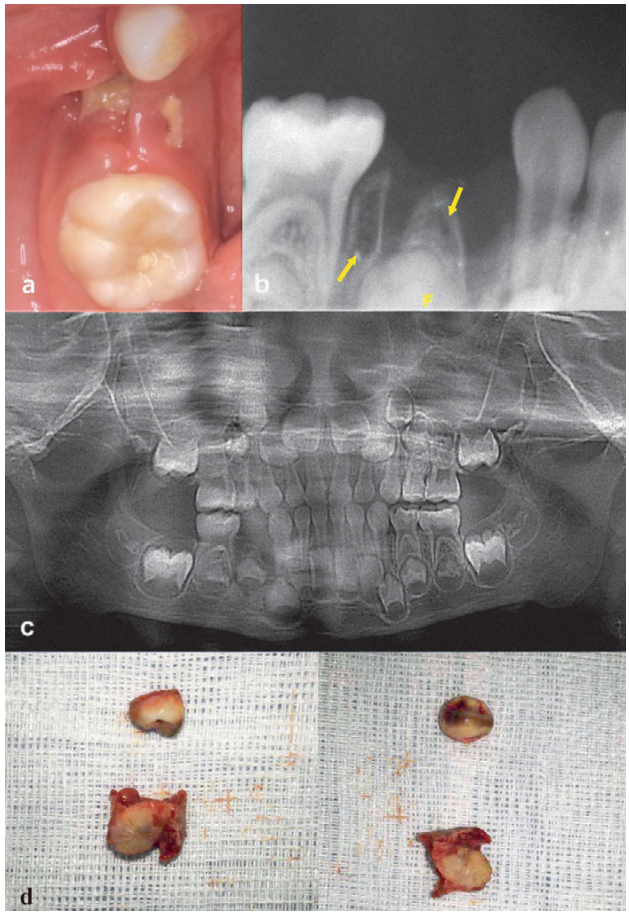

Fig 2a to d Clinical oral examination and radiographic findings at the first visit. Exposed alveolar bone in the primary mandibular right first molar area (white arrows) **(a)**. Periapical radiograph of the radiolucent lesion in the primary mandibular right first molar alveolar bone (yellow arrows) **(b)**. Panoramic radiograph demonstrating radiolucent lesion in the primary mandibular right first molar alveolar bone and the areas surrounding the permanent mandibular right first premolar (blue arrows) **(c)**. Removed sequestrum and permanent mandibular right first molar tooth germ **(d)**.

though the pain and swelling were relieved, the affected tooth fell out spontaneously 1 month before the follow-up examination. The wound remained unhealed and the patient complained of halitosis. The timeline demonstrating the progress of this case is presented in Fig 1.

According to previous medical history and blood testing, the young patient was healthy with no known allergies, systemic diseases or other medications. There was no family history of immunodeficiency disorders.

Clinical oral examinations further revealed poor healing of the socket with alveolar bone exposure in the primary mandibular right first molar area (Fig 2a), and the exposed bone fragment was loose. No fistulae existed in the adjacent mucosa or skin. No other teeth were particularly tender to percussion, and all teeth had a response to dry ice stimulation.

For radiographic examinations, the density of the mandibular right alveolar bone decreased in the periapical radiograph (Fig 2b), and the panoramic radiograph revealed a radiolucent demarcation line between the alveolar socket of the extracted primary mandibular right first molar and permanent mandibular right first premolar germ (Fig 2c).

The clinical diagnosis of arsenic trioxide–induced osteonecrosis was made based on the history of arsenic trioxide sealing, symptom of halitosis, clinical finding of sequestrum and radiographic finding of decreased local bone density. The patient was then referred to the Department of Oral and Maxillofacial Surgery.

The young girl was prescribed a 3-day course of cefaclor and scheduled for a sequestrectomy under general sedation. After the gingiva surrounding the exposed alveolar bone was separated, the loose greyish yellow sequestrum was gently removed with a vascular clamp, and the underlying permanent right mandibular first premolar germ was exposed with a dark yellow

appearance, surrounded by granulation, and detached from the surrounding bone (Fig 2d). Based on the preoperative radiographic examination and changes observed in the colour and mobility of the permanent premolar germ, the surgeon informed the patient's parents that the premolar germ may be affected by arsenic trioxide. After obtaining consent for removal of the germ, the affected tooth germ and granulation tissues were scraped, and the wound was irrigated with chloramphenicol. Histological examination of the removed sequestrum was not performed due to parental refusal.

The postoperative period was uneventful. A soft diet was recommended for the first week, and the patient was prescribed 60 mg cefaclor three times daily for the next 2 weeks after being discharged from hospital. The patient was recalled 1 week later to remove the stitches. Red and swollen gums were observed in the operative area (Fig 3a), so oral hygiene instructions were delivered. One month after surgery, painless healing was confirmed by clinical examination (Fig 3b).

Due to the removal of the permanent tooth germ, two treatment options were considered: maintaining the missing tooth space or allowing mesial movement of the distant molars. The details of each option were explained thoroughly, and the patient's parents chose the latter treatment plan, which involved monitoring the inclination and elongation of adjacent primary teeth, healing of alveolar bone in the operative area and development of adjacent permanent tooth germs.

At the 6- and 12-month follow-ups, intraoral examinations revealed that the primary mandibular right canine and second molar maintained their upright position, whereas the primary maxillary right first molar was slightly elongated without occlusal interference. Panoramic radiographs showed increased bone density in the osteonecrosis area and the development of permanent mandibular right canine and second premolar germs (Fig 3c and d).

The patient did not attend regular appointments for personal reasons until a recent visit for a painful unexfoliated tooth 6 years after surgery. To address the painful symptoms efficiently, only a panoramic radiograph was taken at this visit. In addition to the complete root resorption of the primary maxillary right second molar, the panoramic radiograph also confirmed the complete healing of the mandibular right area and normal development of adjacent permanent teeth germs (Fig 4a). Therefore, the primary maxillary right second molar was extracted, and the patient was recalled 1 week later so the practitioner could check the wound and take intraoral photos. The mesial-distal diameter of the missing tooth area was reduced by 7 mm, with normal gingival colour and texture (Fig 4b). The intraoral examination revealed an acceptable occlusion (Fig 4c). Both the patient and her parents were satisfied with the outcome. Currently, the girl is able to engage in regular activities without any difficulties.

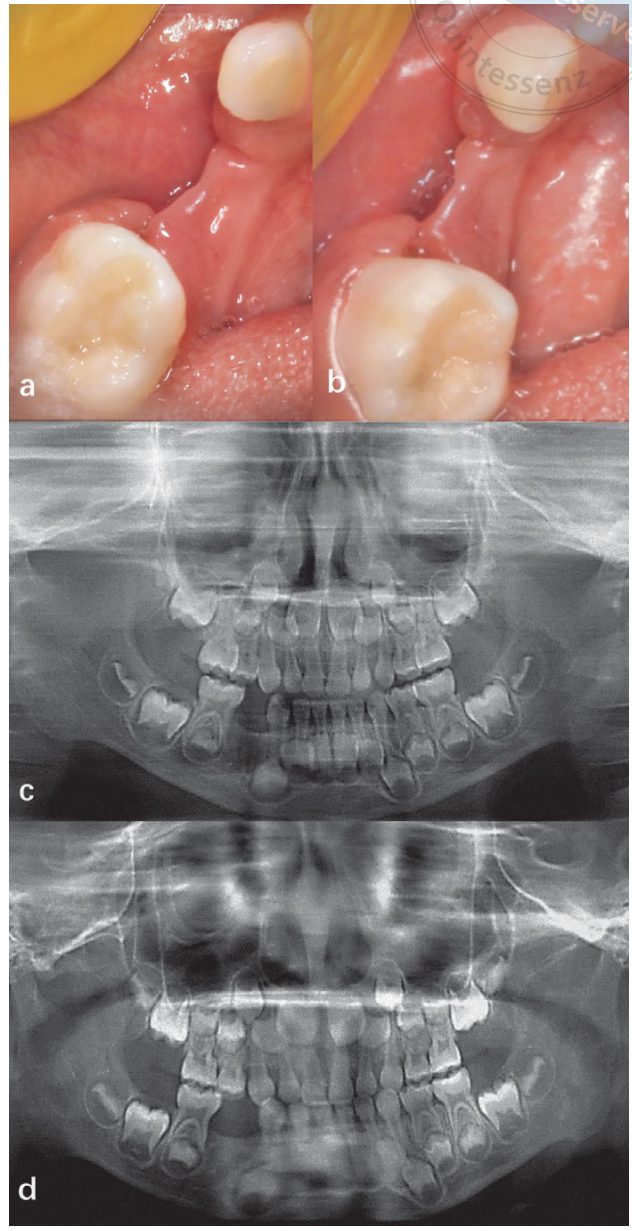

Fig 3a to d Images from 1 week and 1, 6 and 12 months after surgery. Gingival healing observed at the 1-week and 1-month follow-ups **(a and b)**. Panoramic radiographs taken 6 months and 1 year postoperatively demonstrating increased bone density of the lesion site **(c and d)**.

Fig 4a to c Clinical oral examination and radiographic findings at the 6-year follow-up. Panoramic radiograph demonstrating ingrowth of new bone structure and normal development of the permanent mandibular right canine and second premolar germs **(a)**. Complete gingival healing with decreased mesial-distal diameter in the primary mandibular right first molar area **(b)**. Acceptable occlusion of mixed dentition **(c)**.

Discussion

In this case, timely surgical intervention and conservative treatment contributed to a favourable prognosis over the 6-year follow-up period. With regard to the treatment of the involved permanent tooth germ, its removal was necessary due to infection and necrosis of the surrounding bone in reference to the only similar case.[6] The subsequent protocols for space management were formulated in reference to cases of congenitally missing teeth.[7]

Although no reports of osteonecrosis induced by arsenic trioxide used in primary teeth have been retrieved, 27 cases of topical arsenic–induced bone necrosis in permanent dentition have been reported.[8-12] The age range of patients is 14 to 60 years with a gender ratio of 4:5 (male: female). It is noteworthy that the present patient developed symptoms only 1 day after sealing, earlier than all previous cases involving permanent teeth (2 to 7 days). This result aligns with the fact that there are more accessory canals in the pulp chamber floor area of primary teeth than permanent teeth,[13] suggesting that the supporting tissues of primary teeth and their succedaneous tooth germs may be more vulnerable to arsenic leakage from the pulp chamber.

In most cases of drug-induced osteonecrosis in adults, disease-free edges should be exceeded, and healthy bleeding bones should be visible for the resection of necrotic bone, as it is difficult to determine the extent of necrosis.[14] In this case, the surgeons only removed the sequestrum without extended curettage of the surrounding bones. This decision was made based on the physiological characteristics of paediatric jaws, which are more porous, vascularised and resistant to drug invasion than the adult skeleton.[15] The optimal bone repair and normal development of the adjacent permanent tooth germ at the follow-up appointments also support this choice, suggesting that timely intervention for osteonecrosis may not interrupt maxillofacial development.

No histological results for the removed bone were obtained in this case. Although the medical history, clinical symptoms and radiographic findings of this patient all led to the diagnosis of osteonecrosis, histological evidence made it possible to exclude other pathologies.

Conclusion

This is the first case of drug-induced mandibular osteonecrosis involving permanent tooth germ in a child. The sealing of arsenic trioxide in primary teeth may cause more severe damage to the surrounding soft and hard tissues than in permanent teeth. All dental practitioners should be warned against the adverse effects of this agent and avoid using it in practice. For young patients with arsenic trioxide–induced osteonecrosis, timely re-

moval of sequestrum and other necrotic tissue without extended curettage, along with systemic antibiotic therapy, should be considered.

Conflicts of interest

The authors declare no conflicts of interest related to this study.

Acknowledgements

This study was approved by the Ethics Committee of Shanghai Ninth People's Hospital, Shanghai Jiao Tong University School of Medicine with approval number SH9H-2022-T403-1. The mother of the patient gave written consent for personal and clinical details along with any identifying images of her daughter to be published in this case report.

Author contribution

Dr Yue FEI contributed to the conceptualisation, data collection and manuscript draft; Dr Guang Yun LAI contributed to the writing and editing of the manuscript; Dr Jun WANG contributed to the supervision of the study, revision of the manuscript and funding.

(Received Apr 19, 2024; accepted Dec 03, 2024)

References

1. Badescu MC, Rezus E, Ciocoiu M, et al. Osteonecrosis of the jaws in patients with hereditary thrombophilia/hypofibrinolysis-From pathophysiology to therapeutic implications. Int J Mol Sci 2022;23:640.
2. Rosales HD, Garcia Guevara H, Requejo S, Jensen MD, Acero J, Olate S. Medication-related osteonecrosis of the jaws (MRONJ) in children and young patients-A systematic review. J Clin Med 2023;12:1416.
3. Hernandez M, Phulpin B, Mansuy L, Droz D. Use of new targeted cancer therapies in children: Effects on dental development and risk of jaw osteonecrosis: a review. J Oral Pathol Med 2017;46:321–326.
4. Flynn JM, Schwend RM. Management of pediatric femoral shaft fractures. J Am Acad Orthop Surg 2004;12:347–359.
5. Brown JJ, Ramalingam L, Zacharin MR. Bisphosphonate-associated osteonecrosis of the jaw: Does it occur in children? Clin Endocrinol (Oxf) 2008;68:863–867.
6. Mueller MA, Kanack MD, Singh J, Jaffurs D, Vyas RM. Pediatric mandible reconstruction for osteomyelitis during largest reported mycobacterium abscessus outbreak. J Craniofac Surg 2020;31:274–277.
7. Naoum S, Allan Z, Yeap CK, et al. Trends in orthodontic management strategies for patients with congenitally missing lateral incisors and premolars. Angle Orthod 2021;91:477–483.
8. Nezafati S, Ghavimi MA, Yavari AS. Localized osteomyelitis of the mandible secondary to dental treatment: Report of a case. J Dent Res Dent Clin Dent Prospects 2009;3:67–69.
9. Deshpande A, Prasad S, Deshpande N. Management of impacted dilacerated maxillary central incisor: A clinical case report. Contemp Clin Dent 2012;3:S37–S40.
10. Giudice A, Cristofaro MG, Barca I, Novembre D, Giudice M. Mandibular bone and soft tissues necrosis caused by an arsenical endodontic preparation treated with piezoelectric device. Case Rep Dent 2013;2013:723753.
11. Chen G, Sung PT. Gingival and localized alveolar bone necrosis related to the use of arsenic trioxide paste--Two case reports. J Formos Med Assoc 2014;113:187–190.
12. Marty M, Noirrit-Esclassan E, Diemer F. Arsenic trioxide-induced osteo-necrosis treatment in a child: Mini-review and case report. Eur Arch Paediatr Dent 2016;17:419–422.
13. Diéguez-Pérez M, Ticona-Flores JM. Three-dimensional analysis of the pulp chamber and coronal tooth of primary molars: An in vitro study. Int J Environ Res Public Health 2022;19:9279.
14. Hsu KJ, Hsiao SY, Chen PH, Chen HS, Chen CM. Investigation of the effectiveness of surgical treatment on maxillary medication-related osteonecrosis of the jaw: A literature review. J Clin Med 2021;10:4480.
15. Maes C, Kronenberg HM. Chapter 4–Postnatal bone growth: Growth plate biology, bone formation, and remodeling. Pediatric Bone 2012:55–82.

CURRENT BEST PRACTICE

NEW

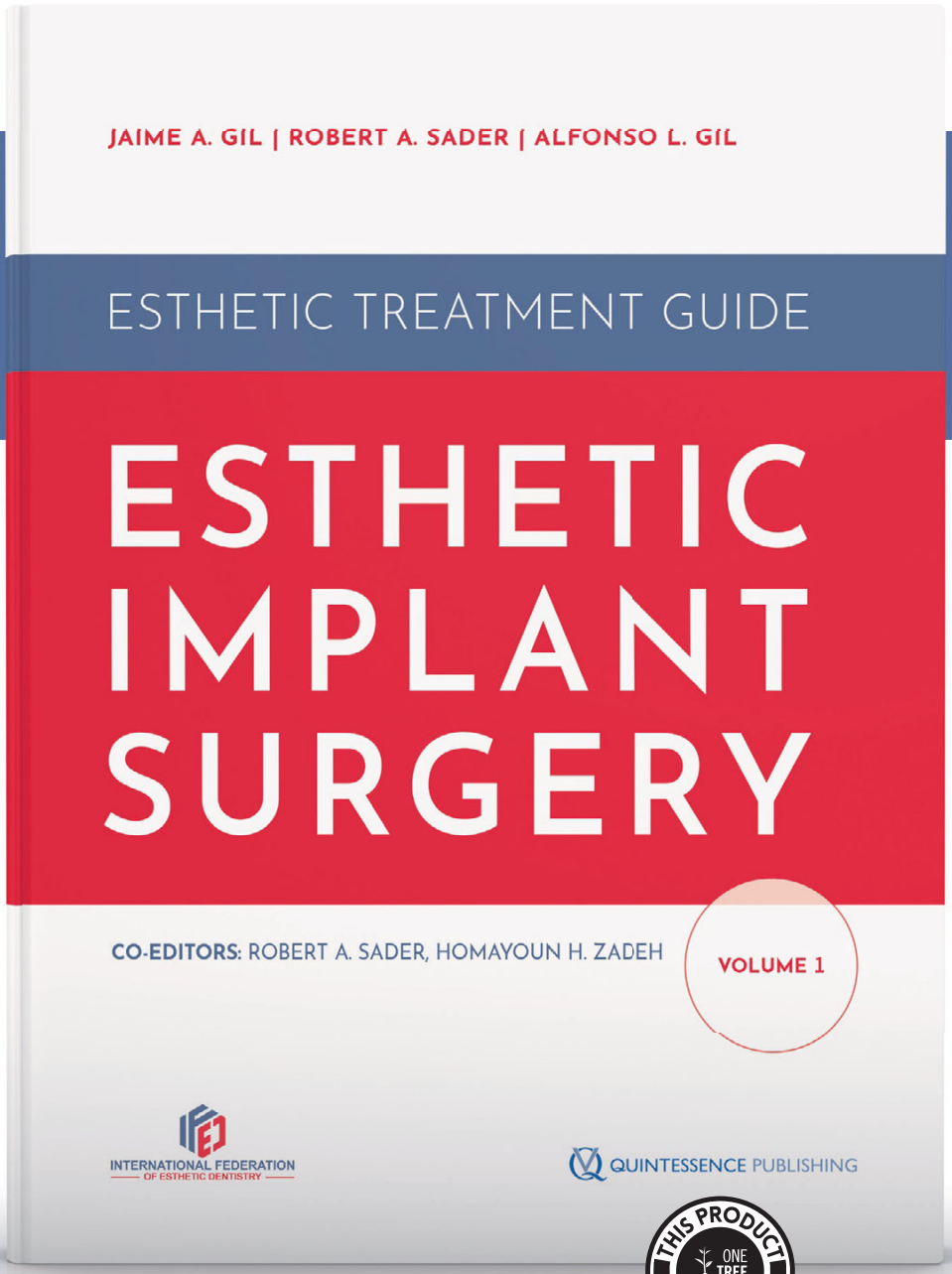

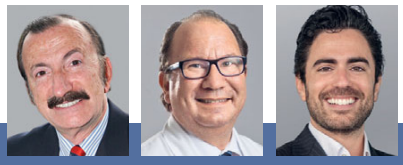

Jaime A. Gil | Robert A. Sader | Alfonso L. Gil

Esthetic Implant Surgery

Esthetic Treatment Guide Vol 1

208 pages, 900 illus
ISBN 978-1-78698-119-6, €128

This guide is a welcome and timely addition to current knowledge in the field of esthetic dentistry. In addition to chapters on esthetic implant site development, ridge augmentation, and managing esthetic complications in implant placement, the book also examines bone, soft tissue, and sinus augmentation, thus providing a comprehensive perspective and description of current techniques and approaches. Implant placement in the esthetic zone and anterior maxilla, which can be challenging for both clinician and patient, is also comprehensively covered. Beautiful illustrations and high-resolution photographs and images help the clinician to understand and apply the described techniques in everyday clinical practice. Case studies complement and further illustrate the issues and solutions highlighted in each chapter, thus grounding theory into real-world practice.

www.quint.link/
esthetic-treatment-vol1

books@quintessenz.de

+49 (0)30 761 80 667

QUINTESSENCE PUBLISHING

fdi World Dental Congress

SHANGHAI 2025

4 DAY exhibition

4 DAY scientific programme

60,000m² exhibition area

35,000+ visitors

8,000 delegates

700+ exhibiting companies

100+ Worldwide speakers

200+ national speakers

Early bird registration deadline: **2 June 2025**

Register Here

See you in SHANGHAI

9 - 12 September 2025